Sedimentary and ecosystem response to Late Cretaceous (Cenomanian - Turonian) paleoenvironmental events along the eastern margin of the Western Interior Seaway, Canada.

by

Danielle Dionne

A thesis submitted to the Faculty of Graduate and Post Doctoral Affairs in partial fulfillment of the requirements for the degree of

Master of Science

in

Earth Sciences

Department of Earth Sciences

Carleton University

Ottawa-Carleton Geoscience Centre

Ottawa, Ontario

ABSTRACT

During the Cretaceous Period, the Western Interior Seaway (WIS) was influenced by both gradual, long-term environmental changes and catastrophic, short-term environmental changes. Vertebrate fossil-rich bioclastic accumulations are particularly well developed along the eastern margin of the WIS within Cenomanian aged strata. In addition to these deposits, the uppermost Cenomanian to Turonian record along the eastern margin is characterized by rich, fairly undiluted planktic foraminiferal assemblages. The major control for the accumulation of these beds is interpreted to be related to a long-term process, namely the timing and magnitude of sea-level fluctuations on the eastern margin of the WIS. Bioclastic elements are interpreted to be concentrated as lags along erosion surfaces during transgressions. Superimposed on this are the effects of short-term processes: the taphonomic character of each bioclastic deposit is interpreted to be linked to the frequency of episodic events that influenced the seaway. Proximal and distal planktic foraminiferal assemblages record a changing environment with frequent catastrophic environmental perturbations including ashfalls and expansion of the oxygen minimum zone into the photic zone. Frequent environmental perturbations affect both distal and proximal settings, though their effect is stronger nearer to the paleoshoreline. Looking at both the depositional and faunal response to these short- and long-term processes that affected the seaway improves our understanding of the dynamics of this epeiric sea during this enigmatic time.

ACKNOWLEDGEMENTS

A big thank you goes to my supervisors Dr. Claudia Schröder-Adams and Dr. Stephen L. Cumbaa for their guidance, instruction, patience and support throughout this project. Research funding for this project was supplied by NSERC Discovery Grants to Dr. C. Schröder-Adams and to Dr S. L. Cumbaa, as well as by an Ontario Graduate Scholarship and the William Sliter Award from the Cushman Foundation for Foraminiferal Research to the author. Special thanks go to Alan McDonald for all his help in the field and with samples on our return to Ottawa, as well as to Michael Jackson for his help cutting and thin-sectioning my fragile samples. My sincere thanks also goes to everyone who has supported me throughout this project; my classmates, officemates, friends, and family, thank you.

TABLE OF CONTENTS

LIST OF TABLES

LIST OF ILLUSTRATIONS

LIST OF APPENDICES

CHAPTER 1 – INTRODUCTION

During the Cretaceous Period, the Western Interior Seaway (WIS) covered much of what is now Western Canada. The WIS was an epeiric sea with shallow, restricted waters that periodically connected the Tethys to the south and the Polar Sea to the north covering central North America and filling the foreland basin, spilling out onto the low gradient of the eastern platform (Cumbaa *et al.,* 2010; McNeil and Caldwell, 1981). Cretaceous strata and their fossil communities preserved within the Western Interior Sedimentary Basin (WISB) document frequent fluctuations in sea-level and attest to paleobiogeographic and paleoenvironmental changes. With no modern analogue for epeiric seas of the scale seen in the Cretaceous, it is difficult to differentiate gradual background processes from event processes in these past settings.

This study is presented in two main chapters addressing a) possible depositional histories and processes that led to the Cenomanian bonebed accumulations found along the the Manitoba Escarpment, at the eastern margin of the WISB; and b) paleoecological history of the planktic foraminiferal assemblage and its response to Cenomanian-Turonian paleoenvironmental changes at the eastern margin of the WIS during this interval.

The Manitoba Escarpment represents the erosional eastern margin of WISB strata. It is a series of uplands with significant Upper Cretaceous exposures, trending southeast to northwest from south-central Manitoba to east-central Saskatchewan. Strata from the Cenomanian-Turonian interval are mostly composed of shales deposited during the global Greenhorn transgressive-regressive cycle (McNeil and Caldwell, 1981; Kauffman and Caldwell, 1993; Schröder-Adams *et al.,* 2001). The Cenomanian-Turonian interval

was a particularly dynamic time in the WIS's history. Strata preserved within the WISB document frequent sea-level fluctuations, especially so on the eastern margin where the shoreline moved rapidly along the shallow gradient of the seafloor (Price *et al.,* 1995; Plint and Kreitner, 2007). Global greenhouse to hothouse conditions affected the seaway as did significant changes in water chemistry, including the global Ocean Anoxic Event 2 (OAE-2) and periods of anoxic or dysoxic bottom waters (Leckie *et al.,* 2002; Schröder-Adams, 2014). It was a period of increased volcanism, resulting in multiple ash falls within the seaway, documented with the strata of the WISB as bentonites (Schröder-Adams, 2014). In addition, two bolide impacts occured nearby (Grieve, 2006). These paleoenvironmental factors created both short-term and long-term changes in depositional patterns and faunal responses.

The outcrops along the Manitoba Escarpment contain numerous bonebeds—bioclastic horizons rich in vertebrate fossils—that are concentrated within the Cenomanian interval. This study aims to improve understanding of the genesis of the bonebeds by describing their sedimentological, taphonomic, stratigraphic, and paleoecologic characteristics. The Late Cretaceous Steen River and Deep Bay craters are in the WISB or closely positioned to the edge of the basin and are dated at 91 ±7 Ma and at 99±4 Ma repectively (Earth Impact Database). Their stratigraphic placements fall within the studied interval and are therefore of interest to the question whether the bonebeds bear evidence of deposition during short-term events such as tsunami that could be related to the associated impact events, or whether they are more reasonably interpreted as the product of long-term seafloor winnowing. Results will impact the use of these distinct surfaces in regional stratigraphic correlations, identifying sea-level lowstands and subsequent transgression

and/or the frequency of high-energy events such as storms and tsunami, and add to our understanding of catastrophic changes that might have affected paleoecosystems of the WIS.

Short- and long-term environmental changes also have the potential to influence biogenic productivity and faunal elements. The low sedimentation rates of the eastern margin of the WIS (Kauffman, 1977b; McNeil and Calwell, 1981; Schröder-Adams *et al.,* 2001) allow for the preservation of rich, nearly undiluted planktic foraminiferal assemblages. Due to their abundance in the geological record and their sensitivity to environmental changes, foraminifera are considered an invaluable tool for identifying paleoecological changes and reconstructing marine palaeoenvironmental histories (e.g. Schröder-Adams *et al.,* 1996; Keller and Pardo, 2004b; Waskowska, 2011; Schröder-Adams*,* 2014) and will provide information about the paleoenvironmental conditions present in the seaway. This study focuses on the response of foraminifera to short-lived, possibly catastrophic, environmental change at the eastern edge of the dynamic Cenomanian-Turonian WIS by drawing correlations between an outcrop section, located proximal to the paleoshoreline, and a subsurface core, located farther basinward. Furthermore, this study focuses on the biotic response of planktic foraminiferal assemblages to frequent ash falls that marked this time period in the WIS (Bagshaw, 1977; Bloch *et al.,* 1993, 1999; Schröder-Adams *et al.,* 2001; Keller and Pardo, 2004b; Tyagi *et al.* 2007). Planktic foraminiferal response to increased volcanism has been particulary well-studied at the Cretaceous-Tertiary boundary interval (e.g. Peryt, 2004; Keller, 2008), but, within the Canadian portion of the WIS, short-term environmental changes during this interval are less well-studied.

In detail, the following objectives are addressed: 1 – create a classification scheme for vertebrate bioclast-rich accumulations; 2 – determine whether the bonebeds are a result of short term events or the result of long-term accumulation; 3 – investigate whether the bonebeds contain evidence for deposition during tsunami and/or bolide impacts; 4 – characterize the foraminiferal response to short-term, possibly catastrophic, environmental changes in proximal and more distal settings; 5 – correlate strata between the proximal outcrop section to the distal subsurface section along the eastern margin; and 6 – characterize the foraminiferal response to frequent ashfalls in the WIS. This study of depositional and faunal response to short- and long-term processes that affected the shallow eastern margin adds to our understanding of the dynamics of an epicontinental sea during a greenhouse climate.

CHAPTER 2

VERTEBRATE FOSSIL-RICH ACCUMULATIONS FROM THE EASTERN MARGIN OF THE LATE CRETACEOUS (CENOMANIAN) WESTERN INTERIOR SEAWAY, CANADA: DEVELOPMENT OF A CLASSIFICATION SCHEME

ABSTRACT

In the Cretaceous Period, the Western Interior Seaway covered a substantial portion of the interior of North America, including much of what is now western Canada. The Albian to Santonian Colorado Group in the Western Interior Sedimentary Basin records the frequent paleogeographic and paleoenvironmental changes of this dynamic time. Mudrock-dominated strata are interrupted by vertebrate fossil-rich bioclastic beds that can be found in outcrop and core, and these are particularly common in Cenomanian successions. Reduced sediment input along the eastern margin in the Manitoba Escarpment allowed for a remarkable concentration of bioclastic components that attest to what must have been a rich assemblage of vertebrates inhabiting the Western Interior Sea. Based on sedimentological, taphonomic, stratigraphic, and paleontological characteristics, these accumulations are classified into four categories: inoceramites, calcareous bone-biophospharenites, non-calcareous bone-biophospharenites, and glauconite-rich organic deposits.

Inoceramites reflect long-term accumulation of material farther from shore as well as reworking of bioclastic material by storms and/or tsunami. Calcareous bone-biophospharenites show evidence of varying degrees of influence by waves and currents in addition to the effects of episodic events such as storms and/or tsunami. They are interpreted to have generally been deposited in shallow water near-shore environments. Non-calcareous bone-biophospharenites represent deposition in deeper water far from the shoreline and may be related to a single event. Glauconite-rich organic deposits, on the other hand, reflect a slow rain of material in deeper distal waters, mainly unaffected by events such as storms or tsunami. In addition to providing a wealth of

paleoenvironmental and paleobiogeographical information, these accumulations have potential as valuable stratigraphic markers useful for the recognition of major events such as extra-terrestrial impacts, tsunamis, and the timing and magnitude of sea-level fluctuations on the eastern margin of the Western Interior Seaway.

1. INTRODUCTION

During the Cretaceous Period, the Western Interior Seaway (WIS) extended from the Arctic Ocean to the Gulf of Mexico, covering much of what is now Western Canada, the west-central United States, and parts of Mexico. Cretaceous strata from the WIS preserved within the Western Interior Sedimentary Basin document frequent fluctuations in sea-level and attest to paleogeographic, paleobiogeographic and paleoenvironmental changes. Research focused on Upper Cretaceous strata of the Colorado Group has documented the occurrence of bonebeds and bioclastic horizons, particularly in Cenomanian-aged strata. These horizonss can be found in outcrop on both margins of the WIS in western Alberta, eastern British-Columbia, east-central Saskatchewan, and west-central Manitoba, and are found abundantly in cores of subsurface wells (e.g. McNeil and Caldwell, 1981; Schröder-Adams *et al.,* 1996; Schröder-Adams *et al.,* 2001; Tyagi *et al.,* 2007; Phillips, 2008; Cumbaa *et al.,* 2010; Cumbaa *et al.,* 2013). Concentrations of phosphatic elements in these beds tend to be highest along the eastern margin of the Cenomanian Western Interior Seaway, as sediment input derived from the Canadian Shield was only minor. In contrast, high sediment input derived from the Cordillera affected the western margin and as a result bioclastic material is increasingly diluted (Schröder-Adams *et al.,* 2001). These fossil-rich horizons commonly contain teeth, bone fragments, scales of marine vertebrates, and, infrequently, terrestrial vertebrate fossils (e.g. Schröder-Adams *et al.,* 2001; Cumbaa *et al.,* 2006, 2010, 2013). Some are dominated by calcite prisms of inoceramid molluscs, and some contain valves of the oyster, *Ostrea* (e.g. Sageman, 1996; Phillips, 2008). Previous studies of these bioclastic concentrations have focused on outcrops along the Manitoba Escarpment, including

localities in the Pasquia Hills, Saskatchewan, and near Riding Mountain, Manitoba (McNeil and Caldwell, 1981; Nicholls and Russell, 1990; Russell, 1993; Bloch *et al.,* 1999; Cumbaa and Tokaryk, 1999; Collom, 2000; Schröder-Adams *et al.,* 2001; Cumbaa *et al.,* 2006; Phillips, 2008; Cumbaa *et al.,* 2010; Barker *et al.,* 2011; Cumbaa *et al.,* 2013). These studies have described the remarkable fossil content of these horizons, have identified faunal composition, and have interpreted taphonomic data. They have also determined the stratigraphic position of the bonebedswith the aid of foraminiferal studies, the dating of the regionally recognized X Bentonite, and detailed work on macrofossils.

The Cenomanian was a particularly dynamic time in the Cretaceous Period. Long-term changes were related to climate fluctuations, tectonically and eustatically-driven sea-level fluctuations, and oceanic anoxic events (OAEs) (Plint and Kreitner, 2007; Gale *et al.,* 2008). At least two bolide impacts occurred near or possibly in the WIS (Earth Impact Database; Grieve, 2006). Global climate reached a thermal maximum in the late Cenomanian and was coupled with the globally recognized OAE-2 at the Cenomanian - Turonian boundary (Price *et al.,* 1995; Leckie *et al.,* 1998; Leckie *et al.,* 2002; Norris *et al.,* 2002; Keller, 2008; Hasegawa et al 2012; Hay and Floegel, 2012; Friedrich *et al.,* 2012). In addition, sea-level fluctuated rapidly in the Western Interior Seaway (Plint and Kreitner, 2007; Gale *et al.,* 2008). Changing paleogeography allowed for Tethyan- and Polar Sea-derived watermasses to enter the seaway, resulting in watermass stratification causing periods of anoxic or dysoxic bottom waters (Schröder-Adams *et al.,* 1996, 2001). This time was also marked by two bolide impacts falling in or near the WIS (Earth Impact Database; Grieve, 2006), possibly generating tsunami that affected sedimentation throughout the seaway.It is within this context that the Cenomanian bonebeds were

deposited. By analyzing the sedimentological, taphonomic, and paleoecologic characteristics of bonebed samples collected from several localities along the Manitoba Escarpment and in the Wapawekka Hills, north central Saskatchewan (Fig. 1), this study aims to improve understanding of the genesis of these bonebeds in the Cenomanian and to develop a classification scheme as has been proposed for shell beds (e.g. Kidwell, 1986; Kidwell *et al.,* 1986) to discriminate between the sedimentary processes that have led to observed differences. Studies of vertebrate bonebeds have mainly focussed on non-marine environments (Cumbaa *et al.,* 2013). Modifications to these schemes allow these vertebrate fossil-rich accumulations to be separated into groups based on their sedimentological, taphonomic, stratigraphic, and paleoecologic characteristics. The similarities which define each group may reflect a similarity in hydrodynamic processes at work during their deposition and hint at the duration of their formation.

This chapter focuses on bioclastic concentrations found in outcrop exposure along the Manitoba Escarpment and in the Wapawekka Hills, north central Saskatchewan (Fig. 1).

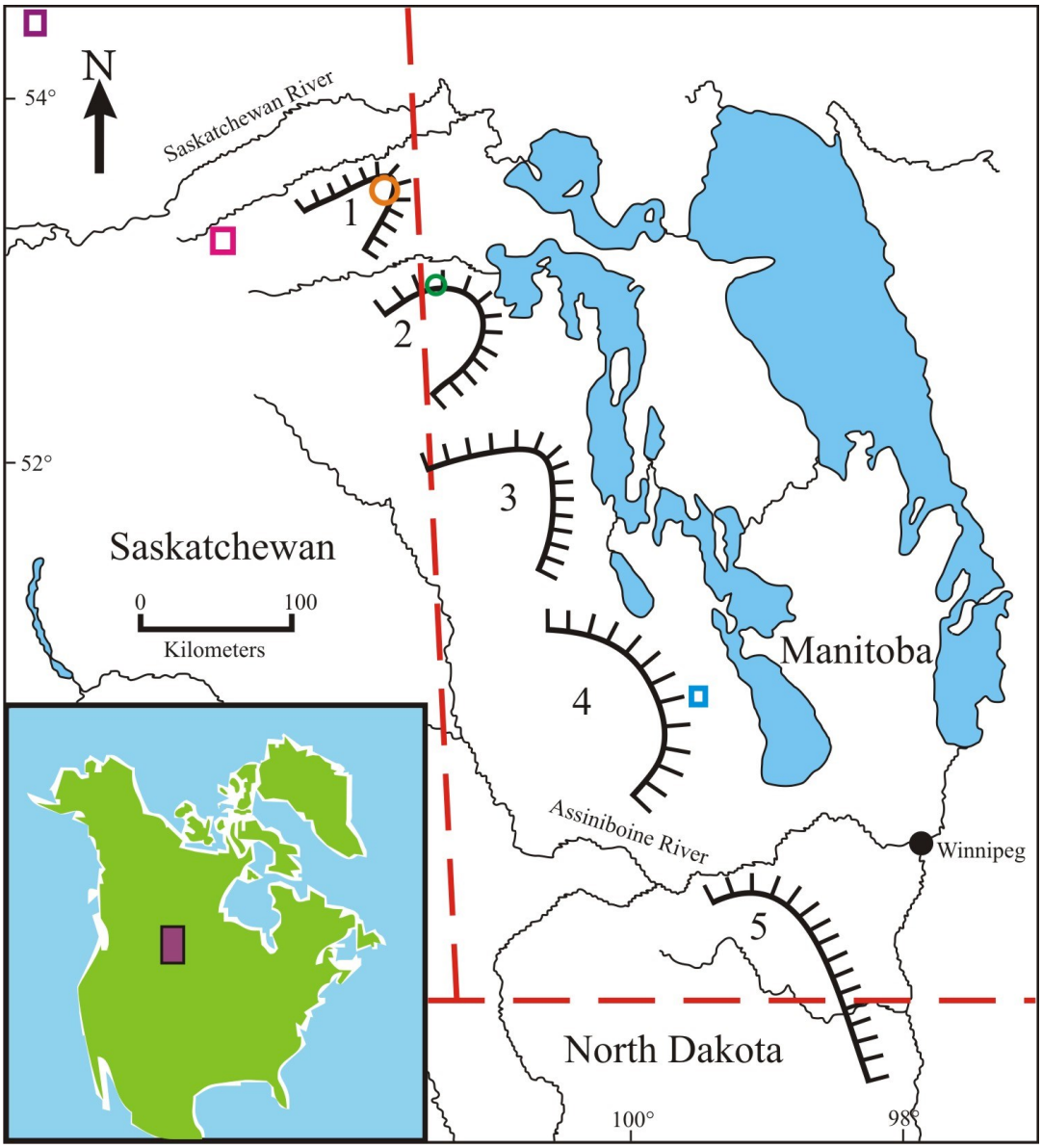

Figure 1: Map of the Manitoba Escarpment showing the locations of sampled bonebeds and bioclastic horizons. Modified from McNeil & Caldwell (1981) and Schröder-Adams *et al.* (2001). 1) Pasquia Hills, 2) Porcupine Hills, 3) Duck Mountain, 4) Riding Mountain, 5) Pembina Mountain. Localities are the Bainbridge river sites (BR1 and BR3), the orange circle; Carrot River sites (DH1 and DH3), the pink square; Van der Voort Farm, the blue square; Camp Seven River sites, the green circle; and the Wapawekka Hills locality, the purple square.

The objective was to determine whether these bonebeds were the result of short-term events, such as storms or tsunami, or whether the accumulation of fossil material was gradual over time, such as during long-term seafloor winnowing. A better understanding of the genesis of these bioclastic concentrations may contribute to our knowledge of event deposition versus long-term seafloor winnowing processes, which will in turn shed further light on sea-level fluctuations within the WIS. Ultimately, a better understanding of significant, regionally correlative beds will also contribute to improved stratigraphic correlations within the basin.

2. GEOLOGICAL SETTING

2.1 Cretaceous Western Interior Sedimentary Basin

The Western Interior Sedimentary Basin (WISB) is a foreland basin (Fig. 2) bordered by the Cordillera to the west and the Canadian Shield to the east (McNeil and Caldwell, 1981). This basin was initiated by pre-Cretaceous tectonic processes (McNeil and Caldwell, 1981). Continental rifting and drifting in the Late Proterozoic to Late Jurassic created the initial Cordilleran margin in North America. Subsequently, in the Late Jurassic, the accretion of allochthonous oceanic terranes began forming the Cordilleran mountain belt, developing a foreland basin (Price, 1994). Tectonism continued to affect the basin throughout the Cretaceous, causing differential uplift and subsidence of the seafloor and changing sedimentation patterns throughout the WISB (McNeil and Caldwell, 1981; Leckie and Smith, 1992; Hart and Plint, 1993; Plint *et al.,* 1993; Plint and Kreitner, 2007; Plint, 2009).

Structurally, the WISB is an asymmetrical trough made up of a foredeep flanked by a fold-thrust belt on the western side, with strata rising eastward to present-day Manitoba (Fig. 2). It can be split into four main zones: the western zone, the west-central zone, the hinge zone, and the eastern stable platform zone (McNeil and Caldwell, 1981). The western zone is marked by the highest subsidence and sedimentation rates. Sediments in this zone are mainly sandstone and conglomerate derived from the tectonically active western uplands. The west-central zone is similar, with high subsidence and sedimentation rates but with shale deposited in the foredeep, with interbedded sandstone derived from western sources. The hinge zone is the broad area between the actively subsiding western zones and the eastern stable platform and includes the forebulge. It is marked by moderate to relatively low rates of subsidence and sedimentation and is dominated by shale with rare carbonate units. Carbonates units become more abundant towards lower paleolatitudes. The eastern stable platform is a broad zone, including the backbulge, with low sedimentation and subsidence rates. Its sediments are mainly shale with rare carbonates. Sedimentary sequences are thin and commonly interrupted by disconformities (Kauffman, 1977b; McNeil and Calwell, 1981).

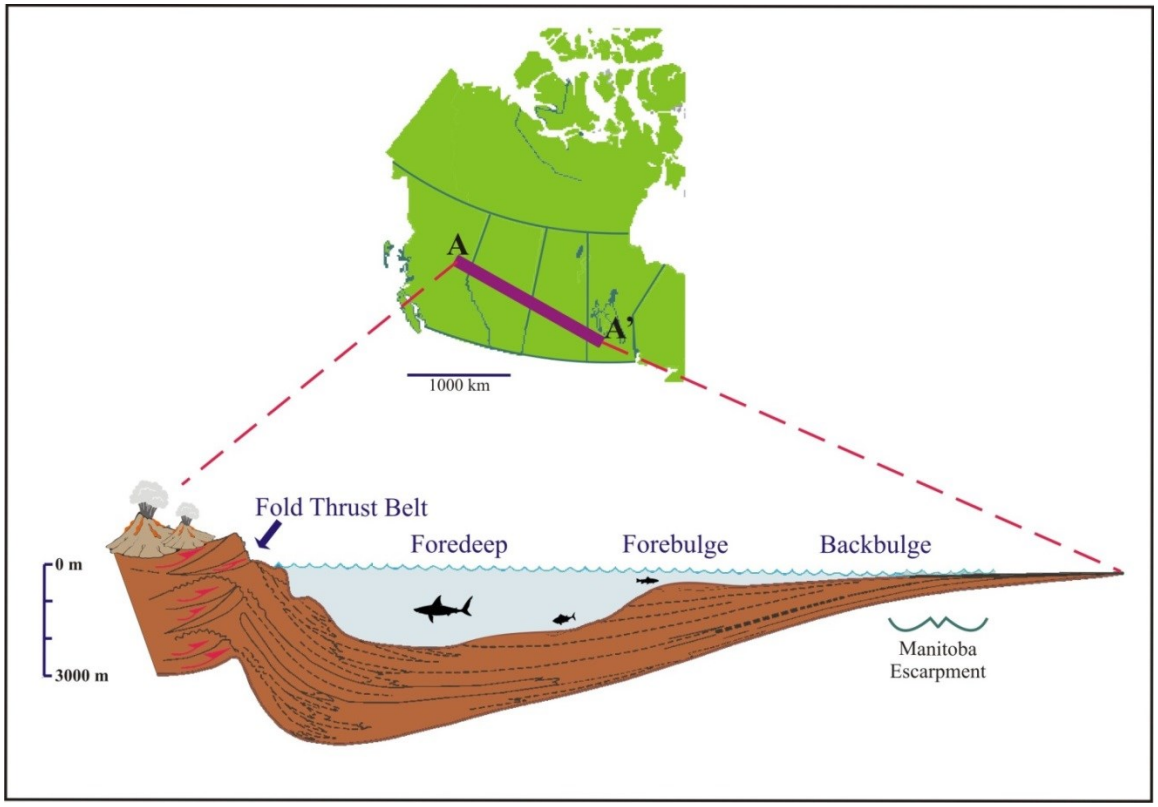

Figure 2: Conceptual cross section of the Western Interior Seaway during a sea level highstand, showing the asymmetry of the basin and long flat gradient of the eastern platform zone. This long expanse of shallow water was strongly affected by sea-level change. Modified from Kauffman (1984) and Phillips (2008).

The Manitoba Escarpment represents the erosional margin of the WISB and is a series of uplands with significant Upper Cretaceous exposures, trending southeast to northwest from south-central Manitoba to east-central Saskatchewan (Fig. 1). The escarpment extends over 675 km and is comprised of Albian to Maastrichthian aged strata up to 600 meters thick (McNeil and Caldwell, 1981; Schröder-Adams *et al.,* 2001). The outcrops along the Manitoba Escarpment contain numerous bioclastic horizons, several of which are investigated here. The Manitoba Escarpment and eastern Saskatchewan are located within the eastern stable platform zone on the backbulge. This area was strongly affected by changes in sea level as the shoreline translated rapidly along the shallow gradient of the seafloor (Fig. 2).

As result of the mainly Cordilleran-derived sediment sources and the increased accommodation space in the foredeep, Cretaceous strata form an eastward tapering wedge (e.g. McNeil and Caldwell, 1981, Bloch *et al.,* 1993; Plint *et al.,* 1993; Plint and Kreitner, 2007; Tyagi *et al.,* 2007). This reduced sediment input along the eastern margin allowed for the remarkable concentration of bioclastic components that attest to rich marine-vertebrate assemblages during the Late Cretaceous (Cumbaa and Tokaryk, 1999; Cumbaa *et al.,* 2006; Phillips, 2008; Cumbaa *et al.,* 2010; Cumbaa *et al.,* 2013).

2.1.1 Western Interior Seaway

The WIS was an epicontinental sea that periodically connected the Tethys to the south and the Polar Sea to the north (Fig. 3), covering central North America and filling the foreland basin, spilling out onto the eastern platform (Cumbaa *et al.,* 2010; McNeil and Caldwell, 1981). Cenomanian strata document a sea-level lowstand and period of

subaerial erosion at the base followed by the transgression during the start of the Greenhorn Marine Cycle (Hattin 1962; 1964; Kauffman, 1977a; Schröder-Adams *et al.,* 2001). The Albian-Cenomanian boundary is marked by a regionally recognizable phosphate-rich bioclastic horizon, the base of the Fish Scales Formation, present throughout Alberta and Saskatchewan. Sea levels continued to rise through the Cenomanian and reached a maximum in the early Turonian connecting the Polar Sea to the Tethys and transforming the restricted Mowry Sea into a seaway (Fig. 3; Hattin 1962; 1964; Kauffman, 1977a). Significant paleoenvironmental changes were occurring in and around the WISB during this time. Cenomanian strata preserved within the WISB attest to multiple, short-lived, sea-level fluctuations that have been attributed to glacioeustasy (e.g. Gardner, 1995; Plint and Kreitner, 2007; Plint, 2009), where sea-level may have fluctuated up to 10 m (Laurin and Sageman, 2007; Plint and Kreitner, 2007).

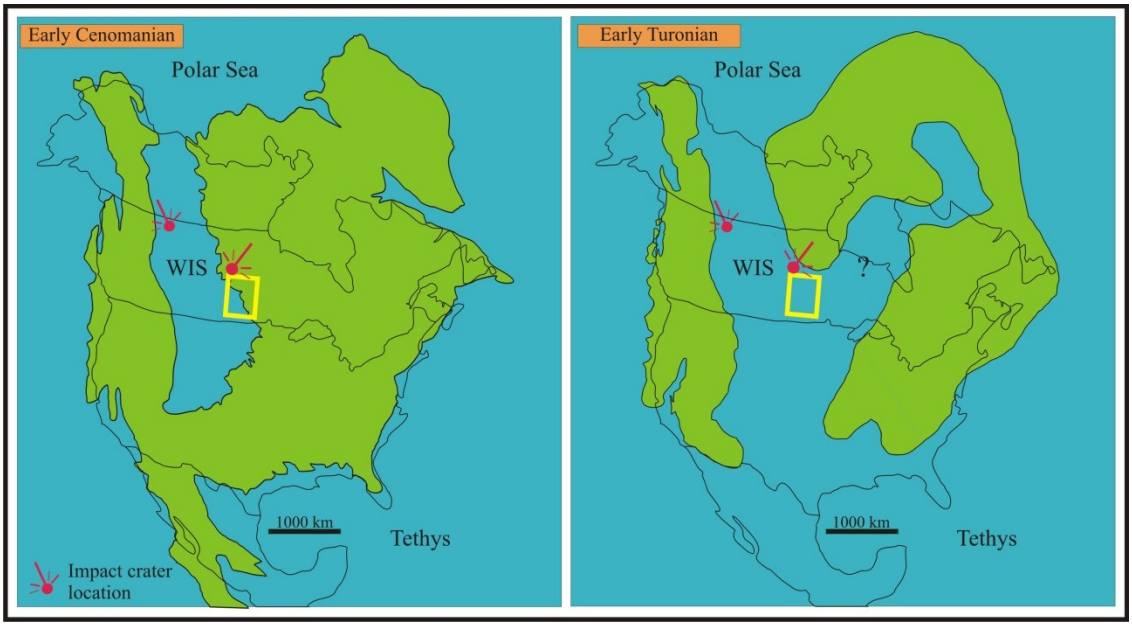

Figure 3: Paleogeographic map showing the extent of the seaway during the earliest Cenomanian, on the left, and during the earliest Turonian, on the right, with the position of the two known Cenomanian-Turonian bolide impact craters shown. The yellow box indicates the field area where bioclastic accumulations were found. Note the nearshore versus offshore position of the study area between these two time intervals. Modified from Bhattacharya and MacEachern (2009).

2.2 Stratigraphic framework

Our current understanding of the eastern margin of the Canadian WIS comes from various studies of the Manitoba Escarpment (e.g. Caldwell, 1975; McNeil and Caldwell, 1981; Schröder-Adams *et al.,* 1996; Schröder-Adams *et al.,* 2001). The strata exposed in the Pasquia Hills, the northernmost upland of the escarpment, are mostly composed of Albian to Santonian aged marine shales deposited during the Greenhorn and Niobrara eustatic cycles (McNeil and Caldwell, 1981; Kauffman and Caldwell, 1993; Schröder-Adams *et al.,* 2001; Cumbaa *et al.,* 2006). These sediments form, in ascending order, the

Ashville, Favel, and the Carlile (previously Niobrara) formations (McNeil and Caldwell, 1981; Bloch *et al.,* 1993; Schröder-Adams *et al.,* 2001; Nielsen *et al.,* 2003; Bamburak and Nicolas, 2009).

2.2.1 Ashville Formation

The Albian-Cenomanian Ashville Formation conformably overlies the underlying Swan River Formation (McNeil and Caldwell, 1981; Bamburak and Nicolas, 2009). It is made up of grey-black non-calcareous shale with thin beds of siltstone, sandstone, and calcarenite. This formation can be divided into several units including, in ascending order; the Skull Creek, Newcastle, Westgate, and Belle Fourche members. The Skull Creek Member is made up of dark-grey, non-calcareous, non-carbonaceous shale overlain by the white to light-grey, fine to coarse grained sandstone and interbedded dark-grey shale of the Newcastle Member. The Westgate Member of the Ashville Formation is dark-grey non-calcareous, non-carbonaceous shale like that of the Skull Creek Member. The base of Fish Scale Zone marks the base of the Belle Fourche Member and points to the division between the Early and Late Cretaceous in the WISB. The grey-black to black carbonaceous and organic-rich beds of the Belle Fourche Member also include three more regionally correlative marker beds: the *Ostrea beloiti* oyster beds, the X Bentonite dated at 95.87 ± 0.10 Ma, and the Bighorn River bentonite dated at 94.29 ± 0.13 Ma and positioned at the boundary of the Ashville Formation and the overlying Favel Formation (McNeil and Caldwell, 1981; Schröder-Adams *et al.,* 2001; Bamburak and Nicolas, 2009; Barker *et al.,* 2011).

2.2.2 Favel Formation

The latest Cenomanian to early Middle Turonian Favel Formation unconformably to conformably overlies the Belle Fourche Member of the Ashville Formation (Bamburak and Nicolas, 2009). It is made up of olive-black chalk-speckled calcareous shale, argillaceous limestones and calcarenite. This formation can be divided in ascending order into the latest Cenomanian Keld and Early to early Middle Turonian Assiniboine members. The uppermost 5 m of the Keld Member is marked by the argillaceous limestone of the Laurier Limestone marker beds and the uppermost 3.5 m of the Assiniboine Member is marked by the fossiliferous calcarenite of the Marco Calcarenite marker bed (McNeil and Caldwell, 1981; Schröder-Adams *et al.,* 2001; Bamburak and Nicolas, 2009).

2.2.3 Carlile Formation

The Middle Turonian to Santonian Carlile Formation disconformably overlies the Favel Formation in the eastern WIS and can be separated into the Morden and Boyne members (Bamburak and Nicolas, 2009). The Morden Member overlies the limestone beds at the top of the Favel Formation and is made up of non-calcareous, carbonaceous shale. It is overlain by the lead-grey shales of the two informal units of the Boyne Member, which consist of calcareous shale beds and chalky shale beds (Bamburak and Nicolas, 2009; Nicolas, 2009) (Fig. 4).

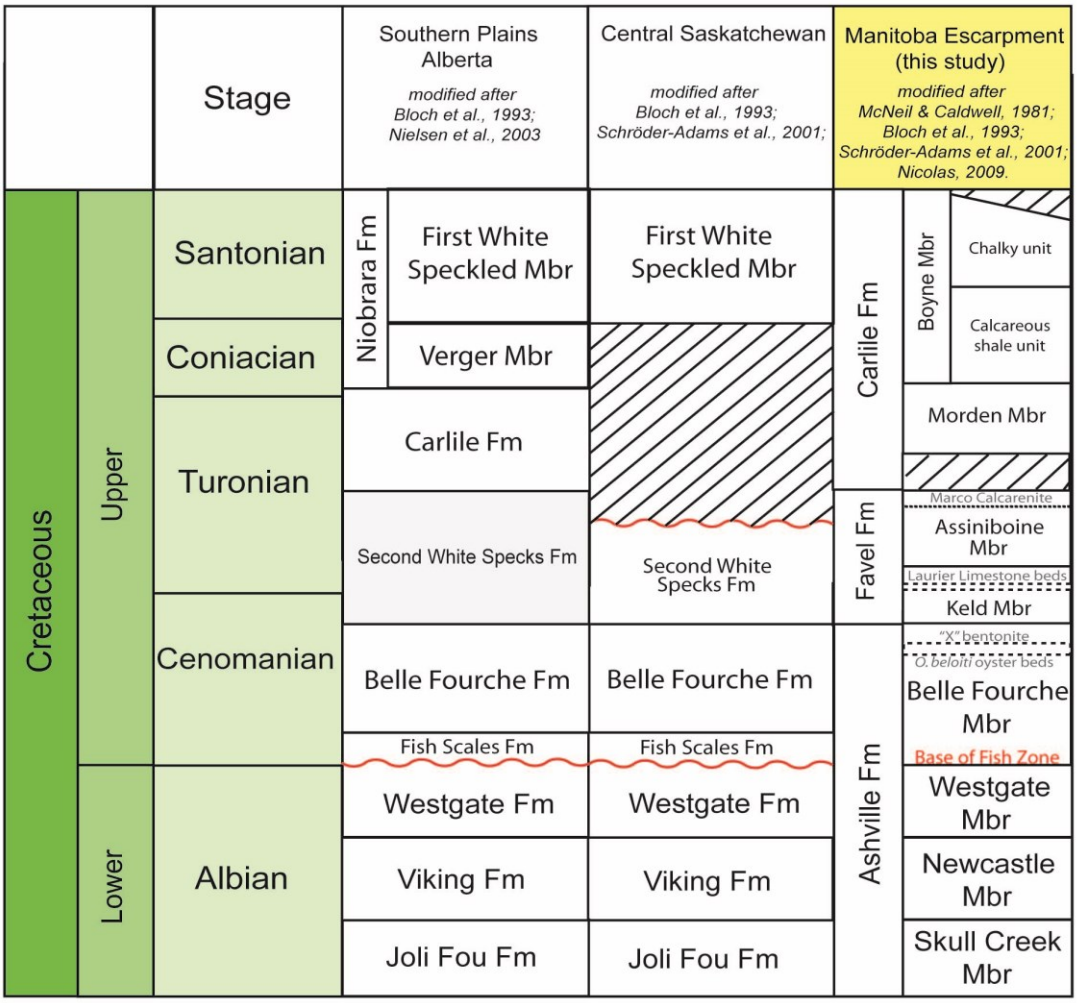

Figure 4: Stratigraphic chart of the Canadian WISB. Modified after Schröder-Adams *et al.* (2001), Phillips (2008), Nicolas. (2009), and Bamburak and Nicolas (2009).

2.3 Paleoenvironment

The Cenomanian-Turonian interval was globally one of particularly dynamic changes that similarly affected the WIS. Marine shales document a complex and variable depositional history and contain evidence of sea level change, poor bottom water oxygenation, increased carbon perturbations, the Oceanic Anoxic Event 2 (OAE-2) and abundant volcanism (Price *et al.,* 1995; Leckie *et al.,* 1998; Schröder-Adams *et al.,* 2001;

Leckie *et al.,* 2002; Norris *et al.,* 2002; Keller, 2003; Grieve, 2006; Plint and Kreitner, 2007; Gale *et al.,* 2008; Keller, 2008; Hasegawa et al 2012; Hay and Floegel, 2012).

The Canadian WIS was contained within a mid-latitude warm humid belt during the Cenomanian to Turonian interval (Hay and Floegel, 2012). Although modern open ocean sea surface temperature rarely exceeds 28-29°C, $\delta^{18}O$ paleothermometry from planktic foraminiferal calcium carbonate shells from the mid to Late Cretaceous indicate greenhouse temperatures near the poles that could have been up to 20°C warmer than today, while surface waters at lower latitudes may have reached 37°C at their peak in the mid to Late Turonian (Norris *et al.,* 2002; Hay, 2008; Hay and Floegel, 2012). Epicontinental seas would be even warmer due to their broad shallow nature. Oxygen isotope analysis of the biogenic phosphate contained in the enamel of fossil shark teeth from the eastern margin of the seaway reveal temperatures exceeding 30°C (Munro, 2000). The presence of crocodilians within the Canadian Arctic in the Turonian also delivers evidence for polar warmth (Huber, 1998; Tarduno *et al.,* 1998; Norris *et al.,* 2002) suggesting a reduced tropics-pole temperature gradient during the Cenomanian (Hasegawa *et al.,* 2012). During these greenhouse conditions, humidity and precipitation rates were high, possibly forming a brackish cap and inhibiting vertical mixing within the water column (Norris *et al.,* 2002; Leckie *et al.,* 1998; Hay and Floegel, 2012; Hasegawa *et al.,* 2012; Price *et al.,* 1995). Climate modelling suggests that seasonality produced strong winds in the winter months, creating a period of increased storm intensity, while it created only weak winds in the summer (Price *et al.,* 1995; Leckie *et al.,* 1998; Hay and Floegel, 2012; Friedrich *et al.,* 2012; Hasegawa *et al.,* 2012).

2.3.1 Bolide impacts

Eleven bolide (meteorite, asteroid, or other extraterrestrial mass) impacts are interpreted to have occurred near the Cretaceous WIS two of which fall within the Cenomanian-Turonian interval (Grieve, 2006; Earth Impact Database). Bolide impacts are interpreted based on the structures they form on impact such as craters, as well as by the ejecta they release during their collision with the Earth's crust (Grieve, 1998; Ormo and Lindstrom, 2000; Grieve, 2006, Reinold and Jourdan, 2012).

The sedimentary signature of a bolide impact on a marine environment is different than that of a subaerial impact due to the features associated with the resurge activity, waves, currents, etc. (Dypvik and Jansa, 2003). Submarine impacts tend to show crater configurations similar to larger subaerial impacts with some key differences (Dypvik and Jansa, 2003). For example, craters of marine bolide impacts generally have larger diameters relative to the size of the impactor, low rims due to the resurge of water back into the crater after impact, and a flat-topped central peak (Dypvik and Jansa, 2003). These differences are reduced when the marine bolide impact occurs in shallow water (Ormo and Lindstrom, 2000), as would have been typical of the WIS. The distal ejecta resulting from marine or subaerial bolide impacts show no significant differences to terrestrial impacts (Dypvik and Jansa, 2003).

When a bolide collides with the Earth's crust, the velocity of impact causes melting and vaporization of silicate materials (Simonson and Glass, 2004). The impact ejecta can be deposited rapidly and over a very extensive area creating excellent stratigraphic markers (Dypvik and Jansa, 2003; Simonson and Glass, 2004). The marker beds may include

tektites or spherules and iridium enriched clays. The force of the impact can also generate shock metamorphic features such as shatter cones and shocked quartz (Stoffler and Lagenhorst, 1994; Langenhorst and Deutsch, 2012). Bolide impacts have been associated with geochemical anomalies such as iridium (Ir) spikes. However, the search for these spikes has commonly yielded mixed results (Grieve, 1998). Impact related materials including geochemical anomalies such as Ir spikes as well as tektite and spherule strewn fields are limited in the stratigraphic record and as such, it is necessary to search for all types of impact indicators (Grieve, 1998; Jansa, 1993).

Impacts can also greatly affect the background sedimentary processes operating in the affected region. Possible consequences of a bolide impact include earthquakes, tsunami, and major changes in water chemistry, as well as short-term and long-term changes in climate, all of which can leave signatures in the sedimentary record (Keller, 2003; 2008; Mitchell *et al.,* 2010). The sedimentary effects of a tsunami traveling through deep water may be very different than its effects on a large, shallow, epicontinental sea. Although there are no modern analogues for the epicontinental seas of the scale seen in the Cretaceous and at other times during Earth's history, modelling approaches may be used (Mitchell *et al.,* 2010). For example, Mitchell *et al.* (2010) modelled the propagation of a tsunami in the Late Jurassic Laurasian Seaway. The modelling experiments lead to several conclusions. There is poor propagation and rapid attenuation (within 1000 km) of tsunami in shallow waters due in part to the frictional effects of the sea bed as well as the possibility of wave -reflection off land masses within the shallow basin. Alternatively, some regional bathymetric geometries could amplify wave heights locally. The modelling experiments indicated that bed shear stresses would be low and would likely

only mobilize sediment on the seafloor near the source. On the other hand, if the source of the tsunami was particularly large, such as a bolide impact within the epicontinental sea, the modelled shear stresses were found to be much higher, though still restricted in extent. These results suggest the effect of a tsunami on sedimentation in an epicontinental sea would be similar to other periodic, high energy events such as surge deposits, storm deposits, and debris flows. These high energy events can all lead to the deposition of sedimentary features such as rip-up clasts, graded bedding, hummocky cross-stratification, and ripples (Dawson and Stewart, 2007; Mitchell *et al.,* 2010). Due to the non-specificity of these features, there is no clear procedure for identifying tsunami deposits (tsunamiites), making them very difficult to recognize (Mitchell *et al.,* 2010). However, if spherules or other evidence of a bolide impact was observed in an event bed, deposition during a bolide-generated tsunami would be difficult to rule out.

The tsunami hypothesis is investigated here in connection to the two aforementioned meteorite impacts that occurred near the WIS during the Late Cretaceous (Fig. 3). The Steen River Crater in Northern Alberta is dated 91 ±7 Ma (Earth Impact Database). This interval includes the Cenomanian-Turonian boundary and the deposition of the upper portion of the Belle Fourche Member of the Ashville Formation and the Keld Member of the Favel Formation in the Manitoba Escarpment (Fig. 4) where an abundance of bioclastic accumulations are found. The Deep Bay Crater in northern Saskatchewan is dated at 99±4 Ma (Earth Impact Database). This interval includes the Late Albian to Early Cenomanian and the deposition of the Westgate Member and the lower portion of the Belle Fourche Member of the Ashville Formation and with that, the Fish Scales Marker Bed (Fig.4). These impacts would have left a signature in the sedimentary record

of the WIS. Paleogeographic maps (Fig. 3) suggest that the Steen River Crater is located within areas then covered by the Western Interior Sea and its location would have resulted in a significant influence on the sedimentary record. This crater is situated near the town of High Level in northwestern Alberta (Grieve, 2006). The crater measures 25 km in diameter and has no surface expression, having been buried by Quaternary sediments (Grieve, 2006). The Deep Bay Crater in northern Saskatchewan is located closer to the Wapawekka Hills of Saskatchewan and the several sample localities that are the focus of this study along the Manitoba Escarpment. This crater is situated at the southern edge of Reindeer Lake in northeastern Saskatchewan (Grieve, 2006). It is a startlingly circular crater 13 km in diameter and 220 m deep (Grieve, 2006). The Deep Bay Crater's relationship to the WIS is debatable due to glacial erosion of the sedimentary cover over the Canadian Shield outside of the crater and the uncertainty of the position of the paleoshoreline during this time. If the meteorite hit terrestrial terrain, the shoreline of the seaway could have not been far from the impact site.

2.3.2 Storm deposits vs tsunami deposits

Since a bolide impact on the WIS would have certainly released a tsunami wave, such a phenomenon needs to be differentiated from large storm deposits. A tsunami consists of a series of pulses of long period waves (Bondevik *et al.,* 1997; Fujiwara and Kamataki, 2007; Marshak, 2012). Their wavelengths can measure hundreds of kilometers and consequently, a tsunami wave base is deeper than the seafloor, and their wave orbitals are elliptical (Dawson and Stewart, 2007; Fujiwara and Kamataki, 2007; Marshak, 2012). Essentially, a tsunami is an immense shallow water wave due to its large wavelength. A tsunami wave height and its speed depend on the size of the disturbance to the water

column but generally, it has a low amplitude and can reach speeds of 700 km/h in the open ocean and, upon reaching shallower coastal water and land, its height is greatly amplified, attaining tens of meters in height, as it slows to 10-20 m/s (Dawson and Stewart, 2007; Morton *et al.,* 2007a,b; Bondevik *et al.,* 1997; Marshak, 2012).

Marine tsunami and storm deposits share many characteristics but also differ in several important ways that may help differentiate them within the geological record. The sedimentary signature of tsunamiites (tsunami deposits) and tempestites (storm deposits) show distinct characteristics. A tsunamiite generally has an irregular base and a near-flat upper surface created by the erosion of substrate during the the early upflow stage of the tsunami wave and the irregular infilling of the scoured surface. On the other hand, a tempestite typically has a sharp, nearly flat base and an irregular upper surface (Dawson and Stewart, 2007). The bed geometry is variable but tsunamiites usually form a sheet-like deposit as a result of the widespread runout of water, while tempestites usually form beds that pinch and swell as a result of the mobilization of sediment by its short period waves (Dawson and Stewart, 2007). The admixture of clasts, including poorly-sorted rounded and angular elements as well as, "exotic fragments" such as plants or beach rock, picked up from a subaerial source, is typical of tsunamiites as the tsunami wave erodes material from shoreface and coastal environments and brings it basinward (Dawson and Stewart, 2007). The alternating flow seen during each successive wave is unique to tsunami and can produce distinctive characteristics including the inverse imbrication of clasts with alternating seaward and landward orientation. Although, deposits are typically massive, multiple fining upward units representing these successive waves may be present (Dawson and Stewart, 2007). The rapid flooding and rapid retreat of water

resulting from the passage of a tsunami wave moving up to 20m/s can erode and entrainsediment into suspension though some sediment may be transported as bedload, creating a inverse to normally graded basal carpet of of coarse-grained clasts (Dawson and Stewart. 2007; Morton *et al.,* 2007a, b). In contrast, the gradual flooding and flow of storm waves travelling up to 5m/s overland erodes and transports sediment mainly by traction (Morton *et al.,* 2007a, b). Only at the end of the event does the water gradually retreat at a slower speed, possibly causing some reworking and redistribution of previously deposited sediment but not at the scale seen in tsunamiites (Morton *et al.,* 2007a, b). Before the backwash of water and sediment moves basinward, the tsunami passes through a zone of zero velocity that allows for the deposition of fine-grained sediment, as does the calm period between each wave. Cross-stratification that includes mud drapes, deposited during these calm periods, can be a diagnostic criterion of an offshore paleotsunami deposit (Dawson and Stewart, 2007).

3. MATERIALS AND METHODS

3.1 Bioclastic Accumulations

This research focused on marine strata deposited near the eastern margin of the Cretaceous WIS in Canada. Samples include vertebrate bioclast-rich lenses and beds from various sites along the Manitoba Escarpment (Fig. 1) such as a) the Carrot River localities 1 and 2 (DH-1 and DH-3) on the flank of the Pasquia Hills, Saskatchewan; b) Bainbridge River localities 1 and 2 (BR1 and BR3), in the Pasquia Hills, Saskatchewan; c) Camp Seven River (C7) in the Porcupine Hills, Manitoba; d) Van der Voort (VDV) east of Riding Mountain, Manitoba; and e) to the north, localities 1 and 2 in the

Wapawekka Hills (WAP1 and WAP2), Saskatchewan (Table 1). Samples were collected in situ as well as in float blocks during field work between 1991 and 2011.

Table 1: Outcrop locations and associated samples. Detailed locations available through the Royal Saskatchewan Museum or the Manitoba Museum.

Bainbridge River	
1. BR1	N53° W102°
Sample (BR1-1)	
2. BR3	N 53° W102°
Samples (BR3-1, -2, -3, -4, -5, -6, -7)	
Camp Seven River (Porcupine Hills, MB)	
C7	N52° W101°
Samples (C7-1, C7-2, C7-3)	
Van der Voort	
VDV	N50° W99°
Samples (VDV-1, VDV-2)	
Carrot River	
1. DH1	N53° W103°
Samples (DH1-1, DH1-2)	
2. DH3	N53° W102°
Sample (DH3-1)	
Wapawekka Hills	
1. WAP1	N54° W104°
Sample (WAP1-1)	
2. WAP2	N54° W104°
Sample (WAP2-1)	

3.1.1 Stratigraphic position of bioclastic accumulations

At the Bainbridge River BR3 locality, the bioclastic accumulations have been assigned a mid to Late Cenomanian in age based on the vertebrate fossil content and the foraminiferal assemblage in the Belle Fourche Member of the Ashville Formation. The largest lens (BR3-7) is situated 2.5 cm above the *Ostrea beloiti* layer, in the soft black shales of the Belle Fourche Member (Schröder-Adams *et al.,* 2001; Cumbaa *et al.,* 2013). The sequence stratigraphic position of this outcrop section has been developed by Schröder-Adams *et al.* (2001) (Fig. 5). The Cenomanian-Turonian WIS was shaped by the Greenhorn transgressive-regressive cycle (Kauffman, 1984). The strata exposed at this locality reflect several periods of lowered sea-level which occurred during the overall transgression. Bainbridge River BR1 locality is situated approximately 300-400m downstream of the BR3 locality. According to McNeil and Caldwell (1981) who worked within this area of the Bainbridge, exposures grow older farther downstream. The bioclastic accumulation found at this locality is unlike that of the large bonebed lenses in BR3. This and its downstream position makes it is probable that the BR1 section is stratigraphically lower than the BR3 exposure.

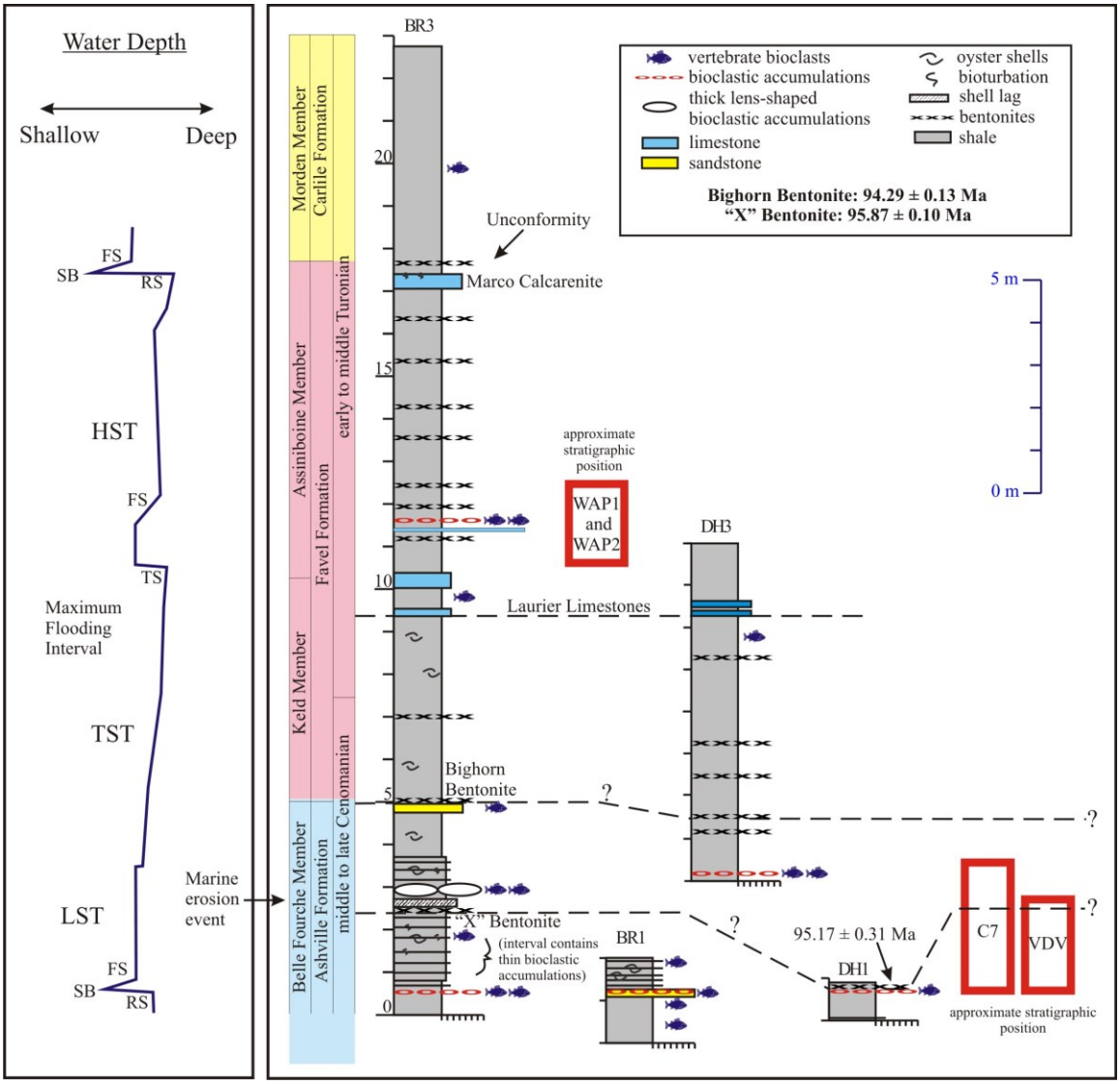

Figure 5: Sequence stratigraphic position of the Bainbridge River BR3 outcrop and stratigraphic position of the different bonebeds relative to the BR3 locality. Modified after Schröder-Adams et al. (2001) and Collum (2000).

At the Carrot River DH3 locality, the presence of two limestone beds interpreted to be the regionally correlative Laurier Limestone beds (Collom, 2000) makes its placement relative to The Bainbridge River (BR3) locality easier. Additionally, Collom (2000) correlated the bentonites between the BR3 and DH3 sites, although without precise dates

for these bentonites, these correlations remain uncertain. The Carrot River DH1 locality, bioclastic deposits have been determined to be mid to Late Cenomanian in age based on the foraminiferal assemblage and radiometric dating (Cumbaa and Tokaryk, 1999; Tokaryk *et al.,* 1997; Schröder-Adams *et al.,* 2001; Cumbaa *et al.,* 2006). The age of the bentonite that overlies the bioclastic accumulation at this locality is closer to the "X" Bentonite than to the Bighorn Bentonite. In addition, the foraminiferal zone and the predominance of algal cysts relate well with that of the basal portion of the BR3 section (Schröder-Adams *et al.,* 2001). Consequently, I place the DH1 section equivalent to the basal portion of BR3 with its bentonite possibly equating with that of the presumed "X" Bentonite in the BR3 section.

The bioclastic deposits from the Van der Voort (VDV) locality have been assigned an early to mid Cenomanian age based on the vertebrate fossil content and the foraminiferal assemblage (Phillips, 2008). The vertebrate fauna, particularly the sharks *Roulletia canadensis* and *Eostriatolamia paucicorrugata*, are endemic to the northern waters of the WIS, and are thus far have only been observed in Cenomanian strata (Phillips, 2008; Cumbaa *et al.,* 2010; Underwood and Cumbaa, 2010). Camp Seven River (C7) samples were collected as float and thus their stratigraphic position is uncertain, although the faunal content is consistent with the other calcareous bone-biophospharenite samples (Cumbaa, pers. comm).

The bioclastic accumulations from two neighboring outcrop localities in the Wappaweka Hills (WAP1 and WAP2) are described by Langford (1973) who considered the shales to be Late Cretaceous in age.

3.2 Methods

Analyses began with macroscopic observations and photography of the raw samples. These observations included the bed shape; bed thickness; the sediment type above and below the bed; whether the bed contained interstratified mudrock laminae or rip-up clasts; and a description of bioclastic components, such as their shape and orientation; and grain size and sorting. Thin sections were prepared in order to make further observations on a microscopic scale including sedimentological features such as the shape of the bioclasts, their proportion within the accumulation, the degree of sediment packing, grain orientation, as well as taphonomic features such as the level of fragmentation of the bioclasts. Sedimentological analysis also included the search for impact criteria. Samples were examined for grains of shocked quartz or impact derived spherules, as well as important differences in textures. The information gathered through macroscopic and microscopic observations of the various bioclastic accumulations (Table 2) was used in order to form a classification scheme based on the investigated characteristics for these accumulations of bioclastic material.

Table 2: List of characters used to describe the bioclastic accumulations. Modified after Kidwell (1986), Kidwell and Holland (1991), and Williams (1995). The characters in bold were particularly important for the classification of bioclastic accumulations.

Sedimentological features	*Stratigraphic features*
Close-packing of vertebrate bioclasts: (dense/loose/dispersed)	**Thickness of the bed**
Percent volume of bioclasts	Scale relative to facies
Shape of vertebrate bioclasts: (platy/elongated/compact)	Laterally extensive (yes/no)
Size-sorting of vertebrate bioclasts: (well/bimodal/poor)	**Geometry of the bed**
Size of vertebrate bioclasts	Sharp basal contact (yes/no)
Type of matrix	Stratigraphic contacts (erosion surfaces/omission surfaces/etc.)
Size-sorting of matrix (well/bimodal/poor)	Internal complexity (simple/complex)
Size of matrix grains	Number of fining upwards sequences
Relative sizes and hydraulic equivalence of bioclasts and matrix grains	Position within depositional sequence
Orientation of bioclasts (in plan view and in cross-section)	***Paleoecologic features***
Associated physical and biogenic sedimentary structures	Number of species/groups/skeletal types
Weathered vs fresh surface	Relative abundance of species/groups/skeletal types
	Taxonomic composition
Taphonomic features	"Life habits" of the assemblage (marine/marginal marine)
	Paleoecological composition (auto/para/allochthonous)
Fragmentation /Breakage (low/moderate/high)	
Surface abrasion (low/moderate/high)	

4. RESULTS

4.1 Characterization of fossil concentrations

This section develops the classification of the bioclastic accumulations in addition to a brief interpretation of depositional environment. The reader is referred to the discussion for more detailed paleoenvirionmental analyses. The classification scheme of dominantly vertebrate-bioclast accumulations addressed here are modified after schemes presented by Kidwell (1986), Kidwell and Holland (1991), and Williams (1995) for shell beds. Macroscopic investigation of the bioclastic concentrations shows a range of characteristics. All of the fossil concentrations were encased in mudrock. Many of these

accumulations occur as lenses while some form sheet-like horizons with sharp upper and lower contacts. In addition, thin sections from all samples were analysed to better interpret these bonebeds and bioclastic accumulations and the diagenetic processes affecting them.

All the bioclastic accumulations are moderately to densely-packed. These bioclast-supported deposits have a variable orientation of elements from those that are randomly oriented to those showing an alignment of platy or elongated bioclasts. Bed thickness and geometry is also variable from thin (~ 1 cm) horizons to thick (up to 10 cm) discontinuous beds or lenses (up to 60 cm at the thickest point of some of the lenses) with simple to complex internal features. Most of the accumulations are ungraded, although a few fine upward. Mudrock interlaminae are common.

The bioclastic accumulations were split into four main categories: 1- inoceramites, 2- calcareous bone-biophospharenites, 3- non-calcareous bone-biophospharenites, and 4- glauconite-rich organic deposits, based on their bulk composition as well as several key characters. These characters include a) the proportion of vertebrate bioclasts present in the sample, from low (< 5%) to high (> 40%); b) whether bioclasts (both vertebrate and non-vertebrate) show a preferred orientation or are randomly oriented throughout the bed; c) the degree of packing of vertebrate bioclasts; d) the sorting of vertebrate bioclasts, from poorly sorted to well sorted or bimodal; and e) the dominant shape of the vertebrate bioclasts, whether elongated, platy, or compact. In addition, features of the beds such as their geometry (lenses or sheets), their thickness, and their lateral extent were considered (Table 2).

4.2 Category 1 - Inoceramites

The inoceramite category includes samples C7-2 and -3 from the Camp Seven River locality; VDV-1 and -2 from the Vandervoort Farm locality; and BR3-1, -2, -3, -4 from Bainbridge River locality #2. Inoceramites are made up of accumulations dominated by inoceramid-derived calcite prisms. They are technically calcarenites due to the abundance of calcareous material, but are termed *inoceramites* here because the calcite consists primarily of disaggregated remains of inoceramids (cf. Cobban and Scott, 1972). In addition to the predominance of inoceramid-derived calcite prisms, samples rarely contain partial inoceramid valves and varying proportions of oyster valves and phosphatic vertebrate bioclasts. Petrographic and sedimentological observations are summarized in Table 3.

Table 3: Summary of observed petrographic and sedimentological characteristics for category 1 (inoceramites) samples based on characteristics in Table 2.

1	Classification	Inoceramites							
	Characteristics	C7-2	C7-3	VDV-1	VDV-2	BR3-1	BR3-2	BR3-3	BR3-4
Sedimentological features	Inoceramite-derived calcite prisms	High > 40%							
	Vertebrate bioclasts	Low < 5%	Low < 5%	Low < 5%	Moderate ~10%	Moderate ~10%	Moderate ~10%	Low < 5%	Low < 5%
	Close-packing of vertebrate bioclasts	Loosely packed							
	Relative grain size (vertebrate bioclasts)	Small							
	Size-sorting of vertebrate bioclasts	Poor							
	Vertebrate bioclasts dominant shape	Elongated and platy		Platy and elongated		Elongated and compact			
	Mud layers	Absent	Present	Absent				Present	Absent
	Preferred orientation of bioclasts	Randomly oriented		Somewhat oriented	Randomly oriented	Randomly oriented	Randomly oriented	Somewhat oriented	Randomly oriented
	Fining upward trend	No							
Other components	Mud content	Low-Moderate	Moderate	Trace	Trace	Trace			
	Coprolites	Absent	Absent	Common	Rare	Rare			
	Oysters	Common	Common	Common	Rare	Abundant	Rare	Rare	Abundant
	Siliciclastic grains	Trace							
Taphonomic features	Fragmentation of vertebrate bioclasts	Minimal							
Other features	Geometry of the bed	Tapered	Tapered	Lens	Tapered	Sheet-like	Lens	Lens	Lens
	Bed thickness	~ 1 - 2 cm	~ 2 - 5 cm	~ 2 - 5 cm	~ 0.5 - 1 cm	~ 3 - 4 cm	~ 2 - 4 cm	~ 2 - 3 cm	~ 2 - 4 cm
Diagenetic features	Pyrite	Common							
	Compaction	Low							

4.2.1 Macroscopic description

Using the characters from Table 2, inoceramites are defined as accumulations dominated by inoceramid-derived calcite prisms with low to moderate percentages of phosphorous vertebrate-bioclast material. Inoceramite layers occur as relatively thick but discontinuous lenses or as tabular beds (Fig.6a). The vertebrate bioclasts, made up primarily of the teeth of sharks and bony fishes, are relatively well-sorted and are within a matrix of sand-sized inoceramid-derived calcite prisms and fragments. The abundance of oyster shell fragments is variable; some samples contain only very few (Fig.6b) while others contain an abundance of disarticulated and fragmented valves (Fig.6c). The valves do not show a preferred orientation within the bed. The abundance of coprolites is also variable; they are common in some samples and rare in others. Macroscopically, the inoceramites are massive with the exception of one sample, which contains alternating calcarenitic beds and fine mud laminae (Fig.6d).

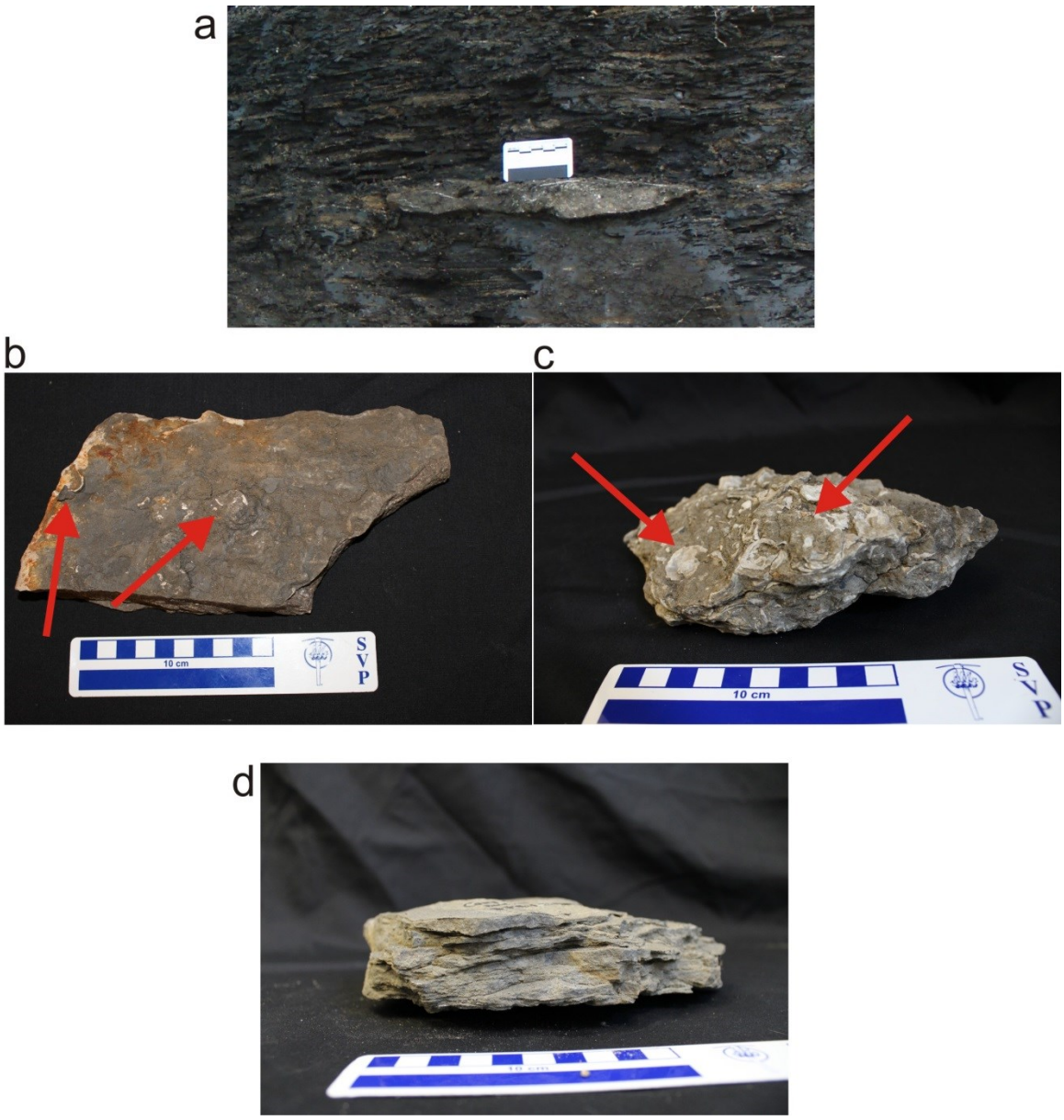

Figure 6: Macroscopic characteristics of category 1 (inoceramites) samples. **a)** *In situ* lens-shaped deposit with no visible internal sedimentary features at Bainbridge River locality #2 (BR3-2). **b)** Inoceramite containing few disarticulated oyster valves (BR3-2) indicated with arrows. **c)** Inoceramite containing abundant oyster valves forming the *Ostrea beloiti* bed (BR3-4). **d)** Inoceramite made up of several mudrock layers interbedded with the inoceramid-derived calcite prism-dominated layers (C7-3).

4.2.2 Petrographic description

Samples are dominated by calcite (80-90%), a large proportion of which consists of inoceramid fragments and inoceramid-derived calcite prisms with a sparry calcite cement (Fig.7a). The abundance of vertebrate bioclasts is variable: samples contain low (< 5%) to moderate (> 20%) proportions of dominantly elongated or platy elements and fewer compact elements. The vertebrate bioclasts are sand-sized (dominantly 1-2 mm in size), rarely fragmented and show only minor abrasion (cf. Phillips, 2008). Siliciclastic grains are very rare and generally only trace amounts of argillaceous material are present (Fig.7b). Pyrite euhedra and framboids are common. Significantly pyritized grains are rare.

Although samples appear massive to the naked eye, in thin section the bioclasts are commonly concentrated along indistinct laminae (Fig. 7c). The laminae are sometimes inclined (VDV-1), as though the sample was cross-laminated (Fig. 7d), or possibly as if discrete planes were present within the lens (BR3-3) that ran nearly parallel to the lens's surface (figs 6e). Bioclasts are also commonly concentrated under oyster valves. The inoceramite samples are described individually below.

C7-2 and C7-3: Sample C7-2 consists mostly of calcite (> 80%), and contains a relatively small proportion of phosphatic vertebrate bioclasts (< 10%). The bioclasts are mainly elongated and platy. The bed contains a moderate amount of mud disseminated through the matrix and abundant oysters. Sample C7-3 also consists mostly of calcite (> 80%), though it contains fewer phosphatic vertebrate bioclasts (< 5%). The bioclasts are mainly elongated and platy fragments. This bed, unlike the other inoceramite samples,

contains several thin (1-2 mm) mudrock laminae that in turn contain rare partial inoceramid valves (Fig. 7f). Pyrite is relatively common in both samples from this locality and occurs most frequently within grains of the inoceramid-derived prismatic calcite (Fig.7g).

BR3-1, -2, -3 and -4: These samples are very similar to one another. They consist mostly of calcite (> 80%). There are moderate proportions of vertebrate bioclasts in BR3-1 and BR3-4 (> 20%) and abundant oysters, while BR3-2 and BR3-3 contain fewer oysters and a lower proportion of vertebrate bioclasts (< 5%). Bioclasts are elongated. A small number of compact elements are present in BR3-1 and BR3-4. Pyrite is relatively common in the samples and occurs most frequently within grains of the prismatic calcite and sometimes in the intragranular pore spaces of phosphatic clasts (Fig.7h).

VDV-1 and VDV-2: These samples also closely resemble each other petrographically. The samples are dominated by calcite (> 80%) with a low proportion of phosphatic bioclasts (< 10%). The bioclasts include mainly platy and elongated elements, with fairly common compact elements and rare coprolite. In VDV-1, the bioclasts are commonly concentrated along low angle cross lamination planes (Fig. 7d) while in VDV-2 they show no preferred orientation. Pyrite is relatively common in the samples and occurs most frequently within grains of the prismatic calcite and less commonly in the intragranular pore spaces of phosphatic clasts.


a
I
b
O
A
V
c
d
O
V
e
V
f
M
I
g
I
P
h
P
1 mm

Figure 7: Category 1 (inoceramites) specimen in thin section. **a)** "Articulated" portion of inoceramid shell (I) and fragmented inoceramid-derived prisms in a sparry calcite cement in sample BR3-1. **b)** Argillaceous material (A) and a phosphatic vertebrate bioclast (V) sheltered under an oyster valve (O) in sample BR3-1. **c)** Random orientation of bioclasts (inoceramid-derived calcite prisms). Arrows indicate the random orientation in sample VDV-2. **d)** Oyster fragment (O) and rounded phosphatic vertebrate bioclasts (V) concentrated along low angle cross-lamination planes, indicated by the arrow, in sample VDV-1. **e)** Phosphatic vertebrate bioclasts (V) concentrated and aligned along a plane that nearly parallels the bed surface in sample BR3-2. Inoceramid-derived calcite prisms also appear aligned in the same direction. **f)** Articulated portion of an inoceramid valve (I) in sample C7-3 below a mudrock layer (M). **g)** Pyrite (P): the black material indicated by the arrow, associated with the inoceramid-derived calcite prism to the right of the "articulated" fragment of inoceramid (I). **h)** Pyrite (P): the black material indicated by the arrow within the pore space of the vertebra in the center of the image.

4.2.3 Depositional environment

The internal structure of the inoceramites, with the occasional concentration and alignment of bioclasts, and the abrasion and hydraulic sorting profiles from the Van der Voort locality (Phillips, 2008) indicate physical transport and reworking of the bioclasts possibly by storms affecting the eastern margin of the WIS. The analyzed inoceramites are interpreted to represent a sediment-starved, distal paleoenvironment (Speyer and Brett, 1991) where bioclastic material was concentrated in deeper waters just above or at storm wave base and distant from the shoreline.

4.3 Category 2 - Calcareous bone-biophospharenites

This category includes samples BR1-1 from Bainbridge River locality #1; BR3-5, -6, and -7 from Bainbridge River locality #2; C7-1 from the Camp Seven River locality; DH1-1, and -2 from Carrot River locality #1; and DH3-1 from Carrot River locality #2. Calcareous bone-biophospharenites are made up of accumulations dominated by phosphatic vertebrate-fossil material (>50%) with variable abundance of inoceramid-derived calcite prisms. Due to variability in sedimentological and taphonomic characteristics, the calcareous bone-biophospharenites are split into three subgroups: A) thin deposits interbedded with mudrock, B) thick and commonly lens-shaped deposits, and C) deposits contained within an inoceramid shell. Petrographic and sedimentological observations are summarized in Table 4.

Table 4: Summary of characteristics for category 2: calcareous bone-biophospharenite samples based on characteristics in Table 2.

2	Classification	Calcareous bone-biophospherenites							
	Sub-group	A			B				C
	Characteristics	BR3-5	BR3-6	C7-1	BR3-7	DH1-1	DH1-2	BR1-1	DH3-1
Sedimentological features	Inoceramite-derived calcite prisms	Low < 5%			Low < 5%	Trace	Trace	Trace	Trace
	Vertebrate bioclasts	High > 50%			High > 50%				Moderate-high ~30%
	Close-packing of vertebrate bioclasts	Moderate-dense			Moderate-dense	Dense		Dense	Loose-moderate
	Relative grain size (vertebrate bioclasts)	Small			Large	Small (with large grains)		Small	Medium
	Size-sorting of vertebrate bioclasts	Poor			Moderate	Moderate		Well	Moderate
	Vertebrate bioclasts dominant shape	Elongated			Elongated and compact	Elongated		Elongated	Elongated
	Mud layers	Present			Present				Absent
	Preferred orientation of bioclasts	Randomly oriented			Randomly oriented	Somewhat imbricated		Somewhat imbricated	Somewhat aligned
	Fining upward trend	No			Yes				No
Other components	Mud content	Trace			Low to Moderate				Moderate
	Coprolites	Rare			Abundant	Rare to Absent		Rare	Common to rare
	Oysters	Absent			Absent	Absent		Absent	Abundant
	Siliciclastic grains	Trace			Trace	Absent		Trace	Trace
Taphonomic features	Fragmentation of vertebrate bioclasts	Moderate			Minimal	Moderate		Moderate	Moderate
Other features	Geometry of the bed	Tapered	Wave-like Tapered	Tapered	Lens	Lens		Tapered	Lens
	Bed thickness	~ 0.5 - 1 cm	~ 0.5 - 1 cm	~ 0.5 - 1 cm	~ 5 - 20 cm	~ 2 - 4 cm		~ 6 - 10 cm	~ 4 - 10 cm
Diagenetic features	Pyrite	Common			Common	Abundant		Common-Abundant	Abundant
	Compaction	High			Very low	Moderate		Moderate	Moderate

4.3.1 Macroscopic description – subgroup A

Subgroup A consists of sample C7-1 from Camp Seven River locality and samples BR3-5, and -6 from Bainbridge River locality #2. These samples are thin, discontinuous but densely-packed accumulations. Vertebrate bioclasts make up over half of the samples. They are small and are poorly sorted overall, and include fish vertebrae, shark teeth, and various other unidentifiable vertebrate bone fragments. The bioclasts do not appear to have a preferred orientation. Sand-sized prismatic calcite crystals are common and coprolites are common to rare. Most samples are thin (~ 1 cm), contain thin (~ 2 mm) shale interlaminae, and drape the underlying strata (e.g. BR3-6 has a wave-rippled shape (Fig. 8a)).

4.3.2 Petrographic description – subgroup A

The samples contain an abundance of densely-packed (> 50%) vertebrate bioclasts with a sparry calcite cement. Bioclasts are dominated by elongated elements with variable proportions of compact elements and few platy elements. They lack preferred orientation (Fig. 8b) and are highly fragmented (Fig. 8c). Inoceramid-derived calcite prisms are common throughout the samples but appear to be concentrated in indistinct layers (Fig. 7d). Like the inoceramites, siliciclastic grains are very rare and mud content is low. However, pyrite is common. Samples belonging to this subgroup are described individually below.

C7-1: The sample is dominated by phosphatic bioclasts (> 50%), most of which are elongate... The bed is classifiable as a grainstone to rudstone cemented by sparry calcite crystals. Linear contacts between grains are common. Fragmented vertebrate elements are

also common (Fig.8c). Inoceramid-derived calcite prisms are common (Fig.8d) and pyrite is fairly abundant within the intragranular pore spaces of phosphatic clasts.

BR3-5 and BR3-6: Samples BR3-5 and BR3-6 are dominated by phosphatic bioclasts (> 50%), most of which are elongate. These beds are also classifiable as grainstones to rudstones cemented by sparry calcite crystals. Linear contacts between grains are common as are fragmented vertebrate elements. Inoceramid-derived calcite prisms are not as abundant as in C7-1, but a partial inoceramid valve forms the top of BR3-6 (Fig.8e) Pyrite is fairly abundant in the intragranular pore spaces of phosphatic clasts as well.

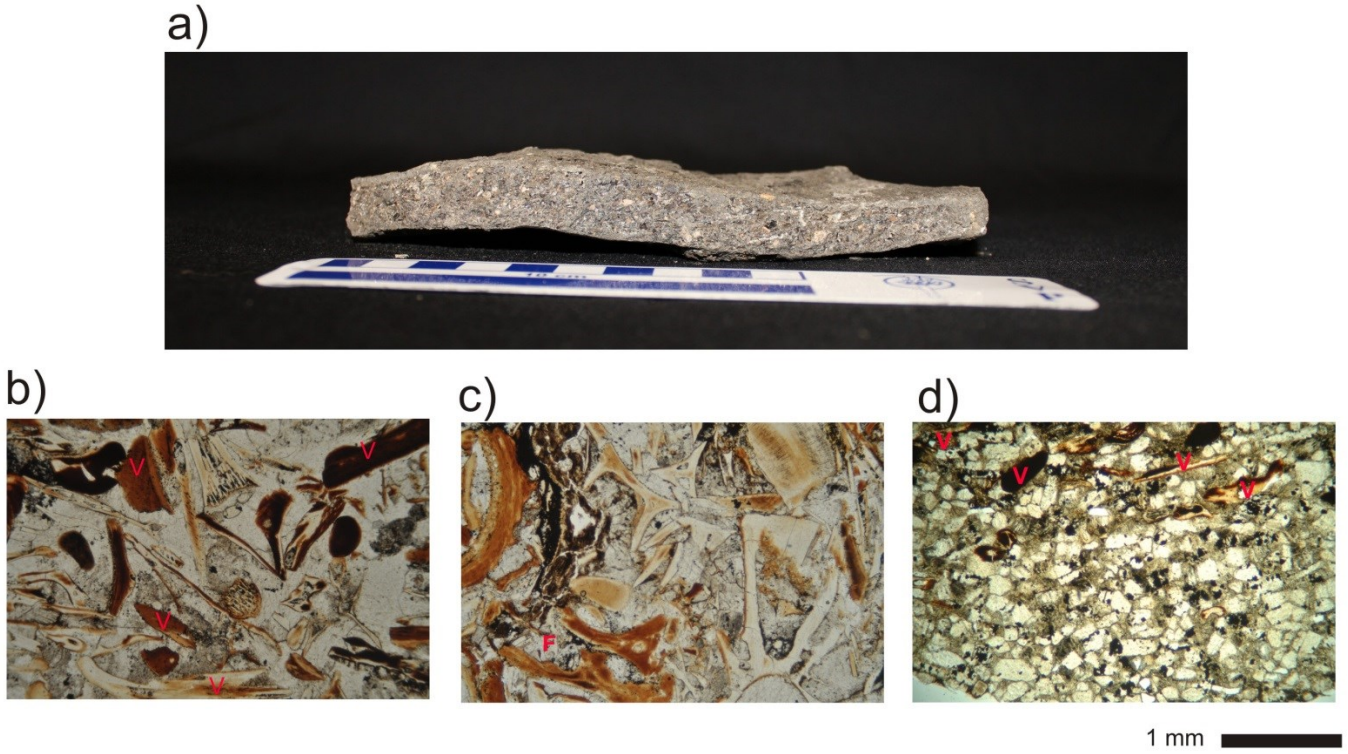

Figure 8: Characteristics of subgroup A of the calcareous bone-biophospherenites (category 2). **a)** Wave-rippled shape of a bone-biophospharenite (BR3-6). **b)** Vertebrate bioclasts (V) are moderately-packed and show no preferred orientation, (BR3-6). **c)** Vertebrate bioclasts are highly fragmented (F). (BR3-5). **d)** Inoceramid-derived prisms occur throughout the deposits but are often concentrated into layers, here below the vertebrate bioclasts (V) (C7-1).

4.3.3 Depositional environment – subgroup A

The thin interbedded calcareous bone-biophospharenites analysed here are interpreted to represent a shallow sediment-starved paleoenvironment proximal to the shoreline and near or at fair weather wave base. Waves concentrated these densely-packed deposits and the multiple interlaminae of mudrock represent episodic sedimentation events.

4.3.4 Macroscopic description – subgroup B

Subgroup B includes samples BR1-1 from Bainbridge River locality #1, BR3-7 from Bainbridge River locality #2, and DH1-1 and -2 from Carrot River locality #1. Sedimentological and taphonomic characteristics of samples in this subgroup are extremely varied. The bioclastic accumulations are thick and discontinuous, often lens-shaped, and bounded by mudrock (Fig. 9a and b). Concentrations are of moderately to densely-packed vertebrate bioclasts in sparry calcite cement. The vertebrate bioclasts are larger on average (many larger than 3 mm) than those in subgroup A and show varying degrees of alignment. Sorting of vertebrate bioclasts is poor to moderate, and bioclasts are dominantly compact or elongated in shape. Beds contain thin mudrock laminae (Fig. 9b) and also locally fine upward (Fig. 9c).

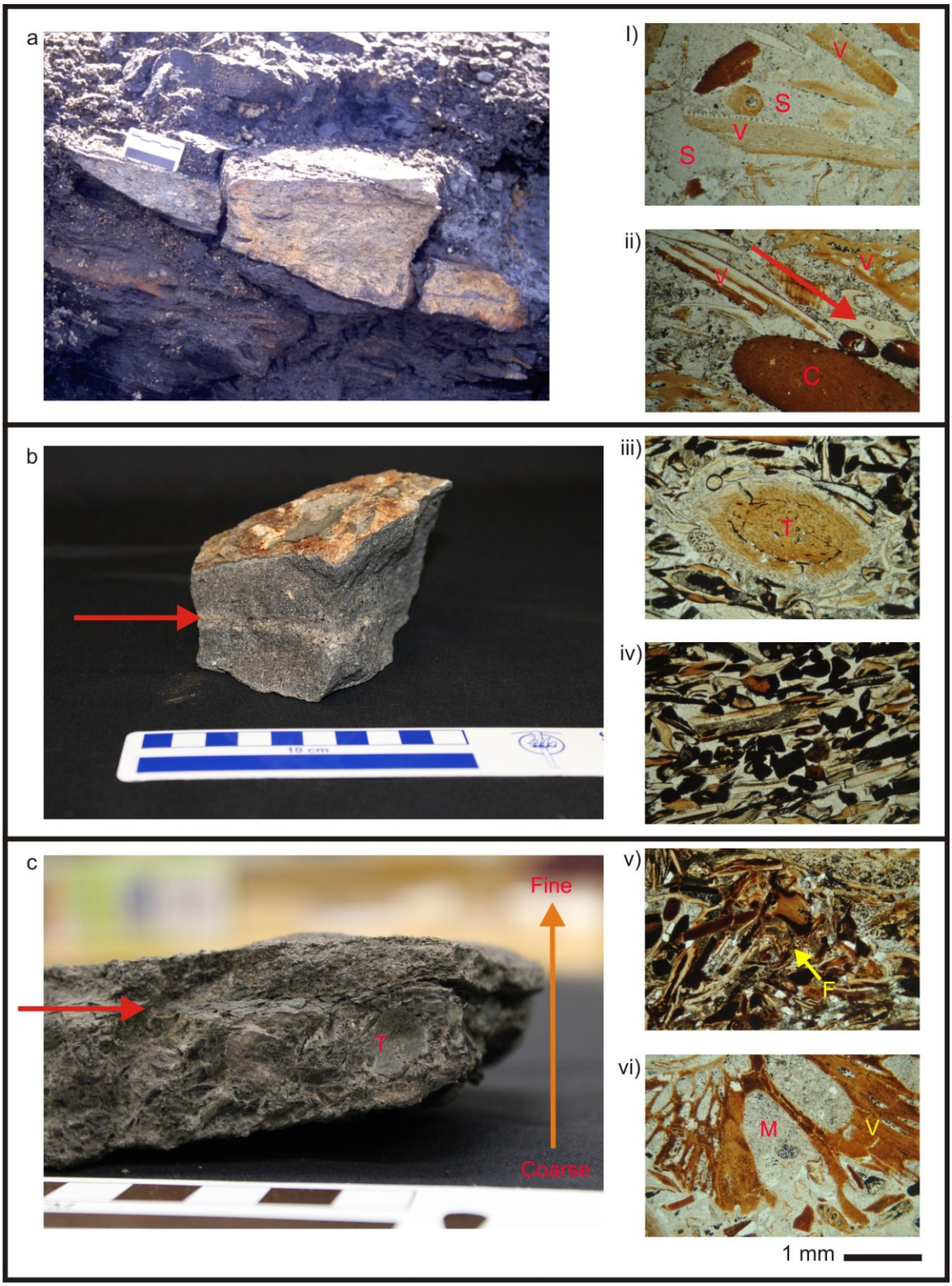
a
i)
V
S
V
S
ii)
V
V
C
b
iii)
T
iv)
c
Fine
T
Coarse
v)
F
vi)
M
V
1 mm

Figure 9: Characteristics of subgroup B of the calcareous bone-biophospharenites (category 2). **a)** *In situ* lens (BR3-7) bounded by mudrock. ***i)*** Vertebrate bioclasts (V) within this accumulation are largely supported by the sparry calcite cement. (S); ***ii)*** Larger, elongated vertebrate bioclasts (V) as well as coprolites (C) are often slightly aligned near-parallel to the surface of the bed, as indicated by the arrow. **B)** Mudrock lamina, indicated by the arrow, in a bioclastic accumulation (BR1-1). ***iii)*** Bioclasts are often fragmented; note the increased compression crushing the tooth (T). ***iv)*** Bioclasts are imbricated; note the increase in linear grain contacts. **C)** Locally, these beds show a fining upward trend; note the large tooth (T) below the mudrock interbed, indicated by the arrow (DH1-2). ***v)*** Bioclasts are slightly imbricated; note the abundant linear grain contacts, increased compaction, and frequent splintered grains (F). ***vi)*** Although mostly calcite-cemented, localized micritic (M) cement is rarely present within the vertebrate bioclasts (V).

4.3.5 Petrographic description – subgroup B

Although they are superficially similar, the samples in this subgroup are petrographically different from one another.

BR3-7: This sample appears moderately sorted, with grain sizes typically ranging from 1-3 mm (the largest average grain size of any of the samples examined). The uppermost 2 cm of the bed fines upward. It contains gutter casts at its base, several thin mudrock laminae, rip-up clasts composed of bentonitic material with recrystallized rims, and abundant undeformed coprolites. Phosphatic vertebrate bioclasts are generally supported by the calcitic cement (Fig.9a *i*), and include platy, elongated, and abundant rounded and compact fish bones, bony fish teeth and shark teeth, as well as abundant coprolites. Elongated vertebrate bioclasts show a slight alignment (Fig.9a *ii*). A few bones of terrestrial organisms, an enantiornithine bird and one or more lizards, have been found in

other bioclastic samples from the same discontinuous bioclastic layer (Cumbaa *et al.,* 2006; Phillips, 2008; Cumbaa *et al.,* 2013). Preservation of clasts is varied, with many fragmented bioclasts showing moderate levels of abrasion (Phillips, 2008). Inoceramid-derived prismatic calcite is relatively rare. Argillaceous material and siliciclastic grains are rare to absent. Pyrite was commonly observed and occurs primarily in and around coprolites and inoceramid-derived prismatic calcite crystals.

BR1-1: A second bone-biophospharenite occurs along the Bainbridge River at locality BR1. Compared to BR3-7, the sample is well sorted, with grain sizes ranging from approximately 0.3 to 1 mm in length. Linear contacts between grains are more common here than in BR3-7; broken grains are common (Fig. 9b *iii*); and vertebrate bioclasts are slightly imbricated (Fig. 9b *iv*). Relative to locality BR3-7, BR1-1 contains a higher concentration of phosphatic bioclasts and less calcite cement. Phosphatic bioclasts are predominantly elongated, with occasional platy or compact clasts, and consist largely of bone and tooth fragments with only rare coprolites. This uppermost 3 cm of the bed fines upward. Inoceramid-derived prismatic calcite is rare to absent. Pyrite is more common here than in all but the Carrot River (DH1) samples, and occurs predominantly within porous phosphatic bioclasts.

DH1-1 and DH1-2: These Carrot River samples are also dominated by elongated phosphatic debris, primarily fish bones and teeth. The phosphatic debris is more concentrated than in other samples within this subgroup (accounting for > 60%). A small number of terrestrial vertebrate bones, including those of a dinosaur and an enantiornithine bird, have been found in other bioclastic samples from this discontinuous layer (Cumbaa *et al.,* 2006). The sample is moderately sorted and slightly imbricated

(Fig.9c *v*), with an average grain size of <1mm, but with occasional large grains (2-4 cm), which appear to be oriented in the same direction. These samples contain very few coprolites, and linear contacts between bioclasts are common, as are broken grains. Pyrite is more abundant in these samples than in any other. Pyrite is present within pore spaces of phosphatic grains, and partially pyritized phosphatic grains are common. In addition, many of the larger grains and teeth have a blue rim, which is interpreted as vivianite. In contrast to the sparry calcite cement seen elsewhere in the sample, some of the larger bioclasts seem to contain calcareous cement that appears more micritic (Fig. 9c *vi*).

4.3.6 Depositional environment – subgroup B

The thick, often lens shaped calcareous bone-biophospharenites of subgroup B are interpreted as representing a shallow water paleoenvironment. Their position is believed to be near fairweather wave-base, however, energy conditions concentrating the bioclastic components might have varied.

4.3.7 Macroscopic description – subgroup C

Sample DH3-1, from Carrot River locality #2, is placed in its own subgroup because it is made up of poorly-sorted vertebrate bioclastic material and disarticulated oyster valves contained within the articulated valves of an intact inoceramid shell above a layer of shale (Fig. 10a). Macroscopically, the accumulation appears massive. Overall, the vertebrate bioclasts do not appear to be preferentially oriented and this accumulation contains no distinct mudrock interlaminae like those seen in all samples from subgroup A and B, although it has higher dispersed mud content throughout.

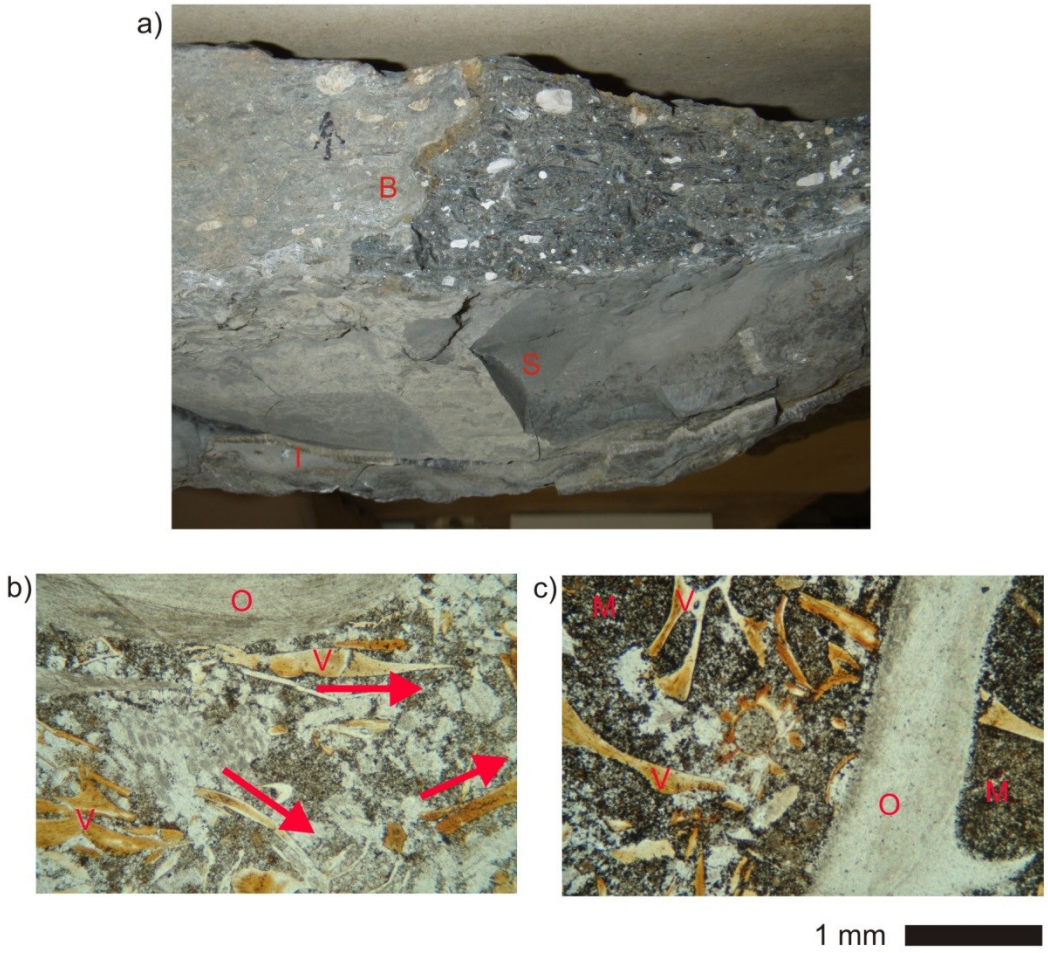

Figure 10: Characteristics of subgroup C (DH3-1) of the calcareous bone-biophospharenites (category 2). A) View of the base of this bioclastic accumulation showing thickened hinge of the inoceramid (I), as well as shale (S) and the overlying bioclastic accumulation (B). B) Vertebrate bioclasts (V) and fragmented oyster valves (O) do not show a preferred orientation within the calcareous matrix, as indicated by arrows. C) Portions of the bioclastic accumulation contain increased mud content (M).

4.3.8 Petrographic description – subgroup C

The DH3-1 bonebed is contained within an intact inoceramid shell and is made up of phosphatic vertebrate bioclastic elements and oyster valves within a sparry calcite

cement. Phosphatic elements are mostly elongated but platy and compact elements are still fairly common but they do not appear to be preferentially oriented (Fig. 10b). Inoceramid-derived calcite prisms are rare and the mud content is fairly high (Fig. 10c). Pyrite is fairly common within the intragranular pore spaces of phosphatic clasts in this sample.

4.3.9 Depositional environment – subgroup C

This subgroup represents deposition in a microenvironment within the valves of an empty, but articulated inoceramid shell that is encrusted with oysters attesting to a low sedimentation rate. This microenvironment provided shelter for the contents of the valves, preserved the higher mud content, and protected the bioclasts from being remobilized and sorted.

4.4 Category 3 - Non-calcareous bone-biophospharenites

This category is represented by a single sample, WAP1-1, from Wapawekka Hills locality #1.Phosphatic bioclastic material is abundant, though it is non-calcareous. Petrographic and sedimentological observations are summarized in Table 5.

Table 5: Summary of observed petrographic and sedimentological characteristics for category 3: the non-calcareous bone-biophospharenite based on characteristics in Table 2.

3	Classification	Non-calcareous bone-biophospherenite
	Characteristics	WAP1-1
Sedimentological features	Inoceramite-derived calcite prisms	Absent
	Vertebrate bioclasts	High > 50%
	Close-packing of vertebrate bioclasts	Dense
	Relative grain size (vertebrate bioclasts)	Medium
	Size-sorting of vertebrate bioclasts	Well
	Vertebrate bioclasts dominant shape	Elongated
	Mud layers	N/A
	Preferred orientation of bioclasts	Imbricated
	Fining upward trend	No
Other components	Mud content	High
	Coprolites	Absent
	Oysters	Absent
	Siliciclastic grains	Absent
Taphonomic features	Fragmentation of vertebrate bioclasts	High (splintered)
Other features	Geometry of the bed	Tapered
	Bed thickness	~ 4 - 6 cm
Diagenetic features	Pyrite	Rare
	Compaction	Very high

4.4.1 Macroscopic and petrographic description

WAP1-1 has an even higher abundance of bioclasts (> 75%) than the calcareous bone-biophospharenites and the bioclasts are very densely-packed within a brown clastic (non-calcareous) mud matrix with common pebble sized mud clasts (Fig. 11a). Bioclasts are densely packed and composed entirely of elongated elements. Vertebrate bioclasts are too fragmented to identify and appear splintered (Fig. 11b). Texturally this bed could be classified as a bone-bioconglomerate. It lacks inoceramid-derived prisms, oyster, coprolites, and quartz grains. Pyrite is rare. The sample shows no distinguishable internal features such as bedding, but is fissile and has abundant fractures (Fig. 11c). The fissile and cracked appearance of this bed, and the intensely splintered vertebrate bioclasts it contains, is anomalous. It appears to have been altered, possibly by exposure to high heat early in its diagenesis.

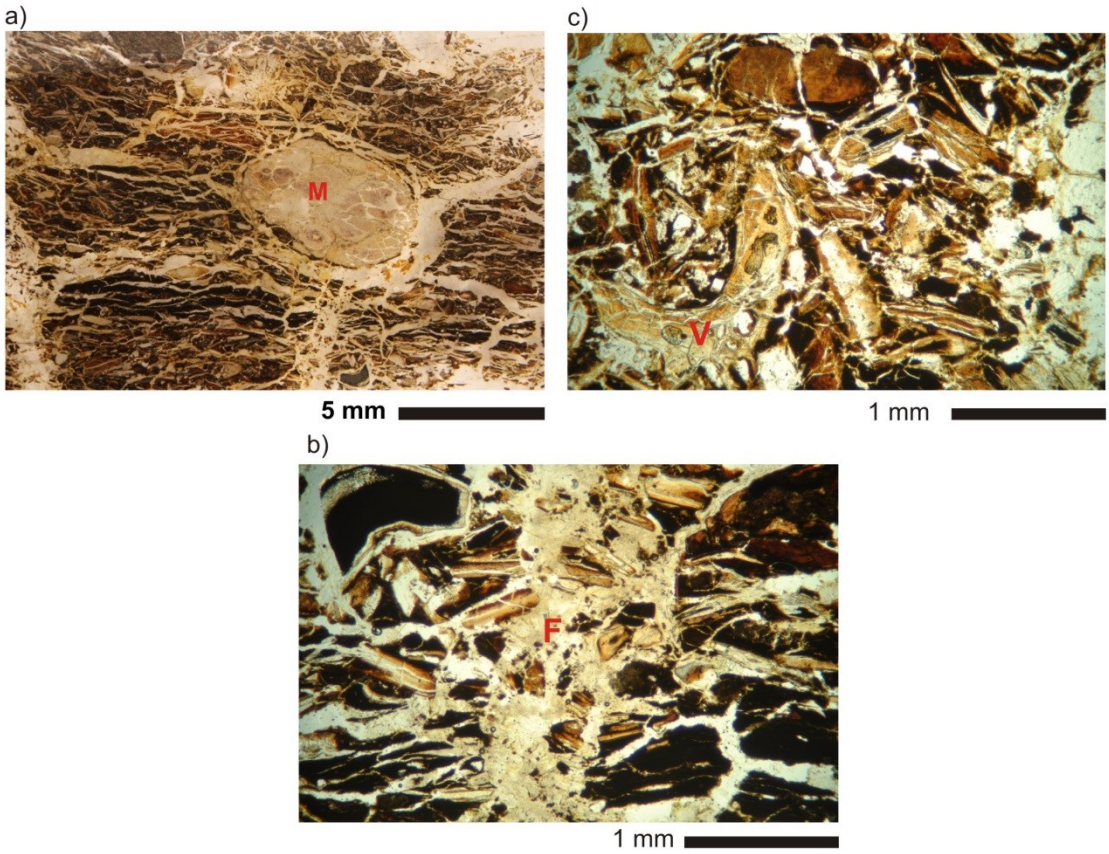

Figure 11: Characteristics of category 3: non-calcareous bone-biophospharenite (WAP1-1). A) Thin section showing a mud clast (M) and densely-packed bioclastic material in a fractured muddy matrix. B) Recognisable vertebrate bioclasts (V) are rare as the bioclasts are extensively fragmented and appear intensely splintered. C) The accumulation contains relatively large fractures (F) throughout and appears to have undergone some alteration.

4.4.2 Depositional environment

This non-calcareous bone-biophospharenite represents a distal environment where the influence from currents is minimal and the deposit was quickly buried below the sulfate reduction zone. The initial mechanism for the deposition of the abundance of phosphatic vertebrate bioclasts is still uncertain but may be event-related.

4.5 Category 4 - Glauconite-rich organic deposit

This category is also represented by a single sample WAP2-1 from Wapawekka Hills locality #2. It contains few bioclasts but abundant mud and organic material, and is classified as an organic-rich deposit. Petrographic and sedimentological observations are summarized in Table 6.

Table 6: Summary of observed petrographic and sedimentological characteristics for category 4: the glauconite-rich organic deposit based on characteristics in Table 2.

4	Classification	Glauconite-rich organic deposit
	Characteristics	WAP2-1
Sedimentological features	Inoceramite-derived calcite prisms	Absent
	Vertebrate bioclasts	Low < 5%
	Close-packing of vertebrate bioclasts	Loose
	Relative grain size (vertebrate bioclasts)	Medium
	Size-sorting of vertebrate bioclasts	Well
	Vertebrate bioclasts dominant shape	Platy
	Mud layers	N/A
	Preferred orientation of bioclasts	Fish scales oriented parallel to bed surface
	Fining upward trend	No
Other components	Mud content	High
	Coprolites	Absent
	Oysters	Absent
	Siliciclastic grains	Absent
Taphonomic features	Fragmentation of vertebrate bioclasts	Very low
Other features	Geometry of the bed	Sheet-like
	Bed thickness	~ 4 cm
Diagenetic features	Pyrite content	Common
	Compaction	Very low

4.5.1 Macroscopic and petrographic description

WAP2-1 is a thick sheet-like horizon containing very few bioclasts (< 5%). It is included here because the sample has an abundance of fish scales on the bottom and top surface of the bed (Fig. 12a). The bed is made up of calcareous mudrock and contains several indistinct bedding planes near parallel to the bed surface. The fish scales within this accumulation are oriented horizontal to the bed surface (Fig. 12b). This bioclastic accumulation contains abundant organic material, pyrite, glauconite (Fig. 12c), and a few planktic foraminifera (Fig.12d), but no inoceramid-derived calcite prisms or coprolites. The presence of rare planktic foraminifera in this sample attests to a higher stratigraphic position, and younger age, when compared to all other samples. In this northern locality planktic foraminifera would have only arrived near the Cenomanian–Turonian boundary. A persistent bioclastic layer was observed at the base of the Second White Specks Formation in cores across the prairies (Schröder-Adams *et al.,* 1996). This WAP2-1 sample might be a time equivalent occurrence to that horizon.

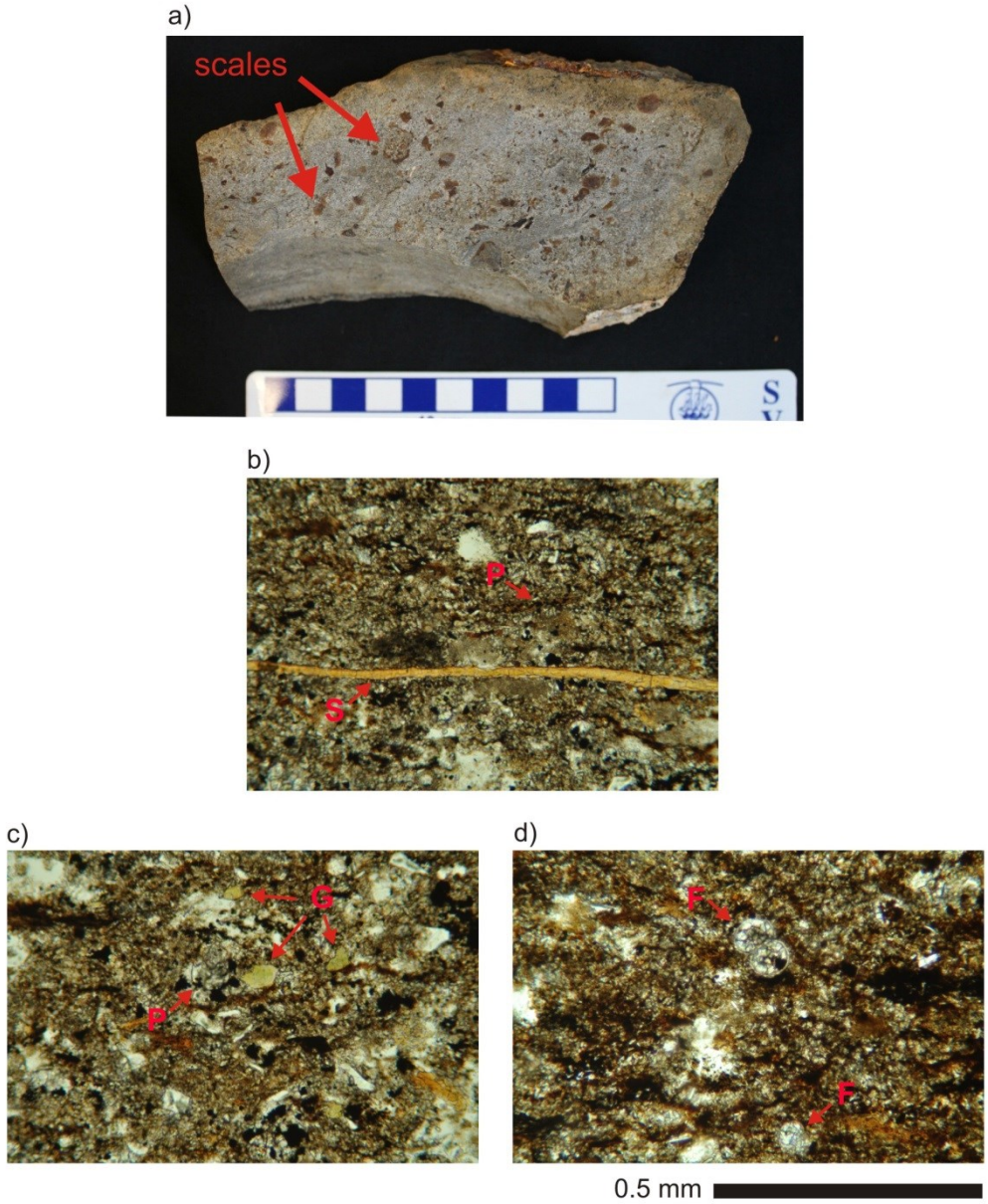

Figure 12: Characteristics of category 4: glauconite-rich organic deposits (WAP2-1). A) Top surface of the accumulation is marked by an abundance of plate-shaped fish scales lying flat (horizontal) to the bedding plane. B) Plate-like scales (S) within the bed are positioned horizontal to the bedding plane within an organic-rich matrix with abundant pyrite (P). C) Glauconite (G) and pyrite (P) are abundant throughout the bed. D) The bed also contains few planktic foraminifera (F).

4.5.2 Depositional environment

This glauconite-rich organic deposit has been interpreted to represent an accumulation of organic debris raining down into relatively deep water over a long period of time below storm wave base. The components of this bed were not reworked by currents or waves. This bed contains abundant pyrite, a low oxygen indicator, and glauconite, an indicator for prolonged hiatus in siliciclastic sedimentation (Canfield and Raiswell, 1991).

5. DISCUSSION

Bioclastic accumulations in the fossil record tend to form because of biogenic processes, sedimentologic (hydraulic) processes, diagenetic processes, or some combination thereof (Kidwell et al., 1986). All of the vertebrate-rich bonebeds described herein, except for category 4 (the glauconite-rich organic deposit) are interpreted to behydraulically concentrated allochthonous bioclast accumulations.

5.1 Duration of accumulation

Several lines of evidence point toward a relatively long period of deposition for most bioclastic accumulations discussed here. Time-averaging was defined as "the mixing of skeletal elements of non-contemporaneous populations or communities" by Walker and Bambach (1971). Determining whether the studied deposits are time-averaged is difficult, due to the lack of precise biostratigraphic ranges for each component within the beds, however the mixture of species from non-contiguous habitats within some of the beds (Phillips, 2008; Cumbaa *et al.,* 2013) suggests a certain time span for accumulations of those deposits. Evidence of abrasion, fragmentation, disarticulation, and sorting by shape and size are also considered to be "sensitive indicators" of time-averaging as well as

sedimentological features which record erosion, transport, and/or low rates of sedimentation (Fürsich and Aberhan, 1990). The elevated levels of fragmentation (breakage) and sorting of the bioclasts similarly indicate a relatively long period of accumulation in a sediment-starved marine environment (cf. Fürsich and Aberhan, 1990). However, the sedimentary record of these accumulations is a combination of background and episodic (event) effects, each overprinted by the other (Speyer and Brett, 1991). The taphonomic attributes created by these background and episodic processes can be correlated to environmental conditions during accumulation. Background taphonomic processes include all preservational processes that operate over long intervals and are mediated by 1) the rate of burial of the bioclast; 2) the environmental energy; and 3) amount of bioturbation (Speyer and Brett, 1991). The rate of burial is the most important factor as it controls the impact of mechanical processes such as sorting, reorientation, fragmentation, and abrasion. Episodic taphonomic processes are sedimentary events that interrupt background processes and operate in short but catastrophic time intervals. These can often superficially resemble background taphonomic effects. Background processes affect the preservation of event-stratified deposits and vice versa, creating an inherently complex taphonomic history (Speyer and Brett, 1991).

Speyer and Brett (1991) describe seven taphofacies models describing the background and episodic taphonomic signatures of different settings. Although these models were created for shell beds, many of the taphonomic signatures can also be seen in dominantly vertebrate-bioclast dominated accumulations as they reflect changes in the amount of time bioclastic grains spent at/near the sediment-water interface, the frequency of

episodic burial or events, and the intensity of current reworking. Taphofacies models described by Speyer and Brett (1991) can be seen in Table 7.

Table 7: Taphofacies models defined by Speyer and Brett (1991) to define shell beds.

Taphofacies model		General features	Background features	Episodic features	Environment
I	Nearshore amalgamated shell beds	• Thick tabular beds • Scour and fill • Shaley partings	• High abrasion • High fragmentation • Hydrodynamically stable orientation of shells and bioclasts **(High level of current winnowing)**	• Completely articulated specimens (echinoderms, trilobites, etc.) • Clasts exhumed from broken hardgrounds **(higher energy event)**	Shallow, proximal setting with variable sedimentation rate and high current energy
II	Current winnowed shell beds	• Thin bedded deposits interbedded with sparsely fossiliferous mudrock • Densely packed • Diverse assemblage	• High abrasion(less than model I) • Variable preservation • Orientation of shells (convex-side up) • Large skeletal components (corals) can be in life position **(Sedimentary shell lag - frequent winnowing of sediments –bypass)**	• Complete crinoids and trilobites on upper surface • Rapid, permanent burial of upper surface **(storm currents)**	Proximal setting with moderate sedimentation rate and relatively high current energy
III	Bioturbated deposits with shelly patches	• Burrow homogenized • Sparsely fossiliferous mud • Patchy "microbioherms"	• Random orientation of shelly debris • Low fragmentation • Shelly debris lags act as substrate for colonization (ex: brachiopods) and impede bioturbators **(Bioturbation is the dominant factor affecting taphononomy)**	• Event-related deposition of winnowed shell layers • Minor events obscured by bioturbation • Thin mud pulses disrupt the growth of colonies **(storms and pulses of fine grained sediment deposition)**	Proximal setting with high sedimentation rate and relatively high current energy
IV-A	Sediment-starved shell beds (proximal)	• Discrete concentrations • Traceable for kilometers	• Disarticulated • Low/no fragmentation • Low/no abrasion • Variable preservation of bioclasts, from poor at base to well preserved near the top of the accumulation **(relative stability with bioclasts exposed for long periods)**	• Well preserved specimen associated with a layer of barren mudrock **(sedimentary events e.g. suspension cloud fallout)**	Proximal setting with low sedimentation rate and relatively high current energy
IV-B	Sediment-starved shell beds (distal)	• Laterally discontinuous patches • Traceable along horizons within one outcrop	• Disarticulated specimen (can be in relict position) • Variable preservation • Low diversity • Shells can be strongly affected by dissolution • Low/no fragmentation **(function of biogenic productivity and duration of accumulation)**	• Top surface buried below mud blanket **(short-duration pulses of fine grained sediments)**	Distal setting (strongly biogenic deposits) with low sedimentation rate, and relatively low current energy
V	Dysaerobic mud-supported shell beds	• Diffusely fossiliferous accumulations	• Low diversity • Early pyritization • High levels of articulation • Low fragmentation and abrasion • No preferred orientation • Common bioturbation **(gradual undisturbed accumulation)**	• Poorly defined layers with and increased abundance of fossil remains (trilobites, blastoids, brachiopods, etc.) **(Event beds are indistinct)**	Distal setting with high sedimentation rate, relatively low current energy, and low oxygen
VI	Exaerobic sediment-starved shell beds	• Low sedimentation • Discrete bedding planes in barren shales • Discontinuity surfaces	• High disarticulation • High fragmentation • Poor preservation • Highly compressed fossil assemblages • Weak preferred alignment • Discontinuity surfaces: accumulated lags of well-preserved chemically resistant (e.g. phosphate impregnated) hard parts **(prolonged surface exposure)**	• Rare occurrences of articulated specimens associated with pulses of burying sediment • Layers within shale **(sedimentary events e.g. storms or debris flows)**	Distal setting with low sedimentation rate, low current energy, and low oxygen
VII	Dysaerobic sediment-dominated shell beds ("barren shales")	• Thick sequences of nearly barren shale, depleted in organic matter	• Scarce and scattered fossils • Poor preservation • Random orientation **(rapid deposition)**	• Very little taphonomic evidence for episodic deposition • Few scattered shell-rich bedding planes • Few complete specimen **(Short-term winnowing events or burial events)**	Distal setting with high sedimentation rate, low current energy, and low oxygen

Inoceramites can be considered "shell beds" as they are dominated by inoceramid-derived calcite prisms and commonly contain abundant oysters in addition to a variable proportion of vertebrate bioclasts. Many of the accumulations in this category occur in laterally discontinuous lenses. The inoceramid shells which dominate these accumulations disaggregate passively, in absence of predation, scavengers, or secondary mineralization, as the organic matrix binding the prisms decays, reducing shell strength (MacLeod and Orr, 1993). Bioclasts in the inoceramite beds vary in their state of preservation but in general fragmentation is low, with little current reworking, presumably because these beds were deposited far from shore, below fair-weather wave-base. These accumulations most closely resemble those described in taphofacies model IV-B - Sediment-starved shell beds (distal). Episodic processes (e.g., storms) are evidenced by the concentration of vertebrate bioclasts and mud, along low-angle cross-laminations within some samples (e.g. VDV-1).

Calcareous bone-biophospharenites show a range of taphonomic characteristics. The accumulations show features related to prolonged exposure on the seafloor, near fair-weather wave-base, such as the fragmented and rounded bioclasts, as well as episodic events, such as the thin mudrock laminae. (Subgroup C was protected from most of the winnowing and reworking by the inoceramid shell in which it is contained.) The variable intensity of currents in this setting is evidenced by slight alignment of grains in some beds (Subgroup B – thick, commonly lens-shaped accumulations), to random orientation in others (Subgroup A – thin accumulations interbedded with mudrock). As a group, they most closely resemble the discontinuity surfaces within taphofacies model VI - Exaerobic sediment-starved shell beds described by Speyer and Brett (1991). Extremely well

preserved fragile elements such as bird bones (BR3-7) within acummulations dominated by rounded and fragmented grains may indicate episodic events which buried these elements resulting in limited to no reworking of these components, whereas the mud laminae suggest that sedimentation was episodic.

The non-calcareous bone-biophospharenite may be the result of a single accumulation event after which it remained undisturbed by currents, possibly in deeper water distal to the paleoshoreline. The glauconite-rich organic deposit was accumulated by background processes including a rain of sediments and fewer bioclasts into a quiet setting, distal to the paleoshoreline, in deeper waters. This deposit most closely resembles taphonomic model V - Dysaerobic mud-supported shell beds described by Speyer and Brett (1991). Episodic events within this deposit are evidenced by the indistinct bedding planes within the accumulation.

5.2 Diagenetic signals

In addition to the taphonomic features, petrographic examination of these bioclastic accumulations shows differences in diagenetic signals. These differences are mainly related to timing of calcite precipitation which in turn affected the degree of compaction. In addition, the abundance of authigenic pyrite varies within the samples. Despite the differences in mineralogy between the inoceramites, calcareous and non-calcareous bone-biophospharenite, and the glauconite-rich organic deposit, all samples can be compared in regards to these two diagenetic signals.

5.2.1 Compaction

By noting the nature of the contacts between grains and the degree of fragmentation (abundance of broken vertebrate bioclasts) or degree of deformation, one can differentiate between fabrics that indicate early cementation and those that have undergone slight to significant mechanical compaction after deposition (Meyers, 1980; Budd, 2002). Mechanical compaction occurs mostly by the rearrangement of grains, the sliding, and eventual crushing they experience during reworking (Croizé, 2010). Early cementation limits compaction. In beds that have undergone early cementation, point contacts between grains are commonly observed, as are "floating" grains in cement, and bioclastic grains tend to be undeformed and unfragmented (Meyers, 1980; Budd, 2002; Croizé, 2010). In contrast, increased mechanical compaction is represented by densely-packed bioclasts with abundant linear grain contacts and an increased abundance of fragmented and deformed bioclasts (Meyers, 1980; Budd, 2002).

In general, the inoceramite samples (category 1) show common point and linear contacts between bioclasts but fragmentation and deformation of vertebrate bioclasts are rare. These beds are interpreted to have been cemented relatively early; the $CaCO_3$ from the inoceramid-derived prisms likely provided the source for calcite cementation, limiting the effect of compaction (cf. Speyer and Brett, 1991).

The calcareous bone-biophospharenites (category 2) show more variability in the level of compaction. Samples with lower abundances of inoceramid-derived calcite prisms tend to show more compaction than those with abundant calcite prisms. Consequently, the non-calcareous bone-biophospharenite (category 3) is more densely packed than any of

the other types of bioclastic accumulates and contains a higher percentage of fragmented (splintered) and deformed bioclasts. In contrast, the glauconite-rich organic deposit (category 4) shows no sign of compaction. Bioclastic grains float in the organic-rich mud matrix and show no sign of plastic deformation or fragmentation.

The low levels and the variable levels of compaction seen in the inoceramites and in the calcareous bone-biophospharenites, respectively, is interpreted to be related to mechanical processes such as the reworking of the accumulations by currents and waves causing the bioclasts to slide against each other, rearrange, and eventually begin pressing on each other (Croizé, 2010). Variation in the energy levels at time of deposition in addition to the timing of cementation, which can strongly limit mechanical compaction, has affected the diagenic features seen in these deposits.

5.2.2 Pyrite

The Cenomanian-Turonian interval within the WISB contains abundant evidence of poorly oxygenated bottom waters. For example, benthic foraminifera are absent or appear as sparse, low-diversity assemblages. Furthermore, the lack of bioturbation throughout most of the interval, as well as the periodic presence of the biomarker isoreniaratane indicates a stratified water column and bottom-water anoxia reaching the photic zone, possibly the result of increased runoff caused by humid greenhouse conditions (Schröder-Adams *et al.,* 2001; Cumbaa *et al.,* 2013).

In addition, pyrite precipitates were observed in biogenic grains of most bioclastic accumulations. This phenomenon results from the formation of low pH (reducing) microenvironments in the bones and coprolites by the microbial metabolism of collagen,

which enhances rapid pyrite mineralization within and around the bioclasts (Trueman *et al.,* 2003). Further pyrite precipitation within biogenic grains results from the decay of remaining organic matter in fecal pellets (coprolites), within pore spaces of vertebrate bones and teeth, and filaments originally present in inoceramid-derived calcite prisms (e.g. Pirrie and Marshall, 1990). In contrast, pyrite is rare in calcite sediments surrounding the bioclasts of all of these accumulations, with the exception of the glauconite-rich organic deposit (WAP2-1). This may reflect the lack of dissolved organic matter in interstitial waters, but in the case of WAP2-1 the matrix of the deposit is organic-rich, and pyrite is abundant throughout the sample. During periods when bottom waters are dysoxic or anoxic, sulfides (pyrite) are mostly produced by biologically mediated reactions between organic compounds and dissolved pore water sulfate in surficial marine sediments (Canfield and Raiswell, 1991). This framboidal pyrite begins to form in the early stages of diagenesis, once sulfide production begins. During later stages of diagenesis, sulfides may become available through non-biologically mediated reactions and form a second generation of pyrite framboids (Canfield and Raiswell, 1991). The maintenance of conditions favorable for pyrite precipitation, namely low pH and low Eh, also inhibits microbial bioerosion of the bones, aiding in the preservation of these fossil accumulations (Trueman and Martill, 2002).

The bioclasts containing the most authigenic pyrite, or those that are the most fully pyritized, tend to be those that have remained the longest within the sulfate reduction zone, near or at the sediment surface (Reeburgh, 1983). Such bioclasts face an increased likelihood of reworking and/or transport, unless they become buried or sit below storm wave base. Within the studied accumulations, pyrite becomes increasingly abundant with

increased signs of mechanical compaction (except for the non-calcareous bone-biophospharenite, which contains almost no pyrite). The earlier cementation occurs, the less likely it becomes that bioclasts can be remobilized. Being buried with an abundance of inoceramid-derived calcite prisms improves the chances of early cementation, limiting compaction and reworking in the sulfide-redox zone.

The distribution of coprolites in the calcareous bone-biophospharenites supports the interpretation that samples from subgroup A as well as samples BR1-1 and DH1-1 and -2 from subgroup B spent more time being reworked on the seafloor before cementation, removing the soft coprolites. Coprolites can significantly vary in hardness depending on the individual producer; however, even the fecal pellets at the harder end of the spectrum would have no more than a paste-like consistency (Hattin, 1996). For these to have accumulated and be preserved intact and undeformed, as seen in sample BR3-7, they would need to have been deposited in an environment that promotes hardening enough to resist disaggregation and/or compaction by winnowing, transportation, sorting, reworking and burial. An environment prone to long periods of calm would thus be required, as well as one which inhibits disturbance of fecal pellets by detritovores or bioturbators. The lesser degree of transport resultant from early cementation interpreted for BR3-7 is also supported by the presence of bentonite rip-up clasts throughout the lenses of this deposit (Schröder-Adams *et al.,* 2001; Cumbaa *et al.,* 2013).

5.3 Paleoenvironmental setting

Traditional genetic interpretations of coarse bioclastic fabrics often rest on two major assumptions. The first is that fine-grained intervals, such as mudrock, are representative

of low energy background conditions and deposits accumulate over long periods of time with few disturbances (Nichols, 2009). The second is that coarse-grained intervals, such as bonebeds or accumulations of bioclastic debris, are representative of high energy conditions needed to transport these larger grains, and deposits accumulate over a short period of time, deposited during an event such as a pulse of storm activity or a tsunami, depositing new material or reworking existing material (Brett *et al.,* 2008). These assumptions have been maintained due to evidence of storm related features in bioclastic deposits and the relative homogeneity of shale intervals which show only subtle changes in character (Brett *et al.,* 2008). However, Brett *et al.,* (2008) proposed a reversal of these fundamental assumptions by suggesting that shale intervals contain a record of multiple high energy events that are deposited in relatively short intervals while bioclastic accumulations may record a low energy environment representing a long period of deposition under seafloor winnowing conditions (Brett *et al.,* 2008). Using the observed diagenetic and petrographic features, I further refined the paleoenvironment for each group. Figure 13 summarizes the paleoenvironmental interpretations for each accumulation type within the classification scheme.

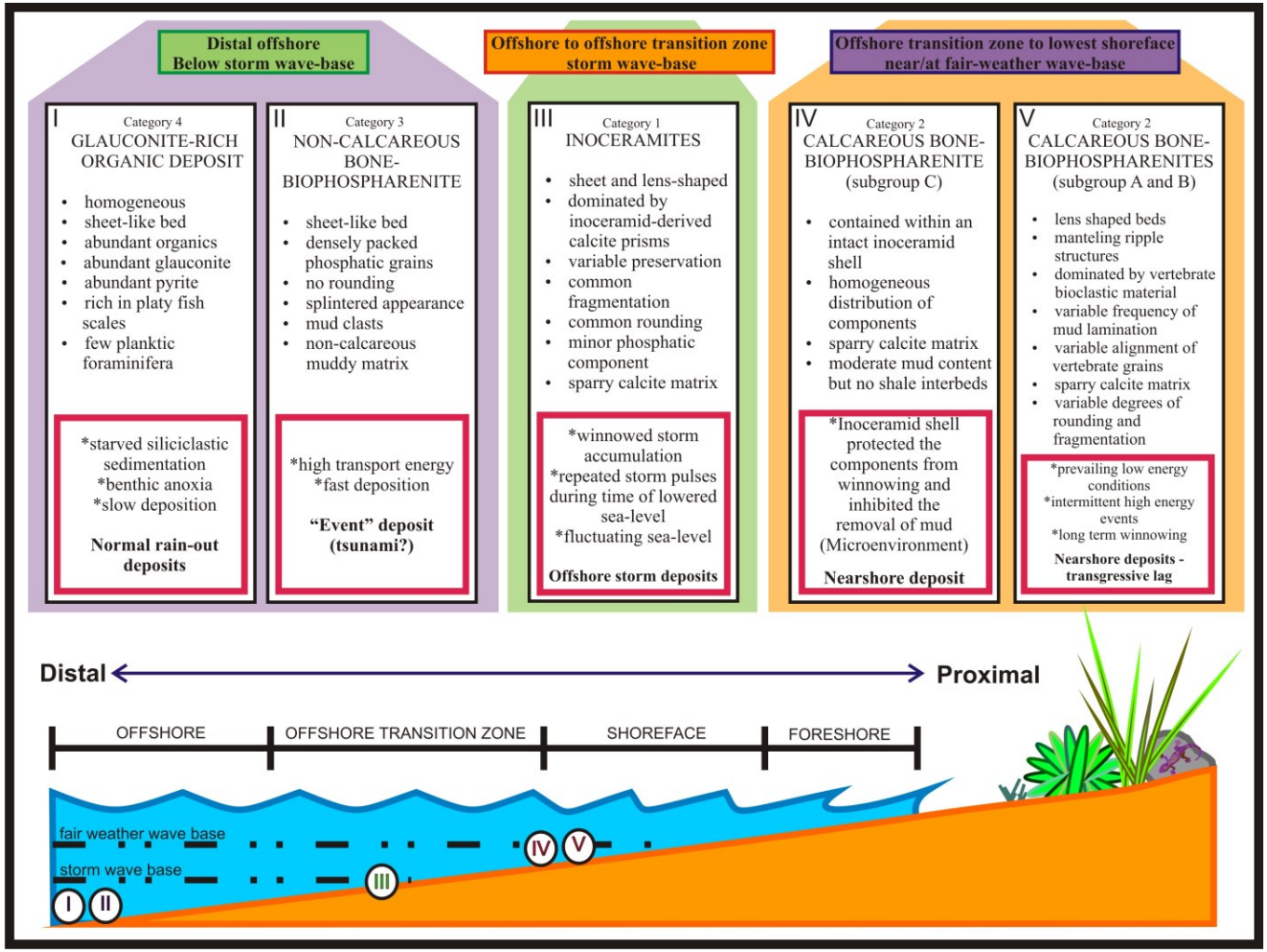

Figure 13: Paleoenvironmental interpretations for each group of bioclastic accumulation.

The disarticulated oyster valves in association with the bioclastic layers in inoceramite samples suggest relatively shallow conditions. In contrast, the taxonomic analysis of one of these accumulations (Phillips, 2008) argues against this interpretation, indicating that these biogenic sediments originated further from shore. A lowering of sea-level is required erode and winnow the bioclastic elements and a subsequent rise in sea-level to concentrate these elements into phosphatic and skeletal concentrations at storm wave base (Kidwell, 1991; Sageman, 1996). Skeletal limestones within the Greenhorn limestones of the Canadian portion of the WIS are very similar to those found in the American portion of the Seaway. Numerous authors have documented these calcarenites interbedded with mudrock from the U.S. portion of the Upper Cretaceous WIS and interpreted them as tempestites formed in response to impingement by storm wave-base during relative sea-level fall and subsequent rise in the basin (e.g., Cobban and Scott, 1972; Kauffman, 1977a, b; Hattin, 1975, 1986; Sageman, 1989, 1996; Shimada *et al.,* 2006; Gale *et al.,* 2008). These beds are regionally correlative and are a useful tool for the recognition of lowstands within the U.S. portion of the seaway (Brett, 1995; Sageman, 1996; Gale *et al.,* 2008). The *Ostrea beloiti* beds of the Manitoba Escarpment, including some of the inoceramites from BR3 locality, are also recognized as regional stratigraphic markers in this area (McNeil and Caldwell, 1981); however, the regional extent of the other Manitoba Escarpment bioclastic concentrations requires further investigation by correlating them to subsurface cores.

The inoceramites studied here are also interpreted as representing a sediment starved, more distal paleoenvironment. Most of these deposits show ramdomly oriented vertebrate bioclasts but some show aligned bioclasts concentrated in laminae and cross-

stratified layers (both calcitic and phosphatic). These features, in addition to the level of abrasion of the vertebrate bioclasts, confirm physical transport and/or reworking (cf. Phillips, 2008). These features are most likely generated by episodic reworking and concentration by storms (cf. Sageman, 1996) but could also be related to other events such as tsunami. These accumulations were concentrated in deeper waters near storm wave-base, like the skeletal limestones of the American portion of the seaway, and away from the shoreline with little influence from currents.

The depositional model previously proposed for the bone-biophospharenite deposits at the Bainbridge and Carrot River localities states that the bonebeds are attributed to amalgamation of bioclasts on the sea floor during early transgression following a drop in sea level and/or as the result of marine erosion events (Schröder-Adams *et al.,* 2001; Cumbaa *et al.,* 2006; Cumbaa *et al.,* 2013). The limited diversity of benthic bivalves is suggestive of stressed ecological conditions. The apparent affinity that inoceramid bivalves had for dysoxic settings (e.g., Kauffman, 1990; MacLeod and Hoppe, 1992; Sageman and Binna, 1997; Kauffman *et al.,* 2007), together with authigenic pyrite precipitation within preserved inoceramid prisms, suggests that this stress was due largely to low oxygen conditions at or near the sediment-water interface. This is consistent with previous interpretations of the Belle Fourche Member of the Ashville Formation in the Manitoba Escarpment at large: finely laminated shales and bentonitic clays were deposited under relatively low energy conditions with very low siliciclastic input and dysoxic to anoxic conditions in bottom waters (e.g. McNeil and Caldwell, 1981; Schröder-Adams *et al.,* 1996; Schröder-Adams *et al.,* 2001).

Calcareous bone-biophospharenites are interpreted as having been deposited in slightly different paleoenvironments based on diagenetic and other trends (Fig. 14). Samples from subgroup A are interpreted as being deposited in a shallow sediment-starved paleoenvironment close to the shoreline near fair-weather wave-base. These deposits are densely-packed with multiple interlaminae of mudrock, representing relatively frequent episodic sedimentation events of unknown origin but likely related to episodic storm pulses delivering suspended mud.

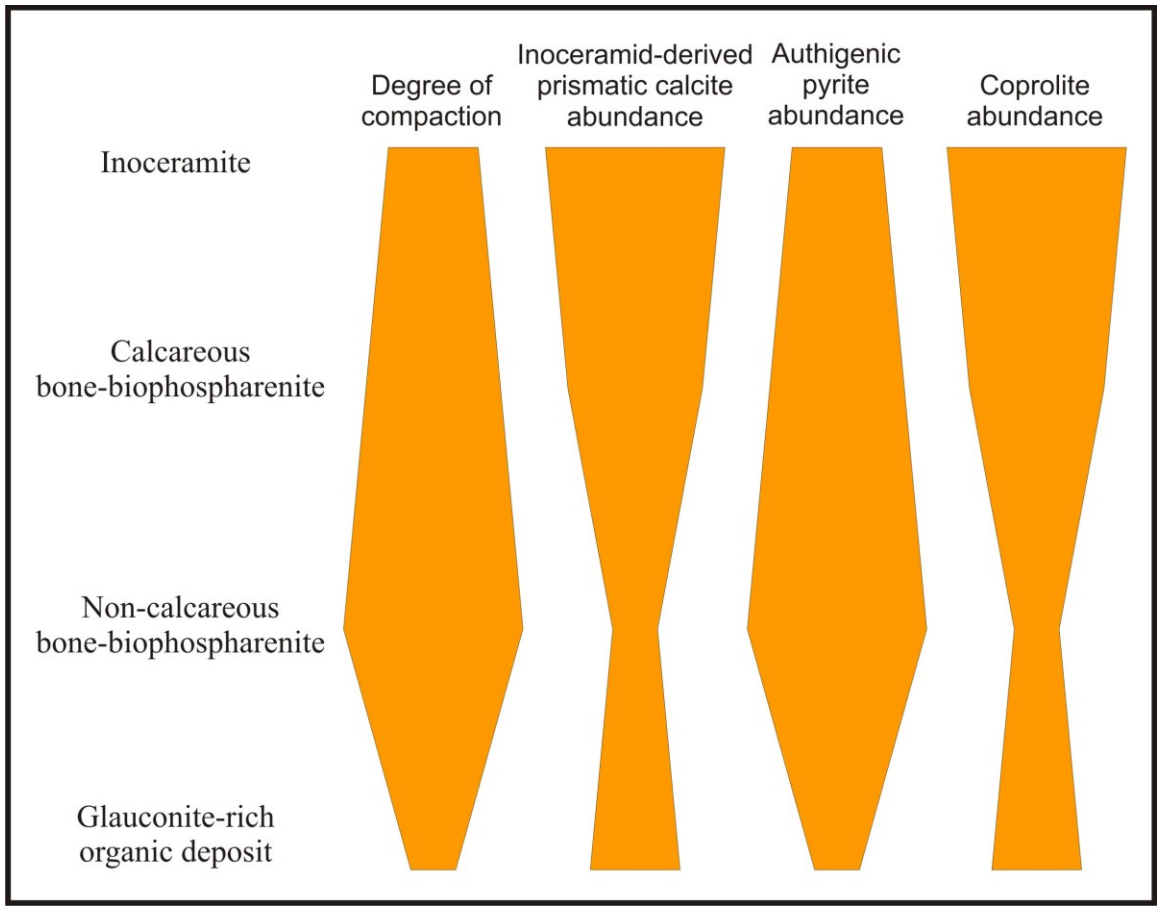

Figure 14: Summary of diagenetic and other trends in the four categories of vertebrate fossil-rich accumulations.

Samples from subgroup B are more variable. Each sample is interpreted as having been deposited under a slightly different set of conditions within a sediment-starved shallow water environment. Sample BR3-7 is interpreted as having been deposited over a long period of time during transgression, after a short-lived marine erosion event, evidenced by the fragile bentonite clasts throughout the lens (Schröder-Adams *et al.,* 2001). This interpretation is consistent with the previous model for this deposit. BR3-7 is interpreted to have accumulated in a shallow environment where the bioclastic grains underwent some winnowing by waves, removing the fines and sorting them, while still being relatively low energy, allowing for the preservation of abundant coprolites. Extremely well preserved bird bones within the bonebed hint at episodic events such as storms or tsunami which could have remobilized the bioclasts and buried the bird bones, protecting them from further fragmentation and abrasion (Dawson and Stewart, 2007). Sedimentary events are also indicated by thin mudrock interlaminae contained within the lens. The bonebed represented by sample BR3-7 experienced early cementation, helping to preserve this accumulation and limiting the compaction seen in other samples of this subgroup.

The bonebed represented by sample BR1-1 is interpreted as having been deposited in a shallow environment near wave-base in a low-oxygen setting. This bed contains highly fragmented bioclasts which are oriented parallel to the bed surface, presumably by persistent currents. In addition, the bones are dark brown to black with phosphate impregnation and they contain abundant pyrite, reflecting an increased time spent at or near the sediment-water interface. A thin mudrock interbed bounded on both sides by larger and better preserved bioclasts may reflect a sedimentary event.

Samples DH1-1 and DH1-2 are interpreted to have been deposited in a sediment-starved exaerobic setting with minor current disturbances. This bed contains highly fragmented bioclasts; the larger bioclasts are slightly aligned while the smaller ones are randomly oriented. Many bioclasts within these accumulations are extensively pyritized, reflecting a significant amount of time when the bioclasts were near the sediment-water interface, subject to reworking and remobilization. In addition, this sample is the only one to contain dinosaur bone fragments and large pebbles, terrestrial elements possibly indicating that the deposition of this bed could be event related. This bonebed contains several of the features typical of a tsunami deposit, including the terrestrially-derived components and the mixture of both rounded and angular clasts.

Subgroup C is interpreted to have been deposited in a similar environment as the other calcareous bone-biophospharenites, near fairweather wave-base; however, it was deposited in its own microenvironment, namely within the valves of an empty, but articulated, inoceramid shell, which mostly protected the bioclasts from being remobilized. The deposition within the shell may have occurred in several phases, resulting in varying mud content within the deposit, protected from waves and currents by the valves of the shell.

The non-calcareous bone-biophospharenite is interpreted to have formed in a distal environment where the influence from currents was minimal and the deposit was quickly buried below the sulfate reduction zone. The initial mechanism for the deposition of the abundance of phosphatic vertebrate bioclasts is still uncertain and may have been the result of a single high energy event that brought the abundance of splintered phosphatic bioclasts and mud clasts into deeper waters below storm wave base. Although no impact

criteria were discovered during the analysis of these accumulations, a bolide impact, such as the two recorded for this time interval, remains a possible mechanism for triggering a high energy event leading to the deposition of this bioclastic bed. In addition, this accumulation underwent intense diagenetic changes after burial. It appears to have been altered by exposure to high heat early in its diagenesis possibly related to the emplacement of kimberlites into Saskatchewan marine sediments in the Late Albian (Leckie *et al.,* 1997).

The glauconite-rich organic deposit is interpreted as being deposited in deeper water where a constant rain of organic debris accumulated over a long period of time below storm wave base. This bed contains abundant pyrite, a low-oxygen indicator, and glauconite, an indicator for prolonged hiatus in siliciclastic sedimentation (Canfield and Raiswell, 1991).

5.3.1 Tsunami

Two bolide impacts may have influenced the WIS during this interval, possibly triggering tsunami. Samples studied here are mid to Late Cenomanian in age based on the foraminiferal assemblage and radiometric dating (Tokaryk *et al.,* 1997; Cumbaa and Tokaryk, 1999; Schröder-Adams *et al.,* 2001). Both the Deep Bay and Steen River impacts are possible candidates for the generation of tsunami waves with the error margins associated with their date of impact (Earth Impact Database). Although no impact criteria were discovered within these deposits future analysis for iridium in these sediments might provide another avenue for testing the hypothesis of the bolide impact on the WIS.

Some of the accumulations studied here contain characteristics which could be attributed to a tsunami; however, because of the non-specificity of these features, it is difficult to distinguish tsunami from other episodic high-energy events, e.g. surge deposits, storm deposits, and debris flows (Dawson and Stewart, 2007; Mitchell *et al.,* 2010). The calcareous bone-biophospharenites DH1-1 and DH1-2 from Carrot River locality #1 are the best candidates for a tsunami deposit. These deposits contain large terrestrially derived clasts including large pebbles and dinosaur bones through these fining upward accumulations. These terrestrially-derived clasts may have been carried seaward by the return flow of a tsunami; however, it is not possible to rule out a riverine origin of these components as proposed in Schröder-Adams *et al.* (2001). The mudrock layer may indicate the period of zero velocity between the landward flooding and return flow of the tsunami, or the time between successive waves, which would differentiate it from storm deposits which would not contain internal mudrock layers. Nonetheless, it was not possible to completely rule out other high-energy events or, more likely, a combination of background processes and episodic events as possible mechanisms for the deposition of these accumulations and origin of the features seen in DH1-1 and DH1-2.

6. CONCLUSIONS

The Manitoba Escarpment records the erosive margin of the Canadian WIS. Cenomanian-aged bioclastic horizons found within the shales of the Belle Fourche Member of the Ashville Formation reflect changing conditions within the seaway. Based on their composition, these accumulations have been classified into four categories: 1) inoceramites, 2) calcareous bone-biophospharenites, 3) non-calcareous bone-biophospharenites, and 4) glauconite-rich organic deposits. Taphonomic features reflect

varying accumulation times, though most of these deposits are interpreted as having been accumulated slowly on the seafloor in a dysoxic environment with a very low sedimentation rate, forming acceptable conditions for inceramids, but inhospitable conditions for benthic foraminifera.

Sea level changes are known to have been frequent and relatively fast throughout the mid to Late Cenomanian and into the Turonian (Plint and Kreitner, 2007; Gale *et al.,* 2008). The average depositional gradient of the eastern margin is less than 1° and thus, even relatively small changes in sea level would have had a dramatic effect on the paleoenvironment of the region. These sea-level fluctuations form the major control for the accumulation and concentration of these bioclastic horizons while episodic events may have a significant effect on the taphonomy of the beds. Sedimentologic and taphonomic features of many of these accumulations do indicate reworking by storms or other high energy events such as tsunami. Although no impact criteria such as shocked minerals and microtektites were discovered during the analysis of these accumulations, these impacts remain a possible mechanism for triggering high energy events which contributed to the sedimentary features seen in some of these accumulations.

These beds are a composite record of background and episodic processes, and it can sometimes be very difficult to untangle the signals found within them to determine a paleoenvironmental setting. These accumulations are made up of concentrated and often randomly oriented vertebrate bioclastic debris of the same composition as the debris found dispersed throughout the shales encasing them. These bioclastic concentrations were often deposited within pre-existing depressions in the seafloor, in the case of lensoid deposits, or as deposits draped over underlying sediments.

In brief, (1) inoceramites were deposited and concentrated over time at storm wave-base and experienced episodic reworking and remobilization of bioclasts by episodic storms concentrating vertebrate bioclasts along slightly inclined cross-laminations seen in some of the beds. (2) Calcareous bone-biophospharenites were deposited under variable paleoenvironmental conditions but were deposited in shallow waters, proximal to the shore, near fairweather wave-base. Evidence of episodic events can be seen in most of the samples as mudrock interlaminae, extremely well preserved bird bones, or as large pebbles and dinosaur bones. (3) The non-calcareous bone-biophospharenite was deposited in a distal environment where the influence from currents was minimal. The initial mechanism for deposition is uncertain but may have been the result of a single high energy event. In addition, this accumulation underwent intense diagenetic changes after burial. (4) The glauconite-rich organic deposit accumulated in deeper waters below fair-weather and storm wave-base. A slow rain of organic-rich debris was accumulated and remained undisturbed over a long period in a low-oxygen and sediment-starved environment.

These accumulations are a useful source of information about this very dynamic time in Earth's history. Because of the narrow time frame of deposition, examination of these accumulations can give us clear indications of lowstands, subsequent transgression, and episodic events during this time.

CHAPTER 3

FORAMINIFERAL RESPONSE TO CATASTROPHIC EVENTS IN THE UPPER CRETACEOUS (CENOMANIAN-TURONIAN) OF THE WESTERN INTERIOR SEAWAY, CANADA

ABSTRACT

The Cenomanian-Turonian interval was globally a particularly dynamic time and is characterized by warm to hothouse conditions, fluctuating sea-level, significant changes in water chemistry, including periods of anoxic or dysoxic bottom waters, periods of increased volcanism, as well as a few bolide impacts. Marine microorganisms such as foraminifera are very sensitive to changes in their environment, and these changes can cause severe biotic effects termed the Liliput effect. This study focuses on the response of foraminifera to short-lived, possibly catastrophic, environmental change as observed at the eastern edge of the Cenomanian-Turonian Western Interior Seaway by drawing correlations between an outcrop section and subsurface core. The studied interval shows little change in foraminiferal assemblages, which are made up almost exclusively of planktic species. This is interpreted to reflect persistent bottom water anoxia in the WIS during this interval. This interval is mostly comprised of resistant and opportunistic species from the genus *Muricohedbergella* and the genus *Heterohelix*, which indicates that conditions on the eastern margin of the Western Interior Seaway were harsh during the Cenomanian-Turonian. The high proportion of particularly opportunistic species such as *Heterohelix globulosa* as well as specimens exhibiting dwarfism was calculated in order to identify times of catastrophic environmental change. Another factor to consider was the frequent ashfalls, their negative effects overprinting the other factors affecting foraminifera. These two different signals must be untangled in order to better understand foraminiferal responses to catastrophic environmental change.

1. INTRODUCTION

In the Cretaceous Period, the Western Interior Seaway (WIS) covered much of what is now Western Canada. Cretaceous strata and their fossil communities preserved within this foreland basin document frequent fluctuations in sea-level and attest to paleogeographic and paleoenvironmental changes. Changes were either gradual or of a short-lived and sometimes catastrophic nature. Long-term, gradual changes were related to climate fluctuations, tectonically and eustatically driven sea-level fluctuations (Plint and Kreitner, 2007; Gale *et al.,* 2008) and oceanic anoxic events (OAEs) (e.g. Leckie *et al.,* 2002; Keller and Pardo, 2004b; Schröder-Adams *et al.,* 2012). Short-lived catastrophic environmental changes may have been associated with two bolide impacts known to have occured during this time, within or very near the WIS (Earth Impact Database; Grieve, 2006) and to frequent volcanic eruptions, which blanketed the seaway with ash (Bagshaw, 1977; Cadrin, 1995).

The Cenomanian-Turonian interval was a particularly dynamic and enigmatic time within the Cretaceous Period. Global climate reached a thermal maximum in the Late Cenomanian (Price *et al.,* 1995; Huber *et al.,* 2002., Norris *et al.,* 2002; Hasegawa et al 2012; Hay and Floegel, 2012; Friedrich *et al.,* 2012) and was coupled with the globally recognized OAE-2 at the Cenomanian-Turonian boundary (Jenkyns, 1980; Hart and Ball, 1986; Leckie *et al.,* 2002; Wilson and Norris, 2003; Coccioni and Luciani, 2005; Guobiao, 2012, Reolid *et al.,* 2012).

Within the Western Interior Seaway, sea-level fluctuated rapidly (Plint and Kreitner, 2007; Gale *et al.,* 2008), and changing paleogeography allowed for Tethyan and Polar

derived watermasses to enter the seaway resulting in watermass stratification causing periods of anoxic or dysoxic bottom waters (e.g. Schröder-Adams *et al.,* 1996; Leckie *et al.,* 1998; Schröder-Adams *et al.,* 2001; Leckie *et al.,* 2002). The Cenomanian-Turonian interval is also marked by periods of extensive volcanism that resulted in abundant ashfalls within the seaway (Bagshaw, 1977; Bloch *et al.,* 1993, 1999; Schröder-Adams *et al.,* 2001; Keller and Pardo, 2004b; Tyagi *et al.* 2007). In addition, two bolide impacts are also documented within this interval, the Steen River Crater in Northern Alberta, dated 91 ±7 Ma, and the Deep Bay Crater in northern Saskatchewan, dated at 99±4 Ma (Earth Impact Database; Grieve, 2006). Marine biota within the WIS had to respond to these environmental regimes (Bagshaw, 1977; Schröder-Adams *et al.,* 1996; Scott *et al.,* 2001; Keller and Pardo, 2004b; Schröder-Adams *et al.,* 2012).

Foraminifera have a global distribution and occur abundantly in marine sediments. Due to their abundance in the geological record and their sensitivity to environmental changes, foraminifera are widely considered as an important tool for monitoring paleoecological changes and reconstructing marine palaeoenvironmental histories (e.g. Schröder-Adams *et al.,* 1996; Scott *et al.,* 2001; Macleod *et al.,* 2000; Keller and Pardo, 2004b; Peryt, 2004; Coccioni and Luciani, 2005; Coccioni *et al.,* 2006; Keller, 2008; Keller and Abramovich, 2009; Tantawy *et al.,* 2009; Waskowska, 2011; Guobiao, 2012; Reolid *et al.,* 2012; Schröder-Adams *et al.,* 2012). This chapter focuses on the response of foraminifera to short-lived, possibly catastrophic, environmental change as observed at the eastern edge of the Cenomanian-Turonian Western Interior Seaway by drawing correlations between an outcrop section and subsurface core. Furthermore, this study focusses on the biotic response of planktic foraminiferal assemblages to frequent ash falls

that marked this time period in the Western Interior. Planktic foraminiferal response to increased volcanism has been particulary well-studied at the Cretaceous-Tertiary boundary interval (e.g. Peryt, 2004; Keller, 2008). On the other hand, the Cenomanian-Turonian strata deposited in the WIS have received abundant scientific attention because they record global hothouse conditions (Schlanger and Jenkyns, 1976; Price *et al.,* 1995; Norris *et al.,* 2002; Wilson and Norris, 2003; Hasegawa et al 2012; Hay and Floegel, 2012; Friedrich *et al.,* 2012) and the globally recognized OAE-2 (e.g. Schröder-Adams *et al.,* 1996; Leckie *et al.,* 1998; Bloch *et al.,* 1999; Leckie *et al.,* 2002; Keller and Pardo 2004b, Schröder-Adams, 2012). However, the question of whether foraminiferal assemblages within these strata responded to short-term changes related to volcanic eruptions and bolide impacts is less well studied and is addressed here.

2. GEOLOGICAL SETTING

2.1 Cretaceous Western Interior Sedimentary Basin

The Western Interior Sedimentary Basin (WISB), bordered by the Cordillera to the west and the Canadian Shield to the east, is one of the largest repositories of Cretaceous sedimentary rock in the world (McNeil and Caldwell, 1981). Structurally, the WISB is an asymmetrical trough made up of a foredeep flanked by a fold-thrust belt on the western side whose base rises eastward to present-day Manitoba (Fig.1). The foreland basin can be split into four main zones: the western zone, the west-central zone, the hinge zone, and the eastern stable platform zone (Kauffman, 1977a,b; McNeil and Calwell, 1981). The western zone is marked by the highest subsidence and sedimentation rates. Sediments in this zone are mainly sand and gravel derived from the tectonically active

western uplands. The west-central zone is the foredeep, the deepest part of the basin. It was also characterized by high subsidence and sedimentation rates. Because it was farther from the mountains, its stratigraphic fill is finer grained. It consists of interbedded sandstone and mudstone grading eastward into mudstone. The hinge zone is the broad area between the actively subsiding western zones and the eastern stable platform and includes the forebulge. It was characterized by relatively low rates of subsidence and sedimentation and is dominated by mudstone and carbonate units. The eastern stable platform is a broad zone that includes the backbulge. Because this zone was farthest from the mountains, sedimentation and subsidence rates were very low, the resultant sedimentary fill consists almost exclusively of mudstone with rare carbonates, and the sediment package is thin and commonly interrupted by disconformities (Kauffman, 1977a,b; McNeil and Calwell, 1981). Rocks of this zone outcrop along the Manitoba Escarpment and underlie eastern Saskatchewan (Fig. 15).

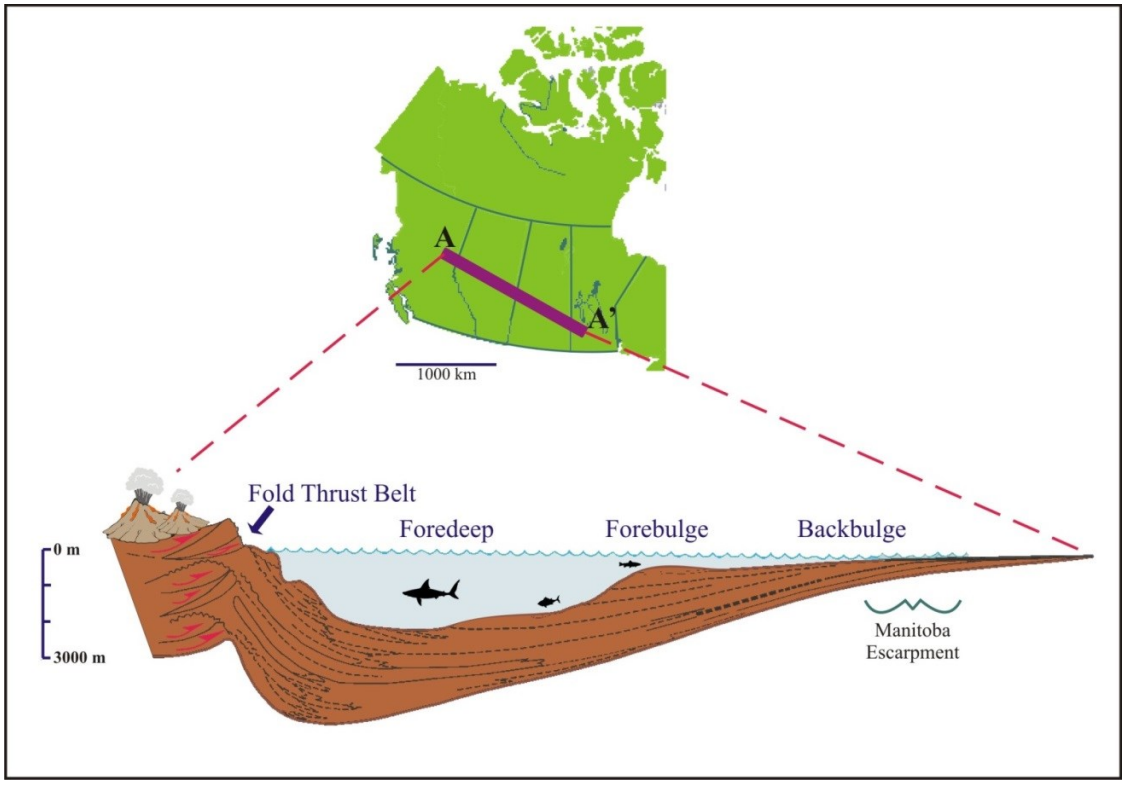

Figure 15: Cross section of the Western Interior Seaway showing the asymmetry of the basin and long flat gradient of the eastern platform zone. Modified from Kauffman (1984) and Phillips (2008).

The Manitoba Escarpment is a 675 kilometer-long series of uplands (Fig. 16) which trends south-sast to north-west along south-central Manitoba and east-central Saskatchewan towards north-central North Dakota. Strata that outcrop along the escarpment are Albian to Maastrichthian in age and are up to 600 meters thick (McNeil and Caldwell, 1981). The low accumulation rates of siliciclastic material in the eastern portion of the WISB, unlike the western portion with its high sediment input and varying accommodation space, have created a condensed section that records rich, fairly undiluted assemblages of planktic foraminifera (Schröder-Adams et al., 2001).

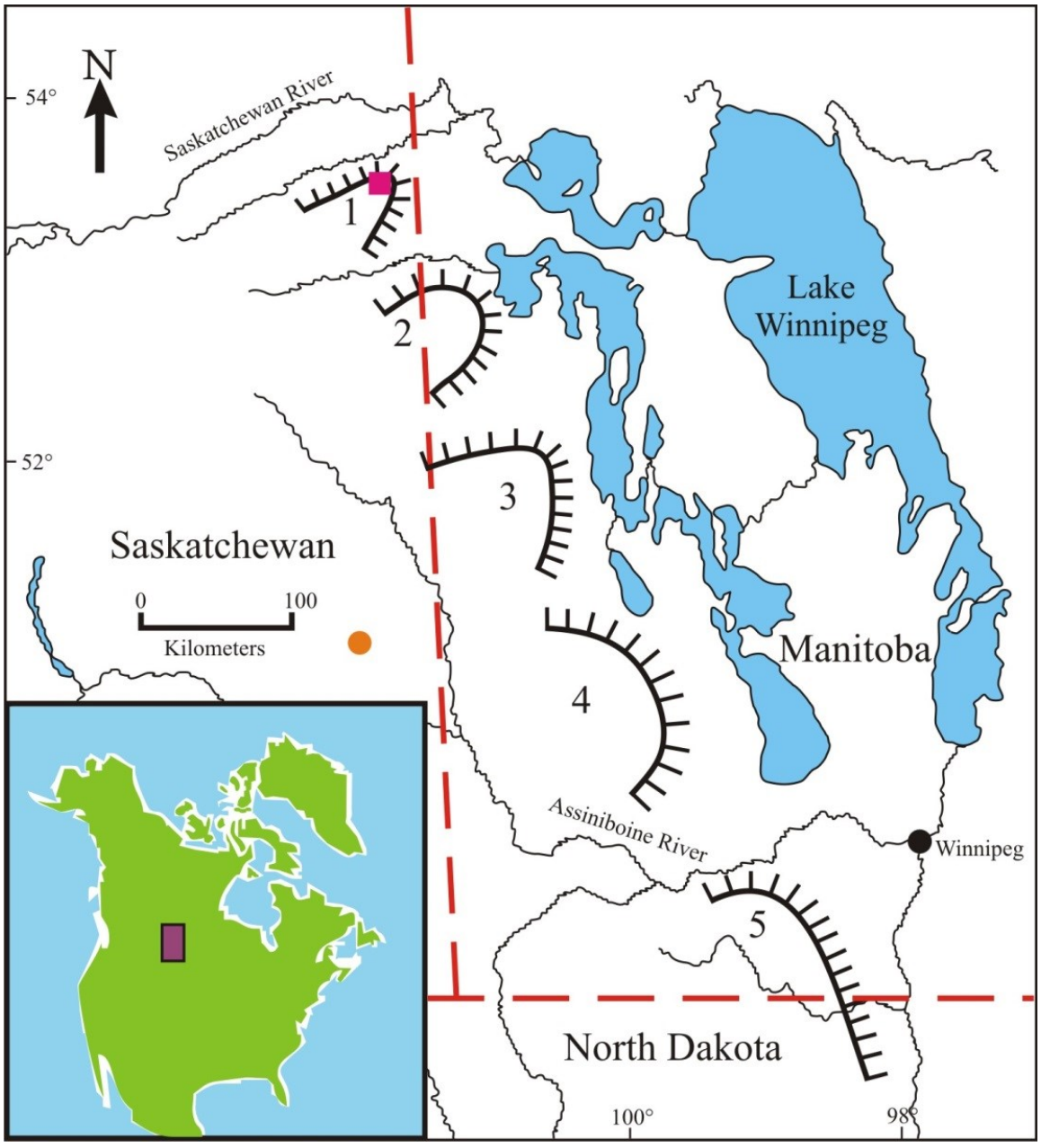

Figure 16: Map of the Manitoba Escarpment showing the locations of the outcrop (pink square) and the core (yellow circle). Modified from Schröder-Adams *et al.* (2001).

2.2 Western Interior Seaway

The Western Interior Seaway (WIS) was an epicontinental sea that periodically connected the Tethys to the south and the Polar Sea to the north, covering central North

America and filling the foreland basin, spilling out onto the eastern platform (McNeil and Caldwell, 1981; Cumbaa *et al.,* 2010). After the sea-level lowstand and subaerial erosion documented at the base of the Cenomanian, transgression occurred during the start of the Greenhorn Marine Cycle (Hattin 1962; 1964; Kauffman, 1977a; Schröder-Adams *et al.,* 2001). As sea levels rose to a maximum in the early Turonian, the Polar Sea connected to the Tethys, transforming the restricted Mowry Sea into a seaway (Fig. 17; Hattin 1962; 1964; Kauffman, 1977a). Significant paleoenvironmental changes were occurring in and around the WISB during this time. Studies of the Canadian and US portions of the WISB have both documented frequent transgressive-regressive events during this interval, where sea-level may have fluctuated up to 10 m (Laurin and Sageman, 2007; Plint and Kreitner, 2007). Due to their short-lived nature and their frequency, fluctuations are interpreted to be the result of glacioeustatic changes (Plint and Kreitner, 2007).

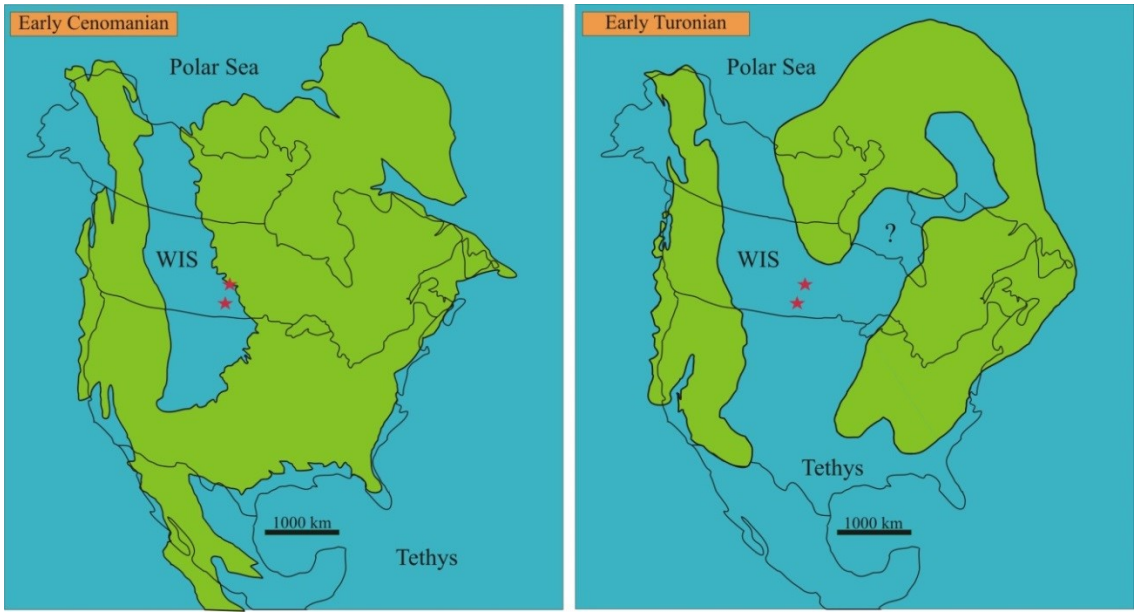

Figure 17: Paleogeographic map showing the extent of the seaway during the early Cenomanian on the right and during the early Turonian on the left. The red stars indicate the outcrop, situated more northerly, and core location, more southerly. Modified from Bhattacharya and MacEachern (2009).

In the earliest Cenomanian, the outcrop location on the Bainbridge River, Saskatchewan, and the studied core were close to the eastern margin of the seaway and were likely to be strongly affected by the sea-level fluctuations while during sea-level highstand in the earliest Turonian, the study localities were farther offshore. During both times, the Bredenbury reference core, situated to the south-west of the outcrop, was in a more basinward position, reflecting a deeper water setting than at Bainbridge. This core location would not have been as strongly affected by sea-level changes.

2.3 Stratigraphic framework

Our current understanding of the lithostratigraphy in the eastern margin of the Canadian WIS comes primarily from studies of the Manitoba Escarpent (e.g. Caldwell, 1975; McNeil and Caldwell, 1981; Schröder-Adams *et al.,* 1996; Schröder-Adams *et al.,* 2001). The strata exposed in the Pasquia Hills, in the northern most portion of the escarpment, are mostly composed of Albian to Santonian aged marine shales deposited during the Greenhorn and Niobrara eustatic cycles (Schröder-Adams *et al.,* 2001; McNeil and Caldwell, 1981; Kauffman and Caldwell, 1993; Cumbaa *et al.,* 2006). In central Saskatchewan, these strata make up, in ascending order, the Joli Fou, Viking, Westgate, Fish Scales, Belle Fourche, and Second White Specks formations (Fig. 18). In parts of central Saskatchewan, there is a significant unconformity between the Second White Specks Formation and the base of the Niobrara Formation. Corresponding units in the Manitoba Escarpment are the Ashville and Favel formations, and the Carlile Formation (previously the Niobrara Formation; includes the Morden Member) (McNeil and Caldwell, 1981; Bloch *et al.,* 1993; Catuneanu and Sweet, 1999; Schröder-Adams *et al.,* 2001; Nielsen *et al.,* 2003; Christopher *et al.,* 2006; Bamburak and Nicolas, 2009; Nicolas, 2009). The Bredenbury core includes sediments from the Joli Fou Formation through to the First White Speckled Member of the Niobrara Formation. The sections that were investigated in this project include, in ascending order, the Fish Scales Formation and Belle Fourche Formation, overlain by the Second White Specks Formation and the Morden Member. The Bainbridge River outcrop includes sediments from the Ashville and Favel formations that in turn are unconformably overlain by the Morden Member of the Carlile Formation.

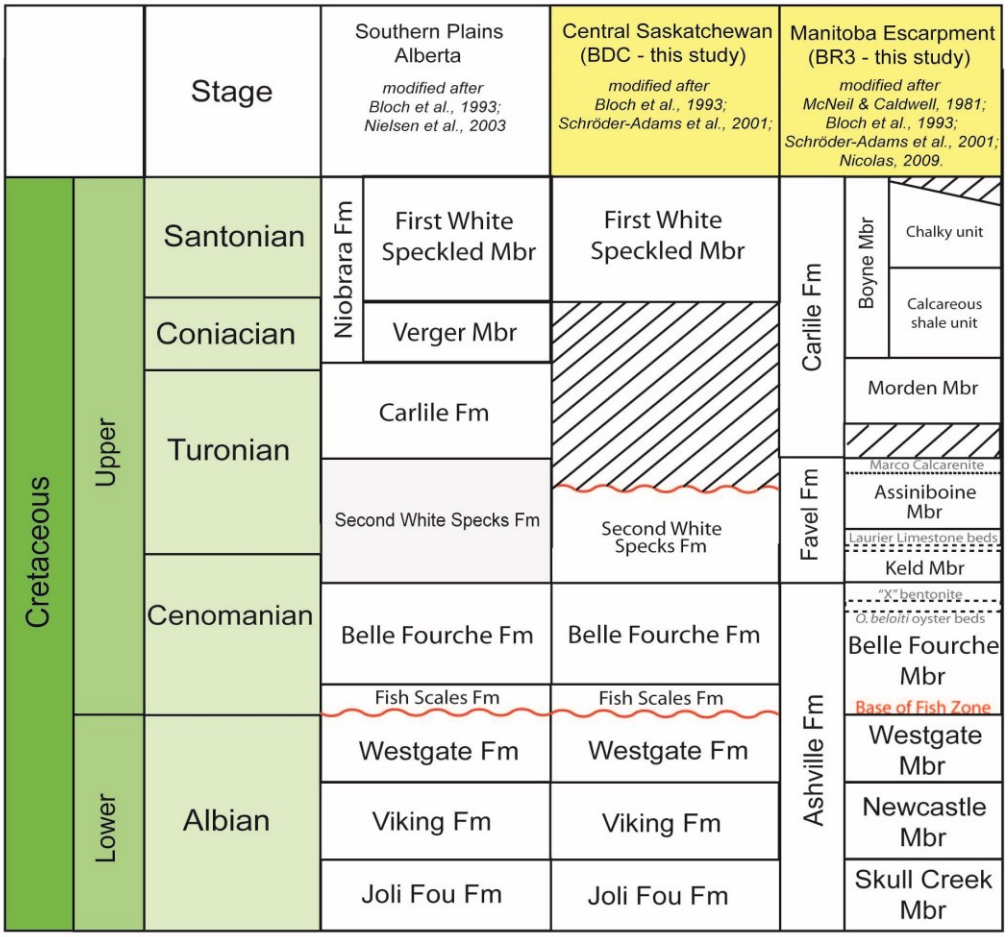

Figure 18: Stratigraphic chart of the Canadian WISB. Modified after Schröder-Adams *et al.* (2001), Phillips (2008), Nicolas, (2009), and Bamburak and Nicolas (2009).

2.4 Paleoenvironment

2.4.1 Paleoclimate

Modern open ocean sea surface temperature rarely exceeds 28-29°C. In contrast, $\delta^{18}O$ paleothermometry from foraminiferal calcium carbonate shells indicates that during the mid Cretaceous hothouse, temperatures near the poles could have been up to 20°C warmer than today, while surface waters at lower latitudes may have reached 37°C at their peak in the mid to late Turonian (Norris *et al.,* 2002; Bice *et al.,* 2006; Hay, 2008;

Hay and Floegel, 2012). Epicontinental seas such as the WIS would likely have been even warmer due to their broad shallow nature. Abundant evidence for high polar temperatures exists in the Canadian Arctic, such as the presence of crocodilians in high latitudes (Huber, 1998; Tarduno *et al.,* 1998; Norris *et al.,* 2002). This polar heat may be a reflection of a reduced tropics-pole temperature gradient during the extreme hothouse conditions of the Cenomanian (Hasegawa *et al.,* 2012). The Canadian WIS was locatedin a mid-latitude warm humid belt during the Cenomanian to Turonian interval and experienced increased humidity and precipitation rates, possibly creating a seasonal brackish lid and inhibiting vertical mixing within the water column (Leckie *et al.,* 1998; Hay and Floegel, 2012). The seaway was also affected by strong eastward-blowing winds in the winter months, creating increased storm intensity, but only weak winds in the summer (Price *et al.,* 1995; Leckie *et al.,* 1998; Hasegawa *et al.,* 2012; Friedrich, 2012; Hay and Floegel, 2012).

The WIS had a unique watermass distribution pattern for which there appear to be no modern analogs. As a result, a diversity of conceptual models for the circulation within the seaway have been proposed (e.g. Eicher and Worstell, 1970; Eicher and Diner, 1985; Hay *et al.,* 1993; Glancy *et al.,* 1993; Slingerland *et al.,* 1996). Circulation within the seaway was affected by many factors including 1) precipitation and evaporation, 2) runoff, 3) wind direction and strength, 4) latitudinal temperature gradients, and 5) the mixing of Tethyan and Polar watermasses (Kump and Slingerland, 1999). Normal warm saline waters moved north along the eastern side of the Seaway while cooler, less saline waters moved south along the west (Eicher and Diner, 1985; Fisher *et al.,* 1994; Schröder-Adams *et al.,* 2001; 2014). This movement is explained by the oceanic

circulation model proposed by Slingerland et al. (1996) and modeled by Kump and Slingerland (1999) accounting for the importance different forcing types. This modeling indicated that the strength of the counterclockwise gyre is strongly influenced by runoff, where eastern drainage flowed northward along the coast and western drainage flowed to the south, creating lower salinity wedges and drawing in the Tethyan and Polar waters. Wind-generated flow, especially during storms, was also a strong factor influencing WIS circulation during this time, and may have resulted seasonal changes in circulation patterns (Kump and Slingerland, 1999). (Fig. 19)

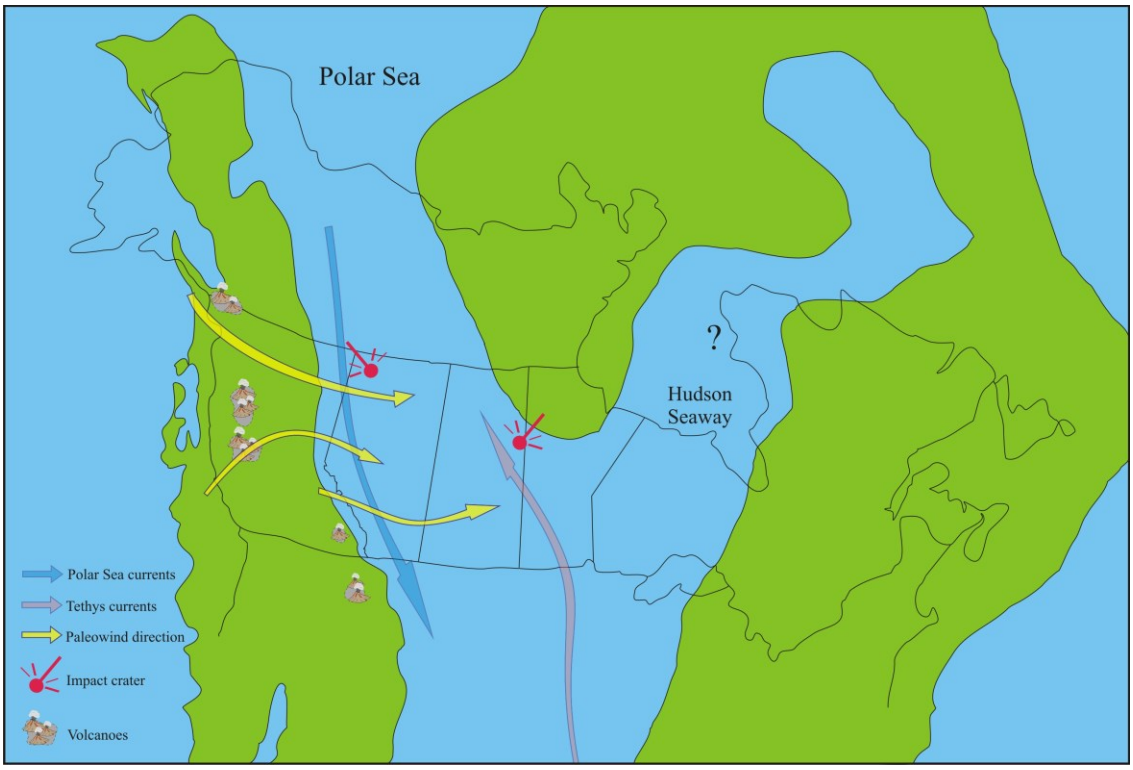

Figure 19: Map of Canada showing reconstructed main wind direction, dispersing ash from the western margin of the seaway throughout the Cenomanian-Turonian interval, currents influencing the seaway, and the locations of bolide impacts; the Steen River impact crater in northern Alberta, dated at 91 ± 7 Ma, and the Deep Bay impact crater in northern Saskatchewan, dated at 99 ± 4 Ma (Earth Impact Database). Modified from Fanti (2009), Grieve (2006), Hay and Floegel (2012), Hasegawa *et al.* (2012), and Price *et al.* (1995).

2.4.2 Volcanism and its effect on biota

The Cretaceous was a period of abundant volcanism at mid oceanic spreading ridges. Volcanism was also occurring near the WISB because of subduction and collision of exotic terranes along the western edge of North America (Kauffman, 1977b, McNeil and Caldwell, 1981; Keller, 2003; Keller, 2008). Within the WISB, an abundance of volcanic

eruptions are documented by single bentonites as well as bentonite swarms, which reflect short periods of intense volcanism (Schröder-Adams *et al.,* 1996; Tyagi *et al.,* 2007; Keller, 2008; Nielsen *et al.,* 2008). Volcanic eruptions can cause both short- and long-term changes in climate (Arthur *et al.,* 1985; Zielinski, 2000; Hay, 1996). In addition, their ejecta, deposited in ash falls, may have increased turbidity in the water column of the WIS, which could have decreased productivity by inhibiting photosynthesis. Alternatively, ash falls may have had the opposite affect: they could have conceivably fertilized the shallow ocean, thereby increasing photosynthesis in surface waters. This would have in turn increased the downward flux of organic matter, which may have led to anoxia at depth as the falling organic matter was decomposed, or an expansion of the pre-existing oxygen minimum zone into the photic zone (Leckie *et al.,* 1998; Frogner *et al.,* 2001; Keller, 2003; Keller, 2008). If such anoxic or dysoxic conditions persisted after an ash fall event they would have presumably exerted asignificant stress on biological communities living within the seaway (Keller, 2003 and 2008; Tantawy *et al.,* 2009; Waskowska, 2011).

2.4.3 Ocean anoxic events and bottom water anoxia

Several global ocean anoxic events, henceforth referred to as OAEs, are interpreted to have occurred during the Cretaceous Period (e.g. Schlanger and Jenkyns, 1976; Jenkyns, 1980; Hart and Ball, 1986 ; Jarvis *et al.,* 1988; Ohkouchi *et al.,* 2006; Forster *et al.,* 2007; Mort *et al.,* 2007; Kuroda *et al.,* 2007; Junium and Arthur, 2007; Jenkyns 2010). Despite extensive scrutiny on the associated stata, there is no concensus as to the cause(s). Past interpretation have linked them to: 1) intervals of greenhouse climate; 2) an increase in marine productivity or a loss of water column stratification (e.g. Erbacher *et al.,* 2001;

Wilson and Norris, 2001; Tsandev and Slomp, 2009); 3) intervals of increased production of oceanic crust (e.g. Jones and Jenkyns, 2001; Poulsen *et al.,* 2001; Snow and Duncan, 2001; Leckie *et al.,* 2002); 4) other large volcanic events (e.g. Keller, 2003; 2008; Turgeon and Creaser, 2008); or 5) some combination of these factors. Cretaceous strata deposited in the WIS contain evidence of the OAE-2, a globally recognized OAE that occurred 93 million years ago at the Cenomanian- Turonian transition (Schröder-Adams *et al.,* 1996; Dean and Arthur, 1998; Simons and Kenig, 2001; Snow *et al.,* 2005; Coccioni *et al.,* 2006; Schröder-Adams *et al.,* 2012). This event may have been triggered by the iron fertilization surface waters resulting from ash falling into the seaway during a period of increased volcanism or alternatively, by the increased presence of warm saline waters, creating favorable conditions for increased primary productivity and the accumulation of abundant organic matter (Leckie *et al.,* 1998; Huber *et al.,* 1999; Leckie *et al.,* 2002; Turgeon and Creaser, 2008).

Several other phases of anoxic or dysoxic benthic conditions also appear to have occurred during the Cenomanian-Turonian interval in the WIS (Schröder- Adams *et al.,* 2001; Simons and Kenig, 2001). These depleted benthic oxygen conditions, during which an oxygen minimum zone is inferred to have formed near the seafloor appear more localized that OAE-2 and could have been triggered by various mechanisms including (1) changes in climate which controlled productivity and/or redox conditions (Leckie *et al.,* 2002); (2) increased input of freshwater into the seaway, which created a freshwater cap and inhibited mixing; or (3) eutrophication of the surface waters, due to the addition of nutrients from runoff or volcanic ash, which resulted in depletion of oxygen within bottom waters (Frogner *et al.,* 2001; Keller, 2003; Keller and Pardo, 2004a; Keller, 2008;

Tantawy *et al.,* 2009). An expansion of this oxygen minimum zone into shallower waters, caused by elevated productivity or the breakdown of water column stratification due to abrubt warming, has been suggested as the cause for the extinction of deep-dwelling planktic foraminifera in the Cenomanian (Leckie *et al.,* 1998, Leckie *et al.,* 2002).

3. MATERIALS AND METHODS

This research project focused on strata deposited near the eastern margin of the Cretaceous WIS of Canada. Two localities were chosen in order to investigate the foraminiferal response to catastrophic environmental change. An outcrop situated on the Bainbridge River in eastern most central Saskatchewan representing a setting proximal to the eastern margin was chosen, as well as a reference core (Bredenbury core: 11-36-22-1W2) situated in southeast Saskatchewan representing a more distal setting (Fig. 15). The localities are approximately 300 km apart. Moving stratigraphically upward, samples were taken at decimeter to one meter intervals in outcrop and one meter to five meter intervals in core. Sampling frequency was increased near critical intervals for paleontological analyses. Samples were prepared for foraminiferal analysis using standard methods (Then and Doherty, 1983); however, in addition to the >63µm fraction used in standard foraminiferal analyses, the remaining fine material (<63 µm) from the outcrop section was picked for foraminera tests in order to identify any particularly small species and/or dwarfed specimens, the latter being common to stressed biotic conditions (Keller and Pardo, 2004a; Keller and Abramovich, 2009). In the previously prepared core samples, species were identified and counted including those of reduced size (dwarfing/Lilliput effect). Representative photographs of the agglutinated foraminiferal

taxa identified in this study can be found in McNeil and Caldwell (1981) and will not be repeated here. Where foraminiferal preservation was poor, identification could only be made to the genus level. Foraminiferal listings (Appendices 1 and 2) reflect the number of specimens picked and identified per sample. Sample volumes vary between core and outcrop due to restrictions in core sampling. The relative abundance and species richness as well as the percentage of the assemblage represented by *Heterohelix globulosa*, the percentage composed of *Whiteinella aprica*, and the percentage represented by both *Clavihedbergella simplex* and *Clavihedbergella subcretacea* were plotted individually in order to facilitate biostratigraphic correlations and better understand the paleoecological and paleoenvironmental changes within the sections. The percentage of the assemblage made up of dwarfed specimens (Lilliput effect), which are defined here as specimens under 0.10 mm in size, was also plotted in order to better understand the foraminiferal response to short term events and to identify periods of catastrophic environmental change.

Furthermore, data from Rock-Eval pyrolysis (Bloch *et al.,* 1993; Schröder-Adams *et al.,* 1996; Schröder-Adams *et al.,* 2001) for both core and outcrop sections was used in addition to foraminiferal data in order to correlate the Bainbridge outcrop section and the Bredenbury core (Appendices 3 and 4). The total organic carbon (TOC) within samples was assessed to gather more paleoenvironmental data, and the hydrogen index (HI) was evaluated to determine the source of the organic matter, with low values associated with a terrestrial source and high values with a marine source (Espitalié, 1977; Bloch *et al.,* 1993; Schröder-Adams *et al.,* 1996; 2001).

4. RESULTS

Benthic foraminifera are relatively rare in the Cenomanian interval and are absent in the Turonian interval. Therefore, this study addresses the planktic component of the Ashville and Favel formations. Representative specimen of the planktic assemblage can be found on Plates 1 and 2.

With the exception of *Heterohelix globulosa* and *Whiteinella aprica*, all specimens identified in the two sections are species of the genus *Muricohegbergella* and *Clavihedbergella*. In the past several years, these groups have undergone major taxonomic revisions and phylogenetic reclassification in order to 1) resolve the taxonomic confusion indicated by inconsistent stratigraphic ranges; and 2) emphasize the importance of wall texture and structure, the primary features used to classify modern planktic foraminifera, over the old typological species concepts (Huber and Leckie, 2011). This has resulted in the genus *Hedbergella*, to which the majority of the species found were previously assigned, being split into several distinct genera. Whereas *Hedbergella* remains, the addition of *Microhedbergella* and *Muricohedbergella* (Petrizzo and Huber, 2006; Huber and Leckie, 2011) results in a revision of species previously identified from the Manitoba Escarpment (McNeil and Caldwell, 1981; Schröder-Adams *et al.,* 2001).

4.1 Systematics

Supergroup RHIZARIA Cavalier-Smith, 2002

Class FORAMINIFERA d'Orbigny, 1826

Order GLOBIGERININA Delage and Hérouard, 1896

Superfamily ROTALIPORACEA Sigal, 1958

Family HEDBERGELLIDAE Loeblich and Tappan, 1961

Genus *Hedbergella* Brönnimann and Brown, 1958

Type species: *Anomalina lorneiana* d'Orbigny var. *trocoidea* Gandolfi, 1942

Emended description: The tests can be small to relatively large in size. Chamber walls are microperforate to finely perforate with the outer wall weakly to densely covered in perforation cones or ridges or rarely small blunt pustules. Aperture is an interiomarginal, umbilical-extraumbilical arch with a thin imperforate rim or narrow lip (Huber and Leckie, 2011).

Species included: *Hedbergella aptiana* (Bartenstein), *H. excelsa* (Longoria), *H. gorbachikae* (Glaessner), *H. praetrocoidea* (Kretzchmar and Gorbachik), *H. ruka* (Banner, Copestake, and White), and *H. trocoidea* (Gandolfi).

Stratigraphic range: species of this genus can be found throughout the Hauterivian to Upper Aptian.

Geographic distribution: species of this genus are cosmopolitan in nature.

Remarks: All previously assigned *Hedbergella* species from the Cenomanian-Turonian strata of the Manitoba Escarpment must now be relegated to a different genus. Most fall into the new genus *Muricohedbergella*, while a few are still unassigned.

Genus *Muricohedbergella* Huber and Leckie (2011)

Type species: *Muricohedbergella delrioensis* (Carsey, 1926)

Description: The tests can be small to moderate in size, coiled and very low to low trochospiral. The spiral side of the tests are evolute and the umbilical side involute. Chambers are globular and never elongated radially, and increase slowly to moderately in size as new chambers are added for a total of 4.5-7 chambers in the last whorl. Chamber walls are finely perforate with the wall pores measuring 1-2.5μm in diameter on adult chambers and variably spaced (Plate 3, 1). Wall surface is moderately to coarsely muricate or pustulose. The aperture is a low interiomarginal, umbilical-extraumbilical arch bordered by a thick flap or lip that can extend partly into the umbilical region (Huber and Leckie, 2011)

Species included: *Muricohedbergella angolae* (Caron), *M. astrepta* (Petrizzo and Huber), *M. crassa* (Bolli), ***M. delrioensis* (Carsey),** *M. flandrini* (Porthault), *M. holmdelensis* (Olsen), *M. implicata* (Michael), *M. intermedia* (Michael), ***M. loetterli* (Nauss),** *M. monmouthensis* (Olsson), ***M. planispira* (Tappan), *M. portsdownensis* (Williams-Mitchell),** *M. praelibyca* (Petrizzo and Huber), and *M. sliteri* (Huber). (Species in bold occur in the Canadian Western Interior Sea).

Stratigraphic range: species of this genus can be found throughout the Upper Albian to Maastrichtian.

Geographic distribution: these species are cosmopolitan in nature.

Full emended descriptions for *Muricohedbergella* species identified in this study can be found as follows: *Muricohedbergella delrioensis* can be found in Petrizzo and Huber (2006), *Muricohedbergella planispira* in Huber and Leckie (2011), emended descriptions for *Muricohedbergella loetterlei* and *Muricohedbergella portsdownensis* have not yet been published.

The clavate "*Hedbergella"* species *Clavihedbergella simplex* (Morrow, 1934), *C. subcretacea* (Tappan, 1943), and *C. amabilis* (Loeblich and Tappan, 1961), though their features are consistent with the genus description, are excluded from the *Muricohedbergella* for their radially elongated chamber and thus, the genus *Clavihebergella* was retained. For a reference list see Appendix 5.

Huber and Leckie (2011) have introduced a new systematic system using wall texture and structure as the primary feature for classification of fossil specimen, as is employed for identification and classification of modern planktic foraminifera, in order to resolve the taxonomic confusion within the foraminiferal fossil record, indicated by inconsistent stratigraphic ranges, and in order to retain the biostratigraphic signal that can be derived from foraminiferal analyses. This resulted in the reclassification of most of species identified in this study into the new genus *Muricohedbergella* and the reassignment of *H. amabilis* into the genus *Clavihedbergella,* with the other species characterized by radially elongated chambers; *C. simplex* and *C. subcretacea*. The extreme similarity between the species previously classified into the genus *Hedbergella* from the Manitoba Escarpment, in addition to the variability within the descriptions of these species among previously

published studies, including their size and morphological features, made identification to species level difficult. This similarity between species, often grading morphologically into each other, was noted in this study and has been proposed previously by Eicher and Worstell (1970) in their work on Cenomanian and Turonian foraminifera from the Great Plains in the United States. They noted that the morphology of *Clavihedbergella amabilis* graded into that of *Muricohedbergella delrioensis* which then graded into *M. portsdownensis*. Furthermore, *M. portsdownensis* has morphological similarities with *Whitinella aprica* which is part of a separate family (Eicher and Worstell, 1970; McNeil and Caldwell, 1981), (Table 8).

Table 8: Morphological similarity between the species previously classified into the genus *Hedbergella* and *Whiteinella aprica* from the Manitoba Escarpment as well as variability between the published descriptions of these species

Species	***M. planispira*** (maybe contains more than one taxon)	***M. loetterlei***	***C. amabilis*** (grades into *M. delrioensis* and *C. simplex*)	***M. delrioensis*** (grades into *C. amabilis* and *M. portsdownensis*)	***M. portsdownensis*** (grades into *M. delrioensis* and *W. aprica*)	***W. aprica*** (grades into *M. portsdownensis*)
Original description	Tappan (1940)	Nauss (1947)	Loeblich and Tappan (1961)	Carsey (1926)	Williams-Mitchell (1948)	Loeblich and Tappan (1961)
Size	tiny - small	small - very large	medium - large	medium - large	medium - large	large - very large
Holotype diameter	G.M.U.S. Pf.3212 = 0.23 mm Pf.3213 = 0.25 mm	G.M.U.S. Pf.3216 = 0.37 mm	G.M.U.S. Pf.3208 = 0.27 mm Pf.3209 = 0.27 mm	G.M.U.S. Pf.3210 = 0.30 mm Pf.3211 = 0.34 mm	G.M.U.S. Pf.3214 = 0.46 mm Pf.3215 = 0.29 mm	G.M.U.S. Pf.3221 = 0.49 mm
Diameter (range)	0.11 mm - 0.26 mm	0.18 mm - 0.7 mm	0.24 mm - 0.45mm	0.23 mm - 0.61mm	0.29 mm - 0.5 mm	0.45 mm - 0.70mm
Thickness	0.11 mm	0.10 mm - 0.4 mm	0.19 mm	0.27 mm	0.24 mm	---
Coil type	Trochospiral	Trochospiral/rotaliform	Trochospiral	Trochospiral/rotaliform	Trochospiral	Trochospiral
Spire height	Variable: slightly depressed - low - flat - nearly flat	Low (dorsal convexity)	Nearly flat	Variable: slightly depressed - low - flat	Low (pronounced dorsal convexity)	Variable: low - nearly flat - moderately convex
number of whorls	2 - 2.5	---	2 - 2.5	2 - 3 (all whorls visible on dorsal side)	2 - 3 (all chambers visible on spiral side)	2.5
number of chambers in last whorl	6 or 7 (5-7)	6 or 7	5 (5-6)	5 (4-6)	5 or 6 (11-12 total in dorsal spire)	5 or 6 (5-7)
chamber shape	globular - subglobular - bulbous	globular - subglobular, closely appressed	morphologically variable: subglobular to slightly elongate	much inflated, nearly spherical - globular (last chamber more inflated) - bulbous	globular not closely appressed, last chamber appearing almost detached in adult stage	globular
increase in chamber size as added	slow - regularly/gradually	rapidly in early stages, later gradually	rapidly	rapidly with few very small initial ones (slower= higher spire)	slowly	gradually (chambers in final whorl increase very little in size)
features of umbilical side	deeply umbilicate	wide umbilicus	broad and open umbilicus	deeply umbilicate and depressed - only the chambers of the last whorl visible	broadly umbilicate (only see chamber of the last whorl-turned under)	broadly umbilicate
sutures	distinct, slightly depressed, radial to gently curved constricted	distinct, depressed slightly curved	distinct, deeply constricted	distinct, deeply constricted/depressed, straight-slightly curved	distinct, deeply constricted radial	distinct, deeply constricted, radial and straight
"wall texture"	finely perforate - finely hispid (or worn smooth)	hyaline, distinctly-finely perforate	distinctly but very finely spinose	distinctly-coarsely perforate early chambers papillate, last less ornamented - sometimes with small projections - surface smooth	hyaline, finely perforate and finely cancellate	finely perforate - coarsely hispid (spines less prominent on final chambers) - weak rugosities on proximal chambers
features of the aperture:lips, flaps, or plates	Narrow bordering lip which expands as a subtriagular flap near the umbilicus, the flaps of previous chambers remain visible around the umbilical depression	no umbilical cover plates	Broad spatulate lip commonly with irregular margins	partially covered by a relatively large spatulate lip which flares slightly at its umbilical end apertural flap borders the top	bordered by a narrow lip, often broken away	narrow bordering rim flaring at the backward margin into a prominent lip. Has umbilical cover plates (high variability in their development but often broken)
test outline	---	rounded	lobate	strongly lobulate	lobulate (broadly rounded)	lobulate, rounded periphery

4.2 Bainbridge River Outcrop

The Bainbridge river outcrop exposes the Belle Fourche Member of the Ashville Formation, the Favel Formation, including the Keld and Assiniboine members, as well as the Morden Member of the Carlile Formation (Fig. 20). For a full discussion and interpretation of the lithology the reader is referred to Schröder-Adams et al. (2001).

A)

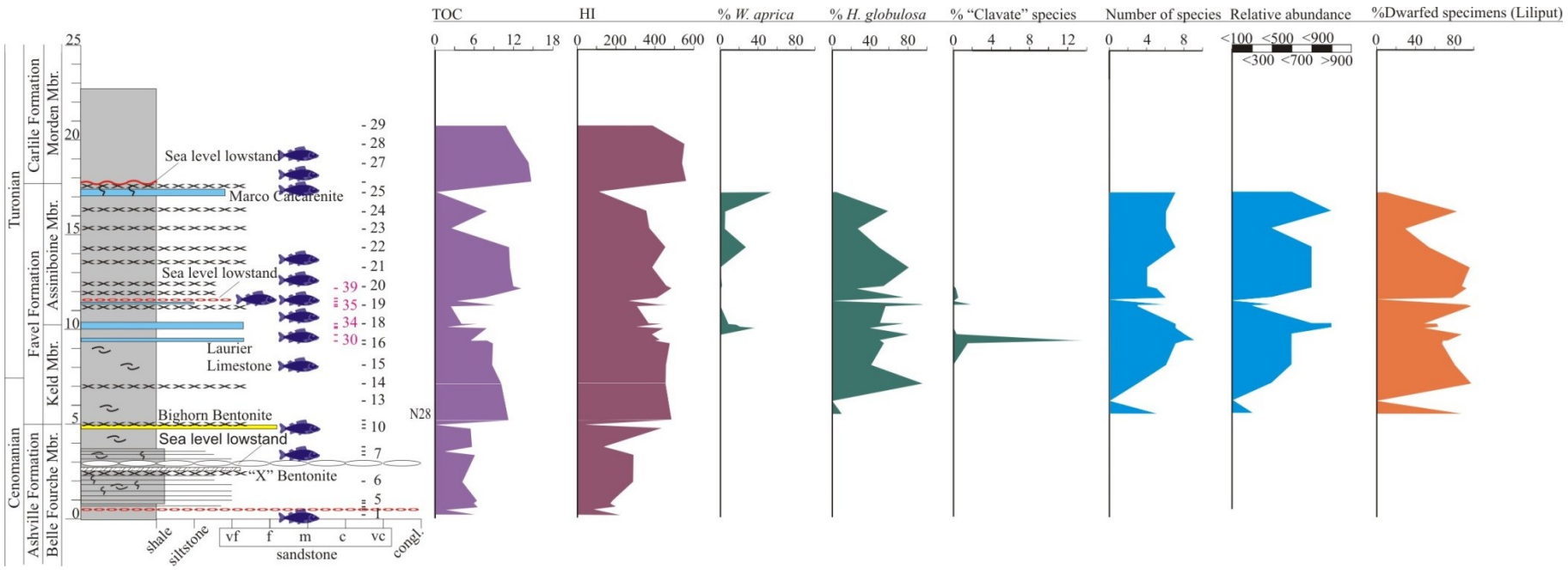
Turonian
Cenomanian
Carlile Formation
Morden Mbr.
Favel Formation
Assiniboine Mbr.
Keld Mbr.
Ashville Formation
Belle Fourche Mbr.
Sea level lowstand
Marco Calcarenite
Sea level lowstand
Laurier Limestone
Bighorn Bentonite
Sea level lowstand
"X" Bentonite
N28
shale
siltstone
vf
f
m
c
vc
sandstone
congl.
TOC
HI
% W. aprica
% H. globulosa
% "Clavate" species
Number of species
Relative abundance
<100 <500 <900
<300 <700 >900
%Dwarfed specimens (Liliput)

B)

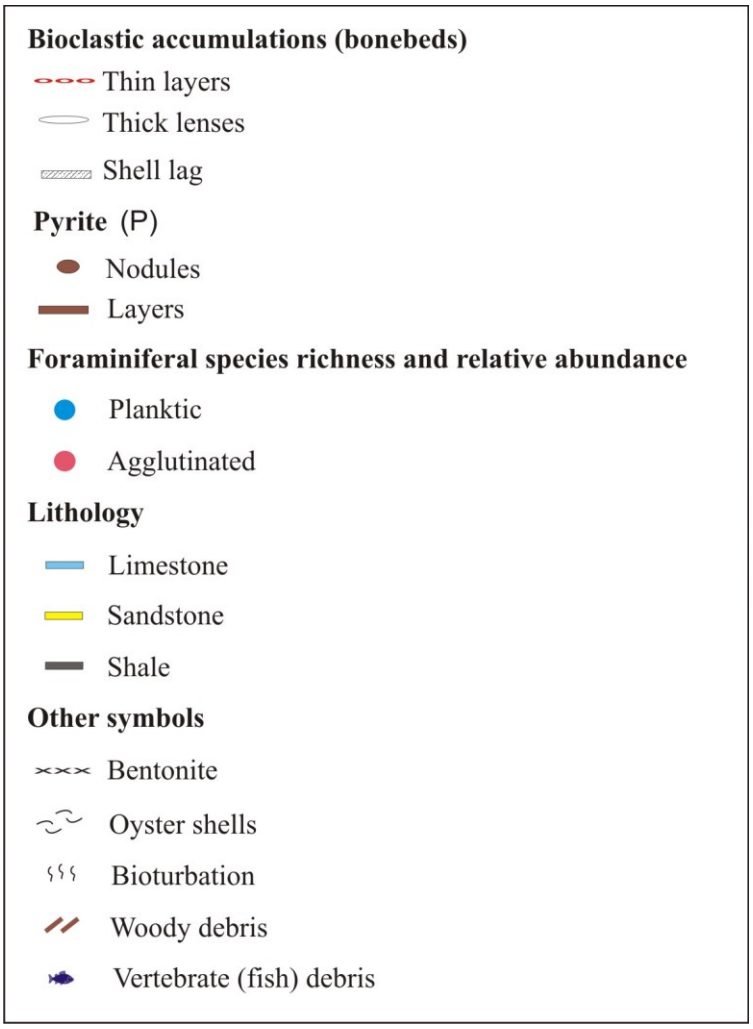

Figure 20: A) Measured section BR3 at Bainbridge River. Modified from Schröder-Adams *et al.* (2001). B) Legend of symbols.

4.2.1 Ashville Formation – Belle Fourche Member

At Bainbridge River, the Middle to Late Cenomanian Belle Fourche Member of the Ashville Formation is composed mostly of non-bioturbated, non-calcareous shale with an abundance of gypsum crystals, especially near its base. A bioclastic horizon forms the base of a coarsening upward trend with interbedded finely laminated mudrock, siltstone, and very fine bioturbated sandstone (Schröder-Adams *et al.,* 2001). A shell lag, the *Ostrea beloiti* layer, widely recognized as a regional stratigraphic marker in the WIS, overlays the X Bentonite and associated with a thick discontinuous lens-shaped bonebed forms the top of the coarsening upwards cycle which is overlain by slightly calcareous shale (McNeil and Caldwell, 1981; Schröder-Adams *et al.,* 2001; Cumbaa *et al.,* 2013). This bioclastic layer and a second marker bentonite, the Bighorn Bentonite (previously thought to be the X Bentonite), marks the base of the overlying Favel Formation and is typically seen at the lower boundary of its correlatives in Saskatchewan and the southern Alberta plains (Bloch *et al.,* 1993). The TOC values are variable, ranging between 0.03 and 6.74 wt% throughout the Belle Fourche Member, but are generally between 4.34 - 6.74 wt% except for the very low values associated with sample 2 (1.73 wt%). This horizon corresponds to a bioclastic accumulation 0.51 m above the base of the section. Sample 11 at 5 m with only 0.03 wt% TOC is the aforementioned Bighorn Bentonite at the boundary between the Ashville and Favel formations. Hydrogen index (HI) values range between 37.5 and 444.50 mg HC/g C_{org}, with a low at sample 2 (85.00 mg HC/g C_{org}) and a peak at sample 10 (444.50 mg HC/g C_{org}) at 4.80 m, suggesting a terrestrial source for the organic matter throughout the Belle Fourche Member. The foraminiferal assemblage contains no planktic species and a few specimens of the agglutinated

foraminifera *Verneuilinoides perplexus* and *Saccamina lathrami* occurring at the base of the section (Schröder-Adams *et al.,* 2001). The foraminiferal zones in the Manitoba Escarpment are the same as those found in Alberta (Fig. 21), and the foraminifera zonal marker *Verneuilinoides perplexus* places the section within the Middle to Late Cenomanian (Caldwell *et al.,* 1978; McNeil and Caldwell, 1981; Schröder-Adams *et al.,* 2001).

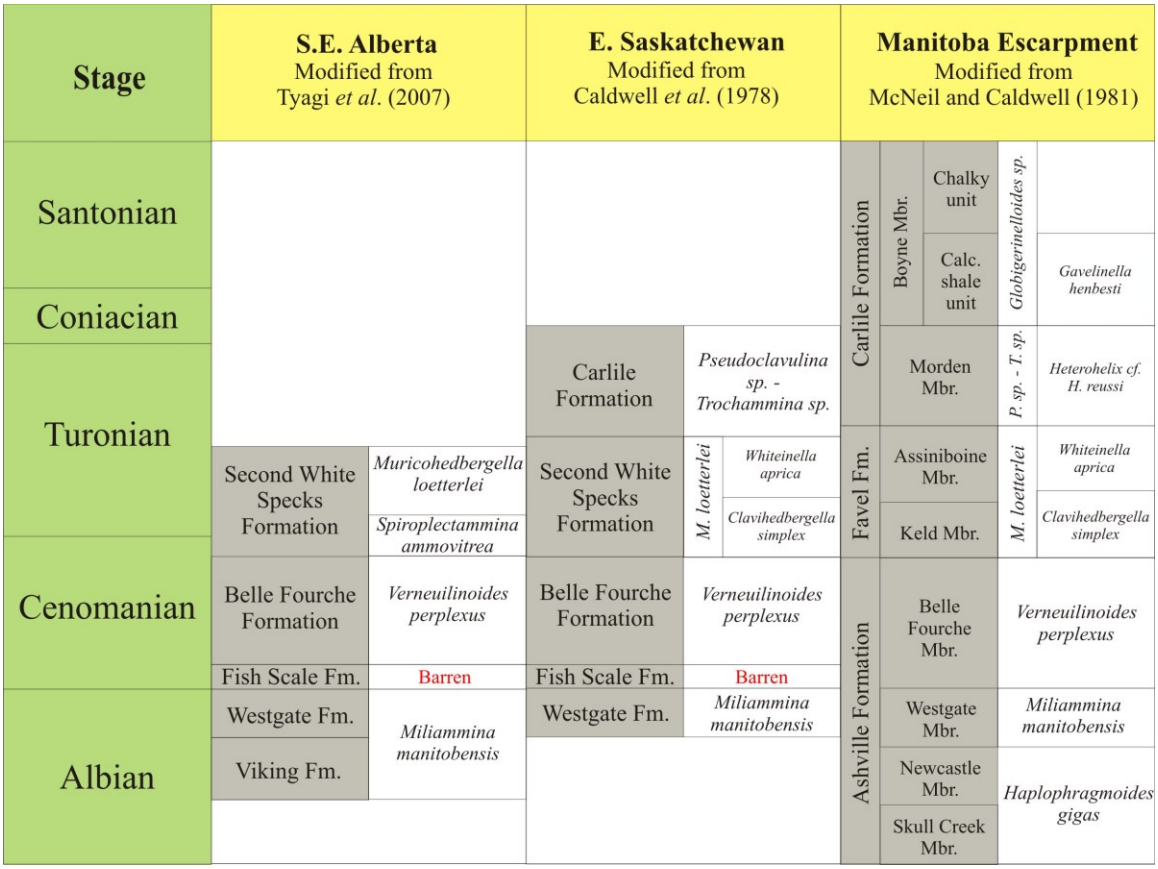

Figure 21: Foraminiferal biostratigraphic zones within the Cenomanian to Turonian Interval. Modified from Tyagi et al., (2007), Caldwell *et al.* (1978), and McNeil and Caldwell (1981).

4.2.2 Favel Formation

The Favel Formation was deposited in the latest Cenomanian through the Early to Middle Turonian and is made up of highly calcareous, finely laminated shale with a high content of organic carbon that is mainly of marine origin (Schröder-Adams *et al.,* 2001). There are abundant disarticulated vertebrate fossils dispersed throughout the formation as well as the rare complete fossil fish skeleton (Schröder-Adams *et al.,* 2001). In addition, the olive-black speckled calcareous shale of this formation contains fairly abundant coccolithophores (Plate 3,2). Inoceramid bivalves are abundant throughout the section and become concentrated to form the Laurier Limestone marking the top of the Keld Member chosen as a marker bed by McNeil and Caldwell (1981) due to its persistence in the Manitoba Escarpment (McNeil and Caldwell, 1981; Schröder-Adams *et al.,* 2001). The concentration of the inoceramid-derived calcite prisms also forms the Marco Calcarenite at the top of the Assiniboine Member (Schröder-Adams *et al.,* 2001). The Marco Calcarenite is bioturbated and its position indicates the unconformable boundary between the Favel Formation with the overlying Morden Member of the Carlile Formation. The Assiniboine Member between the Laurier Limestone and Marco Calcarenite contains seven bentonites. TOC and HI values within the Favel Formation are considerably higher than within the Belle Fourche Member of the Ashville Formation, but are variable. TOC values range between 0.20 and 13.71 wt%, while the HI values range between 112.50 and 499.00 mg HC/g C_{org} indicating at the high spectrum, increased marine productivity. Low values are associated with the Laurier Limestone (1.93 wt%, 309.50 mg HC/g C_{org}), Marco Calcarenite (0.20 wt%, 112.50 mg HC/g C_{org}), sample 37 (3.43 wt%, 269.00 mg HC/g C_{org}) representing a bioclastic accumulation at

11.50 m, and sample 23 (2.65 wt%, 377.50 mg HC/g C_{org}), an interval containing an abundance of siliceous radiolarian tests at 15.31 m.

Planktic foraminifera are abundant within the Favel strata and first appear 1.50 m above the boundary between the Ashville and Favel formations. The assemblage contains nine species including *Heterohelix globulosa*, *Muricohedbergella loetterlei*, *M. delrioensis*, *M. portsdownensis, M. planispira, Clavihedbergella simplex, C. subcretacea*, *C. amabilis*, and *Whiteinella aprica*. *Heterohelix globulosa* is a biserial taxon that dominates most of the interval and is most abundant during the first appearance of foraminifera, 1.50 m above the boundary between the Ashville and Favel formations, and immediately before and after sample 37 (11.5 m), where no foraminifera are present. This absence of foraminifera is associated with a slight dip in TOC and HI values (3.43 wt%, 269.00 mg HC/g C_{org}) and an accumulation of bioclastic material. Foraminifera return after this interval. Two clavate species, *Clavihedbergella simplex* and *C. subcretacea*, occur only near the top of the Keld Member and at the base of the Assiniboine Member in relatively low abundances before and after the barren sample.

An abundance of dwarfed tests, largely composed of *H. globulosa* as well as a smaller proportion of *H. planispira*, was observed during the initial phase of planktic occurrence, above and below the bioclastic accumulation at sample 37, as well as near the end of the planktic occurrence within the section. The benthic calcareous taxon, *Neobulimina albertensis*, was absent from the section but for one specimen observed in sample 15 (8.11 m). Sample 23 (15.31 m) within the Assiniboine Member of the Favel Formation contains fewer foraminifera and an abundance of siliceous radiolarian fossils, indicating high productivity. This assemblage forms the *Muricohedbergella loetterlei* Zone, which

in turn contains two subzones, the lower *Clavihedbergella simplex Subzone* and the upper *Whiteinella aprica* Subzone, the latter of which contains no *C. simplex* or *C. subcretacea* (Fig. 21).

4.2.3 Carlile Formation – Morden Member

The Morden Member of the Carlile Formation uncomformably overlies the Favel Formation. The portion of the Morden Member exposed at the Bainbridge River locality was deposited during the Late Turonian and is composed of black shale without any visible bedding. A thick bentonite (15cm) forms the base of the unit, overlain by one meter of slightly calcareous shale where calcareous nannofossils are present. The upper boundary is not exposed in the Bainbridge River outcrop (Schröder-Adams *et al.,* 2001). Both TOC and HI values are highest within the lower Morden Member, with TOC values ranging between 11.22 and 15.27 wt% indicating high productivity and HI values ranging between 393.50 and 573.00 mg HC/g C_{org} indicating a marine source for the organic matter. There are no foraminifera present in the Morden Member suggesting a different souce of organic matter.

4.3 Bredenbury core

The stratigraphic succession in the Bredenbury core extends from the Mannville Formation to the First White Specks Formation. Approximately 4 m of the sectionin the Westgate Formation was not recovered. This study focuses primarily on the stratigraphically equivalent strata to that seen in the Bainbridge River outcrop above the missing section including the Fish Scales, Belle Fourche, Second White Specks, and Carlile formations (Fig. 22). Bioclasts and phosphatic vertebrate remains are common

throughout the studied section but do not appear in concentrated beds such as those seen in BR3.

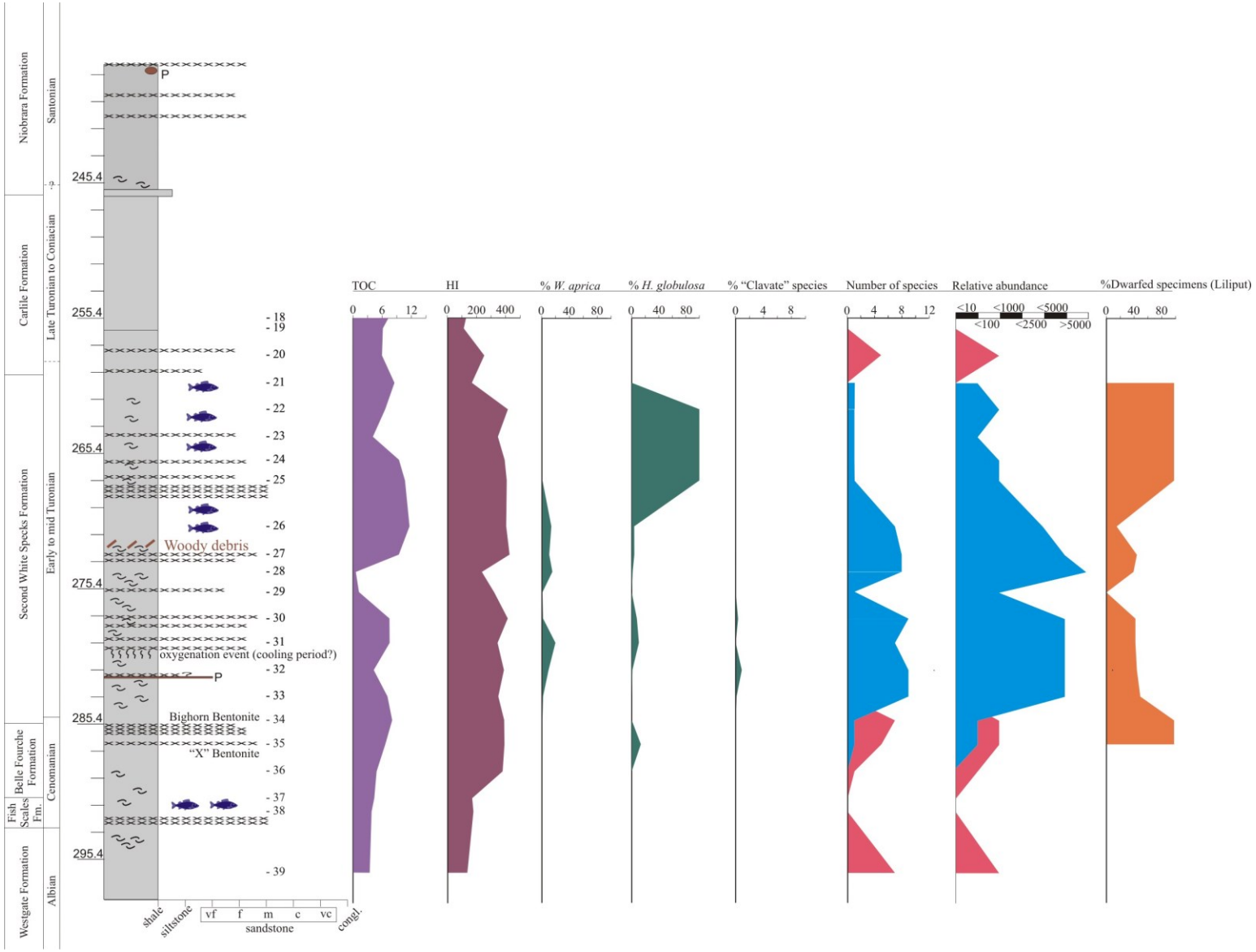
Niobrara Formation
Santonian
Carlile Formation
Late Turonian to Coniacian
Second White Specks Formation
Early to mid Turonian
Belle Fourche Formation
Fish Scales Fm.
Cenomanian
Westgate Formation
Albian
245.4
255.4
265.4
275.4
285.4
295.4
Woody debris
oxygenation event (cooling period?)
Bighorn Bentonite
"X" Bentonite
shale
siltstone
vf f m c vc
sandstone
congl.
TOC
HI
% W. aprica
% H. globulosa
% "Clavate" species
Number of species
Relative abundance
<10 <1000 <5000
<100 <2500 >5000
%Dwarfed specimens (Liliput)

Figure 22: Reference well 11-36-22-1W2 (Bredenbury). See figure 20 for legend.

4.3.1 Fish Scales Formation

The Fish Scales Formation appears to have been deposited over approximately 1.4 million years between 97.2 and 95.8 Ma (Early to Middle Cenomanian) given its dinoflagellate assemblage and stratigraphic position (Singh, 1983; Leckie *et al.,* 1992; Bloch *et al.,* 1993; Schröder-Adams *et al.,* 1996). This formation is composed of shale with abundant bioclasts including a hash of oyster shells, inoceramids, and vertebrate material sometimes appearing to form layers. Two thick bentonites (15cm and 27 cm) can be seen within the formation, the thicker one thought to be the "X" Bentonite, of the late Middle Cenomanian, dated in Western Canada at 95.87 ± 0.10Ma (Barker *et al.,* 2011). The sharp lithological contact formed by a bioclastic layer at the base of the Fish Scales Formation, the regionally recognized Fish Scales Marker Bed, is absent at this locality (Schröder-Adams *et al.,* 1996). Total organic carbon values are low in the Fish Scales Formation, increasing into the Belle Fourche Formation from 4.95 to 5.51 wt%. Hydrogen index values match this trend increasing from 181 mg HC/g C_{org} in the Fish Scales Formation to 401 mg HC/g C_{org} in the Belle Fourche Formation indicating an increasingly marine source of organic matter. This formation has widely been described as being barren of foraminifera (Schröder-Adams *et al.,* 1996).

4.3.2 Belle Fourche Formation

The Belle Fourche Formation was deposited over approximately 2.5 million years between 95.8 and 93.3 Ma, in the Late Cenomanian (Schröder-Adams *et al.,* 1996). The

unit is very thin in this core, possibly related to hiatal surfaces. It is made up of non-calcareous shale with dispersed oysters and oyster hash near the base. A series of bentonite beds is present within this formation and an 11 cm thick bentonite near its top is thought to be the Bighorn Bentonite, recognized elsewhere throughout the WISB and dated at 93.5 ± 0.20 Ma (Tyagi *et al.,* 2007), which places this interval in the earliest Turonian. Total organic carbon values increase upwards in the Belle Fourche Formation, from 5.51 to 8.99 wt%, while the HI values are high and stay relatively stable, ranging between 401 and 421 mg HC/g C_{org}. Agglutinated foraminifera are found within the Belle Fourche Formation including *Trochammina rainwateri* and *Verneuilinoides perplexus* representing the *Verneuilinoides perplexus* Zone (Fig. 20) of the Middle to Late Cenomanian (Schröder-Adams *et al.,* 1996). Planktic foraminifera begin appearing near the top of the Belle Fourche Formation slightly below the Bighorn Bentonite. The low diversity and low abundance agglutinated foraminifera, which form a low diversity, low density assemblage in the Belle Fourche Formation, disappears at the boundary to the Favel Formation. The initial planktic assemblage is made up of small spiral species of *Muricohedbergella*, *Clavihedbergella amabilis,* and the biserial species *Heterohelix globulosa*, all of which are dwarfed in size.

4.3.3 Second White Specks Formation

The Second White Specks Formation was deposited over approximately 2.3 million years between 93.5 and 91.2 Ma, covering the Early to Middle Turonian (Schröder-Adams *et al.,* 1996). The lithology is made up of calcareous shale, almost chalky in this core, with abundant shell material, dispersed fish remains, abundant inoceramids (whole valves,

valve fragments, and individual calcite prisms), and occurrences of planktic foraminifera and calcareous nannofossils throughout (Schröder-Adams *et al.,* 1996). A pyrite layer occurs within the basal unit that is overlain by mudstone containing several bentonite layers, which in turn is topped by a layer containing woody debris. Overlying this layer is a shale barren of shells followed by mudstone containing dispersed bioclastic material and several other bentonite layers. Anoxic conditions in sediment pore waters are evidenced by the growth of pyrite framboids on the foraminiferal tests that were deposited during this time (Plate 3, 3). Total organic carbon and Hydrogen index values are high within the Second White Specks Formation. Total organic carbon values are highly variable, ranging between 0.82 and 12.62 wt%, with particularly low values at sample 28 (273.30 m) and sample 29 (275.60 m). Hydrogen index values are relatively stable, ranging between 177.00 and 447.00 mg HC/g C_{org}.

The base of the Second White Specks Formation is placed where a slightly more diverse planktic foraminiferal assemblage appears. Overall, planktic specimens are extremely abundant, with sample sizes up to five times larger than those from equivalent strata exposed in outcrop in the Bainbridge River. The assemblage contains nine species including *Heterohelix globulosa*, *Muricohedbergella loetterlei*, *M. delrioensis*, *M. portsdownensis, M. planispira, Clavihedbergella simplex, C. subcretacea, C. amabilis* (Loeblich and Tappan, 1961), and *Whiteinella aprica*. *Heterohelix globulosa* dominates the top of the interval, and accounts for 100% of the foraminifera between 262.30 and 268.90 m, while the two clavate species, *C. simplex* and *C. subcretacea*, occur only above and below the pyrite layer at 282.0 m. The low TOC values at sample 29 coincide with a dramatic loss in foraminiferal abundance and diversity. Dwarfed specimens are abundant

throughout most of the Second White Specks Formation but are particularly abundant during and after bentonite layers at the base of the unit, between 290.80 and 291.7 m, as well as at the top of the formation where 100% of *H. globulosa* are dwarfed in size.

4.3.4 Carlile Formation

The Carlile Formation was deposited during the Late Turonian and into the Coniacian and is composed of non-calcareous shale with thin calcareous horizons. Two thin bentonites layers (1 cm each) occur at its base, and it is overlain by the First White Specks Member of the Niobrara Formation. The rock is clay rich. Total organic carbon and hydrogen index values are lower than those in the Second White Specks Formation but higher than the values seen in the Fish Scales Formation. Total organic carbon values range between 6.46 and 7.91 wt% and hydrogen index values range between 134.00 and 274.00 mg HC/g C_{org}. The foraminiferal assemblage within the Carlile Formation is made up of agglutinated foraminifera including *Haplophragmoides hendersonense, Trochammina ribstonenses,* and *Pseudobolivina rollaensis* (Schröder-Adams *et al.,* 1996) suggesting a late Turonian to earliest Coniacian time.

5. DISCUSSION

5.1 Surface to Outcrop Correlation

The Bredenbury core (BDC) and Bainbridge River outcrop (BR3) were correlated using lithology, bentonites, and biostratigraphic information. The following differences in lithology are observed: 1) thick bioclastic accumulations only occur in outcrop, whereas the core has phosphatic material thinly scattered throughout the succession; 2) shelly

concentrates occur in the core while in outcrop they occur as densely packed limestones without terrigenous components; 3) bentonite beds are significantly more abundant in core than in the outcrop; and 4) the overall thickness of the interval thins from west (core) to east (outcrop). These differences are explained by the increasingly proximal position of the outcrop locality where fairweather wave-base is reached, resulting in winnowing processes that in-turn concentrate phosphatic and calcareous bioclastic material and prevent preservation of bentonite beds. The reduced thickness of strata in outcrop is explained by reduced accommodation space and possibly hiatuses throughout.

Biostratigraphic information can also provide information useful for correlation between the core and outcrop sections. The shallow waters and the low gradient make this region particularly sensitive to changes. Consequently, the sea-level fluctuations during this interval have a strong affect on the foraminiferal assemblage. The foraminiferal assemblage also reacts to the frequent perturbations in their environment, such as recurring ash falls, and can provide signs for periods of catastrophic environmental change.

5.2 Biotic stress and the Lilliput effect

Various biotic stresses may have operated during the Cenomanian-Turonian interval. These include the extreme greenhouse warming (Schlanger and Jenkyns, 1976; Price *et al.,* 1995; Norris *et al.,* 2002; Wilson and Norris, 2003; Hasegawa et al 2012; Hay and Floegel, 2012; Friedrich *et al.,* 2012), the increased volcanism (Bagshaw, 1977; Bloch *et al.,* 1993, 1999; Schröder-Adams *et al.,* 2001; Keller and Pardo, 2004b; Tyagi et al. 2007), whose ashfalls are seen in outcrop and core as bentonites, pervasive low oxygen

levels (Schröder-Adams *et al.,* 2001; Leckie *et al.,* 2002; Keller and Pardo, 2004b), as well as changing sea levels on the already shallow margin of the epicontinental sea (Plint and Kreitner, 2007; Gale *et al.,* 2008). These events throughout the Cenomanian-Turonian interval could have impacted the foraminifera both locally and in the broader region.

Negative biotic effects can be seen in the fossil record of foraminifera as a reduction in species diversity, which may coincide with the removal of all benthic or all planktic foraminifera from the assemblage. For example, the absence of benthic species during OAEs in the Cretaceous has been interpreted as the result of inhospitable bottom water conditions during these global events. An expansion of the oxygen minimum zone after OAE-2 is interpreted for the WIS, which created inhospitable surface water conditions and may have caused many planktic foraminifera to become extinct, ex: the keeled genus *Rotalipora* (Eicher and Worstell, 1970; Schröder-Adams *et al.,* 1996; Leckie *et al.,* 2002; Keller and Pardo, 2004b). In addition, biotic effects can include changes in foraminiferal assemblage resulting in an abundance of "disaster opportunists" or other small unornamented opportunistic species (Keller and Pardo, 2004a). These species are tolerant to variable, harsh, and low-oxygen conditions (Keller and Pardo, 2004a). Disaster opportunist species such as the planktic group *Guembelitrinidae*, including the species *Guembelitria cretacea*, become abundant to dominant during periods of high biotic stress (Leckie *et al.,* 1998; Keller and Pardo, 2004a). Due to their small size (38-100µm) they are often missed in routine foraminiferal analysis (Keller and Pardo, 2004a).

In addition to an abundance of these opportunistic species, severe biotic effects can be seen by the presence of "dwarfed" specimens of larger species as well as specimen showing modification in their ontogenetic growth (Keller and Pardo, 2004a). These changes in test size have been noted in foraminiferal assemblages right before extinction events as well as in studies of high stress environments (Keller and Pardo, 2004a; Keller and Abramovich, 2009; Wade and Olsson, 2009; Waskowska, 2011). High stress environments can be a result of several factors including high levels of nutrient influx leading to eutrophic waters and toxic conditions for foraminifera (Keller and Pardo, 2004a). These nutrients can come from terrestrial sources in form of weathering (increased during rapid climate change) and continental runoff, or from volcanic sources such as ash falls (Keller and Pardo, 2004a; Tantawy *et al.,* 2009). High stress can also be induced by environmental changes such as temperature variations associated with volcanism or greenhouse warming (Twitchett, 2006, 2007; Keller and Abramovich, 2009), sea-level fall in shallow nearshore environments, stratification and poor mixing of the water column often resulting in low-oxygen, including dysoxic to anoxic benthic conditions, creating harsh living conditions for foraminifera and other organisms living within the Cretaceous WIS (Schröder-Adams *et al.,* 1996; Schöder-Adams *et al.,* 2001; Keller and Pardo, 2004a; Keller and Abramovich, 2009; Tantawy *et al.,* 2009). At their most severe state, catastrophic environmental changes can cause extinction (Schröder-Adams *et al.,* 1996; Keller and Pardo, 2004a; Peryt, 2004; Keller, 2008; Keller and Abramovich, 2009).

Reduced species richness in association with an increase in number of small species and dwarfed specimens, characteristic of high stress environments, is termed the Lilliput

effect. This term was coined by Urbanek (1993) describing the effects of "post-event syndrome" affecting surviving taxa after an extinction event including low diversities, high abundances, and the reduction in size of tests (Twitchett, 2006 and 2007). This reduction in size can be separated into two main outcomes: 1 – morphological size reduction, evidenced by the removal of large bodied foraminifera from the assemblage, and 2 – intraspecies size reduction, evidenced by dwarfing of the foraminifera test size due to stunted growth. Both these outcomes can be seen in the foraminifera from the BDC and BR3.

Species richness at both study sites is small, totalling up to nine species, but only rarely more than six or seven. The assemblage includes the biserial *Heterohelix globulosa* as well as the closely related group of foraminifera containing *Muricohedbergella loetterlei*, *M. planispira*, *M. delrioensis, M. portsdownensis, Clavihedbergella simplex, C. subcretacea*, *C. amabilis* (Loeblich and Tappan, 1961), as well as *Whiteinella aprica*. This group of foraminifera is known for their abundance in open ocean and epicontinental sea settings (Leckie *et al.,* 1998). They are widely distributed, a few specimens being found as far as the Arctic slope (Tappan, 1962), and as a group, they have been called the "weeds of the Mid-Cretaceous ocean" being among the most widespread and abundant species in the Greenhorn Sea, especially *Muricohedbergella delrioensis, M. planispira,* and *M. loetterlei* (Leckie *et al.,* 1998; Eicher and Worstell, 1970; McNeil and Caldwell, 1981; Schröder-Adams *et al.,* 1996). In addition, *Heterohelix globulosa* is noted for its abundance in warm, shallow proximal waters of epicontinental seas (Leckie *et al.,* 1998). It is not surprising then to find that they are tolerant to even harsh living conditions like those reported throughout the Cretaceous

WIS. In fact, Heterohelicids and Hedbergellids (now Muricohedbergellids) make up the survivor assemblage with some disaster opportunists in some localities after the K/T mass extinction, though their population was much reduced, further showing their tolerance for even the harshest conditions (Keller and Abramovich, 2009).

Foraminiferal diversity throughout the Cenomanian-Turonian interval in the U.S. portion of the seaway is higher than in the Canadian portion though species of the genera *Heterohelix* and *Muricohedbergella* remain the dominant components of the assemblages (Eicher and Worstell, 1970; Keller and Pardo, 2004b). In their study of the Cenomanian and Turonian foraminifera of the Great Plains of the United States, Eicher and Worstell (1970) found that throughout Kansas and eastern Colorado, *Heterohelix* and *Muricohedbergella* were the first planktic foraminifera to appear in an assemblage as well as the last to disappear. To the east and to the north, other foraminiferal genera only appeared much later when compared to locations situated further into the basin. These east and north locations also showed assemblages with lower abundances and lower overall diversity. Eicher and Worstell (1970) split the Cenomanian-Turonian interval into three subintervals; a lower planktic zone corresponding to the Upper Cenomanian, a benthic zone corresponding to the Lowest Turonian, and an upper planktic zone ranging into the Middle Turonian.

The lower planktic zone is almost entirely dominated by planktic foraminifera, with a high proportion of *Heterohelix* and *Muricohedbergella* species, especially in the north, and only few low-oxygen tolerant benthic *Neobulimina albertensis* specimens. Upper Cenomanian assemblages from Pueblo, Colorado show an absence of deeper-dwelling

planktic species such as the keeled rotaliporids and globoruncanids as well as the weakly keeled praeglobotruncanids and dicarinellids, and only contain small numbers of these later in the Turonian (Keller and Pardo, 2004b). Their rarity is interpreted as the result of shallow waters and a well-developed oxygen minimum zone present during this interval. They were more successful in more open sea environments within the WIS (Keller and Pardo, 2004b). This interval is dominated by oxygen minimum zone dwellers, the biserial planktic foraminifera *Heterohelix moremani* and *H. reussi*. Widespread dysoxic conditions that persisted throughout the middle to late Cenomanian, are also documented for parts of the Canadian WIS (Schröder-Adams *et al.,* 1996), evidenced by the limited to absent benthic foraminiferal assemblage and lack of bioturbation throughout the Cenomanian of the studied sections. These conditions could also have inhibited deeper dwelling keeled foraminifera from inhabiting this region. Studied sections also show an abundance of *Heterohelix* though the species present is *H. globulosa.*

The benthic zone noted by Eicher and Worstell (1970) for the early Turonian in the American WIS, represents a short interval of basinwide improvement of bottom water conditions as well as improved conditions throughout the water column. In this zone, they noted the appearance of a diverse assemblage of benthic species as well as a diversification of planktic species. This may be associated with a short-term cooling event documented for this time (Friedrich *et al.,* 2012). In the studied interval at BDC, a short oxygenation event, evidenced by the presence of a bioturbated interval (depth: 280 m), may be the manifestation of this benthic zone in Canada. This bioturbated interval is not present at BR3.

The upper planktic zone in the American WIS signifies a return to limiting bottom water conditions and low oxygen interpreted as the result of a shallowing within the basin (Eicher and Worstell, 1970). In this zone, the genera *Heterohelix* and *Muricohedbergella* are dominant once again, though lower in abundance than in the lower planktic zone. Only a few benthic species such as *N. albertensis* and *Gavelinella dakotensis* persist into this zone in the American WIS before disappearing in the early-Mid Turonian in conjunction with a reduction in planktic diversity. In easternmost Colorado species of the genera *Heterohelix* and *Muricohedbergella* become the only species present in the assemblage and these two genera are increasingly dominant and become smaller in size through the Turonian before disappearing entirely in the Middle Turonian as benthic foraminifera reappear (Eicher and Worstell, 1970). No benthic foraminifera were found before the disappearance of the planktic assemblage at BDC, though one *N. albertensis* specimen was counted at BR3 sample 23, at 15.31 m (Fig. 19). An increase in smaller specimen is also noted in both sections during this interval.

In the US portion of the seaway other species of planktic foraminifera are also common, including globigerinellids in surface waters and Guembelitrids in eutrophic waters representing intervals of ecologically stressful conditions (Keller and Pardo, 2004b). These species are not seen in the Canadian section. The overall reduction in planktic foraminifera diversity northward within the United States into the Canadian WIS can in part be attributed to temperature gradients, especially for the surface dwelling species; however, during the Cenomanian-Turonian interval, extreme hothouse conditions prevailed and temperature gradients were reduced (Hasegawa *et al.,* 2012). The disappearance of deep-dwelling foraminifera such as the keeled genera from the Late

Cenomanian assemblage of the American WIS is interpreted to reflect the reduced open marine conditions and an expanded oxygen minimum zone; the poor stratification of the upper water column was insufficient to support a diverse planktic community (Eicher and Wostell, 1970; Keller and Pardo, 2004b). The abrupt drop in planktic diversity towards the north is also interpreted, not the result of temperature gradients but rather, as a result of changes in conditions within the basin. The location of this abrupt drop in diversity is interpreted to be the manifestation of the approximate limit of circulation from undiluted open ocean currents (Eicher and Worstell, 1970). The drop in diversity to the east is also interpreted to be a result of changing conditions from a deeper and more open ocean setting to a shallow and marginal setting. This paucity of planktic foraminiferal species extends northward into Canada in the Manitoba Escarpment.

5.3 Correlation of planktic foraminiferal assemblages

Five main correlation lines were identified between the studied subsurface and outcrop sections. (Fig. 23; correlation lines ① - ⑤). The lithostratigraphic boundary between the Belle Fourche and Second White Specks formations in the subsurface and the Ashville and Favel formations in outcrop is often placed at the contact between non-calcareous and calcareous shale. This boundary can be diachronous. Therefore, I place that boundary right above the Bighorn Bentonite, a regionally extensive chronostratigraphic surface (Barker *et al.,* 2011). Using the bentonite as datum, planktic foraminifera at Bredenbury (BDC) first appear in the upper Belle Fourche Formation right below the bentonite. At the more proximal site of Bainbridge River (BR3), the planktic foraminiferal assemblage only appears in the lower Favel Formation above the bentonite (Fig. 23; correlation line

1). The poor planktic foraminiferal diversity at both sites is indicative of somewhat inhospitable environmental conditions during this interval. During the deposition of the Belle Fourche Formation at BDC, harsh environmental conditions resulted in stunted growth of the foraminiferal tests deposited there. On the other hand, conditions during the deposition of the Belle Fourche Member of the Ashville Formation at BR3 were not suitable to support planktic foraminifera. The shallower water at this more proximal site was more susceptible to turbidity in the water column. Nonetheless, the initial planktic occurrence at both sites shows a similar pattern, beginning with low diversity, low abundance, and dwarfed test sizes (Fig. 20 & 22), although at BR3 the assemblage is dominated by *Heterohelix globulosa* in this interval, contrary to the higher abundance of spiral foraminifera at BDC. *Whiteinella aprica,* a species that prefers more open ocean conditions, is absent in the initial phase of planktic occurrence at both localities.

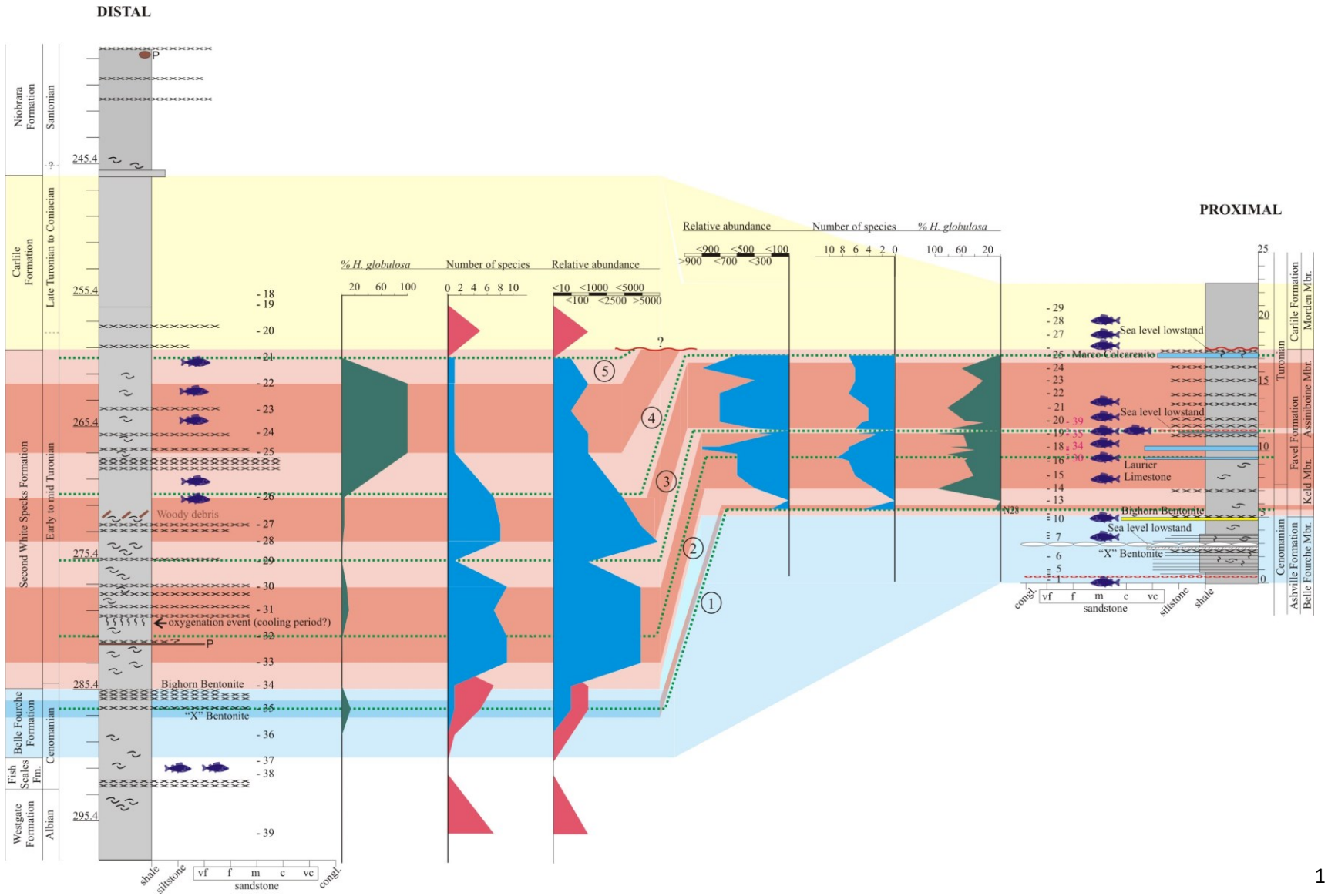
DISTAL
PROXIMAL
Niobrara Formation
Santonian
Carlile Formation
Late Turonian to Coniacian
Second White Speeks Formation
Early to mid Turonian
Belle Fourche Formation
Cenomanian
Fish Scales Fm.
Westgate Formation
Albian
245.4
255.4
265.4
275.4
285.4
295.4
Woody debris
oxygenation event (cooling period?)
Bighorn Bentonite
"X" Bentonite
% H. globulosa
Number of species
Relative abundance
Sea level lowstand
Marco Calcarenite
Laurier Limestone
N28
Turonian
Cenomanian
Carlile Formation
Morden Mbr.
Favel Formation
Assiniboine Mbr.
Keld Mbr.
Ashville Formation
Belle Fourche Mbr.
shale
siltstone
vf f m c vc
sandstone
congl.

Figure 23: Change in planktic foraminiferal diversity and abundance (blue), and % *H. globulosa* at BDC and BR3. Although there are more fluctuations in BR3 (probably due to denser sampling at this site), trends can be seen between the two localities, where dominance in *H. globulosa* coincides with low diversities during intervals of higher biotic stress. The five correlation lines are 1) the initial planktic occurence; 2) the appearance of clavate (*C. simplex* and *C. subcretacea*) species; 3) the presence of very few poorly preserved specimen of *Muricohedbergella sp*. at BDC and loss of all foraminifera in BR3; 4) a decline in foraminiferal diversity and abundance; 5) the loss of the planktic assemblage. See Figure 20 for legend of symbols.

5.3.1 Opportunistic species

The presence of opportunistic species can indicate particularly harsh conditions which can be associated with a variety of stressors within this dynamic time interval. Many of the species observed at the two locations studied are considered opportunistic in nature. The genus *Heterohelix (H. globulosa)* has distinguished itself over the spiral foraminifera in this assemblage as being particularly tolerant to inhospitable conditions, in addition to being low-oxygen tolerant and able to tolerate a large range of ecological conditions (Leckie, 1985; Keller and Pardo, 2004b). This taxon is also one of the few species to thrive in many localities during the OAE-2 and the associated expansion of the oxygen minimum zone (Leckie *et al.,* 1998; Keller *et al.,* 2001; Leckie *et al.,* 2002; Coccioni and Luciani, 2005). The dominance of *H. globulosa* in association with a drop in species diversity in the section, which may indicate an increase in biotic stress, can be correlated between the two sections (Fig. 23), although the higher proportion of *H. globulosa* in the

assemblage at BR3 indicates that this site was a higher stress environment than BDC, possibly related to its more proximal position to the paleoshoreline. In addition, the fluctuations in the percentage of this species appear to show a higher variability of the environment at the seaway margin (BR3) compared to within the, still shallow, basin (BDC); though this may be, in part, caused by the smaller sampling interval at BR3.

At both sites, foraminiferal diversity increases upwards in the Favel Formation and its equivalent, the Second White Specks Formation. The dominance of *H. globulosa* in this interval continues at BR3. *Whiteinella aprica*, a large species, only occurs well up into the Favel Formation at BR3, whereas it occurs at a lower position at BDC, indicating more favorable conditions for foraminifera. The proportion of this large species in the assemblage is associated with the proportion of *H. globulosa*. When *H. globulosa* is dominant, only a small percentage of the assemblage is made up of *W. aprica*, and when the proportion of *H. globulosa d*ecreases, the percentage of *W. aprica* increases.

5.3.2 Elongated forms and anoxia

Near the top of the Keld Member, and again at the base of the Assiniboine Member of the Favel Formation at BR3 there is a sudden appearance of the two clavate species: *Clavihedbergella simplex* and *C. subcretacea.* These species can also be seen in the Second White Specks Formation at BDC, although their prominence in the assemblage is lower. These two species occur over two restricted intervals in both sections. At BR3 the first spike occurs within the accumulation of inoceramid-derived calcite prisms that forms the first of the Laurier Limestone beds (Fig. 23: correlation line 2), while the second occurrence straddles a bioclastic horizon. This horizon is associated with the

sudden disappearance of all foraminifera, and the proportion of clavate species above this layer is very low (<0.5%). At BDC, the first spike falls just after a distinct pyrite layer, at 282.0 m (Fig. 23: correlation line 2), while the second occurrence falls just below sample 29 (275.6 m) which contains only 38 poorly preserved specimens of *Muricohedbergella* sp.

Recently, elongated chambers in planktic foraminifera have been interpreted as an adaptive response to dysoxic conditions due to the increasing abundance of these forms near and within sediments that record OAEs (eg. BouDagher-Fadel *et al.,* 1997; Coccioni and Luciani, 2004, 2005). A recent study by Coccioni et al. (2006) has investigated this phenomenon and has concluded that the conditions related to the development of the OAEs favour the development or foraminifera with elongated chambers, though other environmental factors such as increased upper water column stratification, greater productivity, and/or greater seasonality play a role in the distribution and proliferation of these forms.

The appearance of the two clavate species *Clavihedbergella simplex* and *C. subcretacea* at BR3 and BDC is interpreted as a response to a short-lived but severe change in the environment seen at both localities. At BDC, their first appearance falls just after a distinct pyrite layer, a sign of anoxia (Canfield and Raiswell, 1991), and the other falls within a group of bentonite layers, which has negative effects on biota in the water column including increasing acidity, and increased turbidity which may promote bacterial growth creating eutrophic conditions, which can lead to the formation of dysoxic surface waters (Leckie *et al.,* 2002; Stewart *et al.,* 2006). Interestingly, between the first and

second appearance of *C. simplex* and *C. subcretacea* at BDC there is an interval with intense bioturbation, indicating sufficient levels of oxygen were present for bottom dwellers to survive and alluding to the complex changes in this paleo-ecosystem.

At BR3 the first spike of *C. simplex* and *C. subcretacea* occurs within the accumulation of inoceramid-derived calcite prisms that form the first of the Laurier Limestone beds, indicating that low oxygen conditions dominated for a short time. Their abundance is relatively high but drops suddenly when the abundance of *W. aprica* begins to rise, indicating a return to more normal conditions. The second occurrence of *C. simplex* and *C. subcretacea* at BR3 straddles a bioclastic horizon devoid of foraminifera. The clavate specimens indicate that low-oxygen conditions may have extended up into the photic zone (cf. Coccioni et al., 2006). This expansion of the oxygen minimum zone may have been a major biotic stress affecting the planktic foraminiferal assemblage and causing the overall reduction in foraminiferal abundance and diversity seen in this interval.

Associated with the presence of *Clavihedbergella* species at BR3, species richness and relative abundance (including a low to absent proportion of *W. aprica*) decrease before the sudden loss of all foraminifera, and an increase in the percent dwarfed specimens and an increase in the dominance of *H. globulosa* in the assemblage can be noted, persisting after the recovery of foraminiferal diversity. At BDC, this pattern is not readily apparent, possibly due to the larger sampling interval.

5.3.3 Morphological size reduction and intraspecies size reduction

These changes in diversity within the foraminiferal assemblage are interpreted to be related to variations in environmental stress in the WIS. Changes in diversity have been applied to many continental shelf settings as a measure of biotic stress (Keller and Abramovich, 2009). This same method can be applied to the WIS by illustrating the selectivity (based on size) of the reduction in assemblage diversity, such as the removal of the large species *Whiteinella aprica* in times of high biotic stress (when *H. globulosa* is dominant). Foraminiferal assemblages can be characterized as optimal assemblages, high-stress assemblages, and disaster assemblages (Keller and Abramovich, 2009).

An optimal assemblage—one that existed during ideal living conditions—should exhibit a high diversity of species with species ranging in test size, from small to large, and in test ornamentation, from simple to complex (Keller and Pardo, 2004a; Keller and Abramovich, 2009). The foraminiferal assemblages in BDC and BR3 have low diversities, as is typical of assemblages in epeiric sea strata versus open-ocean strata: the samples typically contain no more than seven to a maximum of only nine species. The assemblages are therefore considered "sub-optimal". In addition, the assemblages at both localities are composed mainly of resistant, opportunistic species (genus *Muricohedbergella* and *Heterohelix*), reflecting the stressed environment (Leckie, 1987; Leckie *et al.,* 1998, Keller, 2003; Keller and Pardo, 2004a). However, evidence of morphological size reduction can still be seen in the assemblage from both sections by observing changes in the proportion of *Whiteinella aprica*, the largest species in the assemblage (Fig. 24). An increase in the proportion of *W. aprica* present in the

assemblage is interpreted to indicate a return to more normal conditions within the seaway while increased environmental stress is reflected by a lower proportion of *W. aprica* and the increased proportion of *H. globulosa*.

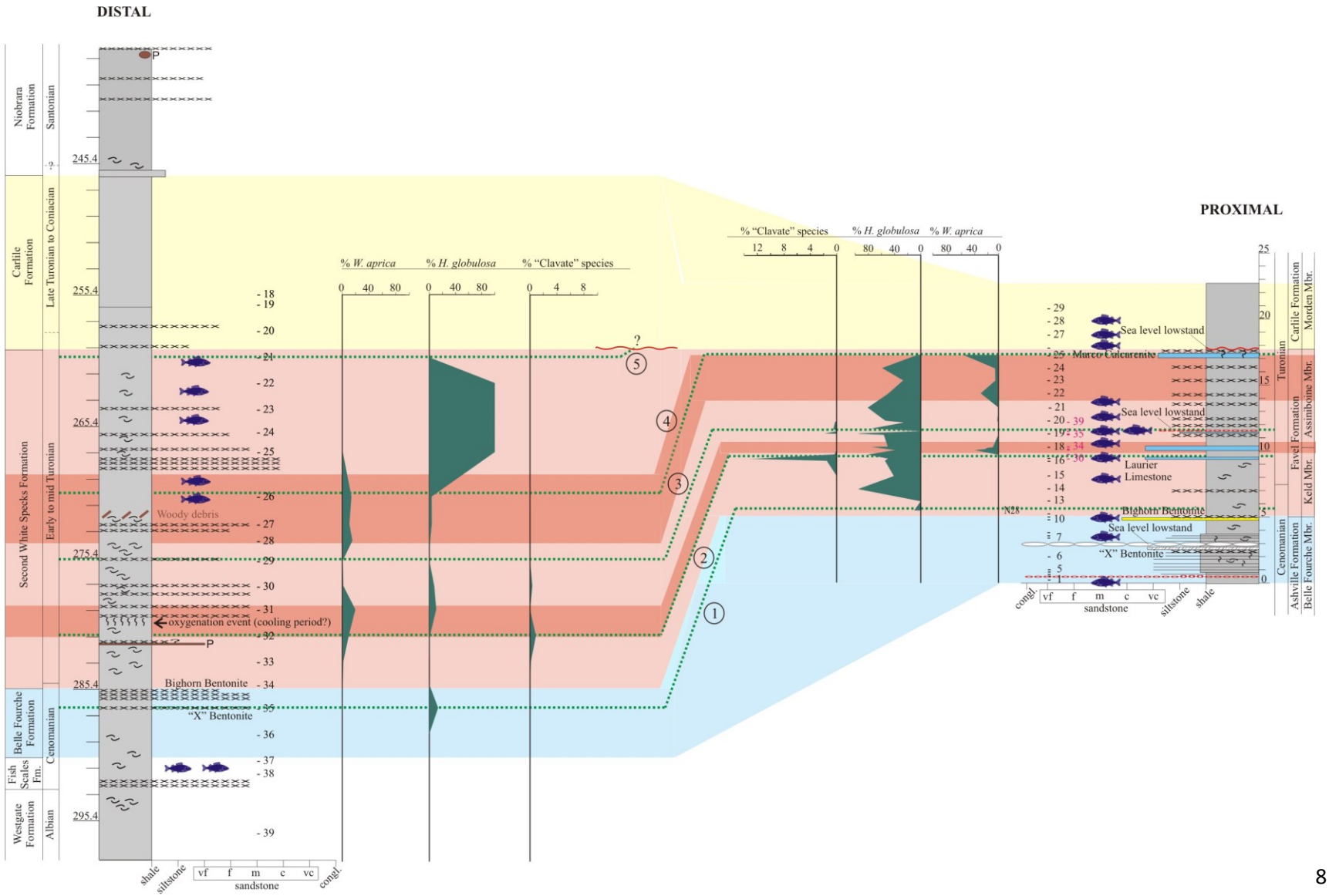
DISTAL
PROXIMAL
Niobrara Formation
Santonian
Carlile Formation
Late Turonian to Coniacian
Second White Specks Formation
Early to mid Turonian
Belle Fourche Formation
Cenomanian
Fish Scales Fm.
Westgate Formation
Albian
245.4
255.4
265.4
275.4
285.4
295.4
Woody debris
oxygenation event (cooling period?)
Bighorn Bentonite
"X" Bentonite
% W. aprica
% H. globulosa
% "Clavate" species
shale
siltstone
vf f m c vc
sandstone
congl.
Sea level lowstand
Murco Calcarenite
Laurier Limestone
Turonian
Cenomanian
Carlile Formation
Morden Mbr.
Favel Formation
Assiniboine Mbr.
Keld Mbr.
Ashville Formation
Belle Fourche Mbr.

Figure 24: Variations in percentage of *Whiteinella aprica* in the assemblage in comparison to more ecologically tolerant species. This large species has a reduced abundance or is removed entirely during intervals with exceptionally high biotic stress. Both BR3 and BDC show two periods of relatively high abundance. Correlation lines are also indicated. See figure 20 for legend.

At BDC, there are two intervals within the Second White Specks Formation where *W. aprica* becomes more abundant. The first is over the interval of bioturbation interpreted as the Canadian record of a cooling event described by Friedrich *et al.,* (2012). This interval has relatively high TOC and HI values attesting to increased marine productivity. This short oxygenation event helped the foraminiferal assemblage attain higher diversity of species and abundance of individuals, including the larger *W. aprica*. At BR3, the first appearance of *W. aprica* is within the interval containing the Laurier Limestone. Numerous authors have documented calcarenites interbedded with mudrock from the U.S. portion of the Upper Cretaceous WISB sediment fill and interpreted them as tempestites formed in response to impingement by storm wave base (e.g., Cobban and Scott, 1972; Kauffman, 1977a, b; Hattin, 1975, 1986; Sageman, 1989; Brett, 1995; Sageman; 1996; Shimada *et al.,* 2006; Gale *et al.,* 2008). These more frequent storms may have interrupted stratification and the oxygen minimum zone, allowing *W. aprica,* possibly a deeper dweller than *Muricohedbergella* and *Heterohelix* (Leckie, 1985), to become more abundant.

At BDC, the second interval with a relatively high abundance of *W. aprica* occurs in the middle of the Second White Specks Formation. Total organic carbon and hydrogen index

values are again high at this time indicating high productivity from a marine source. The woody debris layer contained within this interval is anomalous; however, it could be the result of transportation by a large event such as a storm or tsunami. *Whiteinella aprica* declines in abundance and is replaced by *H. globulosa,* which becomes the only component of the assemblage, after a bentonite swarm in the upper 10 m of the Second White Specks Formation. At BR3 and in the core, where *W. aprica* is abundant, HI values are also high, indicating a marine source of organic material and relatively high TOC throughout, indicating high productivity, but for a short dip at sample 23 (Fig. 24), where *W. aprica* also loses abundance. At BR3, all foraminifera disappear abruptly from the section at the boundary between the Favel and Carlile formations. At the distal setting *W. aprica* remains to the top of the Favel Formation, contrary to the trend seen in BDC. The abrupt loss of foraminifera reflects the unconformable boundary between these formations at this locality.

A high-stress assemblage can be defined as having low diversity and few large species relative to an optimal assemblage (Keller and Pardo, 2004a; Keller and Abramovich, 2009). Foraminiferal assemblages that lack the large species *Whiteinella aprica,* as seen in the Early Turonian strata from both core and outcrop localities, are interpreted to be high-stress assemblages. Within this interval, all foraminifera are lost from the section in BR3, sample 37 (11.50 m), and only few are preserved in BDC, sample 29 (275.60 m) (Fig. 23: correlation line 3). This short-term loss is associated with a bioclastic horizon at BR3 and can be attributed to a lowering of sea-level, eroding the seafloor, winnowing the bioclastic grains, and concentrating them into a bioclastic horizon during the subsequent rise in sea-level. This lowering of sea-level induced a higher level of biotic stress,

strongly affecting the foraminiferal assemblage at both localities and excluding the larger foraminifera *W. aprica.* At the proximal position *W. aprica,* disappears earlier from the assemblage and recovers later than other planktic foraminifera, reflecting the increased biotic stress near the seaway margin at times of lower sea levels. The high stress conditions leading to the reduction in assemblage diversity and morphometric size reduction are often accompanied by other effects on the foraminifera living in these environments such as a stunting of their growth resulting in a dwarfed test size and/or modified ontogenetic growth (Keller and Abramovich, 2009; MacLeod *et al.,* 2000). Evidence of reduced test size and low diversity is seen throughout both sections. The abundance of dwarfed tests is closely linked to the abundance of *H. globulosa* in both localities but especially in BR3. In both BDC and BR3, the interval of lowered sea-level also shows an increase in the percentage of dwarfed specimens. Similarly, the interval where the planktic assemblage first appears also shows a high proportion of dwarfed specimen (Figs. 19 and 21) including *H. globulosa*, dominating the assemblage at BR3, and smaller coiled forms such as *M. planispira*, which are more abundant in BDC. These intervals give further evidence of stressful biotic conditions, which increase in severity towards the paleoshoreline.

Species in the high stress assemblage are generally small and opportunistic, and live at intermediate water column depth (Keller and Pardo, 2004a; Keller and Abramovich, 2009). Abundance of any surviving larger species is low and variable, while the abundance of smaller species can be quite high (Keller and Pardo, 2004a; Keller and Abramovich, 2009). This can be seen in both outcrop and core as *W. aprica* becomes less

abundant, the proportion of *H. globulosa* in the assemblage increases (Fig. 24) while foraminiferal abundances remain quite high throughout (Fig. 23).

There is a decrease in the number and diversity of foraminifera species at the top of the Favel Formation at BR3 (sample 25) and near the top of its equivalent at BDC (sample 26), the Second White Specks Formation, in eastern Saskatchewan (Fig. 23: correlation line 4). At BDC, the trend continues upward, and foraminifera disappear entirely near the contact with the Carlile Formation interpreted as a period of increasing biotic stress (Fig. 23: correlation line 5). This is further supported by the complete dominance of few tiny *H. globulosa* tests at BDC above 268.90 m. This trend is not observed at BR3 where there is an abundance of *W. aprica* before the disappearance of all foraminifera. This is inconsistent with the abrupt disappearance of the assemblage. At this site, the Morden Member of the Carlile Formation unconformably overlies the Favel Formation, which corresponds with the abrupt disappearance of foraminifera.

Dissaster assemblages are found when a major environmental perturbation has altered the ecosystem, often causing mass mortality and leaving behind survivors of only the most resistant opportunistic species (Keller and Abramovich, 2009). These assemblages are made up of a few small opportunistic species as well as disaster opportunist, such as guembelitrids or heterohelicids, which dominate the assemblage (Keller and Abramovich, 2009). The presence of disaster opportunists is the best indication of an event of catastrophic change in the environment (Keller and Pardo, 2004a; Keller and Abramovich, 2009); however, only one specimen of the benthic foraminifer *Neobulimina albertensis,* a documented disaster opportunist and low-oxygen indicator (Friedrich,

2009), was observed in a sample from the Keld Member of the Favel Formation in the very earliest Turonian at BR3. This species has been described from other localities in the WIS and within Cretaceous strata of the tropical Atlantic (Schröder-Adams *et al.,* 2001; Friedrich, 2009). Several species of heterohelicids have distinguished themselves as disaster opportunists during OAEs and extinction events, such as the end-Cretaceous interval (Keller and Abramovitch, 2009). The complete dominance of very few tiny *H. globulosa* tests at BDC above 268.90 m could be considered a disaster assemblage, indicating an interval of harsh conditions which excluded all but the most ecologically tolerant species (*H. globulosa*) before the disappearance of all planktic foraminifera from the assemblage.

5.3.4 The effect of ashfalls on foraminifera

The unfavorable environmental changes associated with volcanic disturbances can cause mass mortality, leaving only the most tolerant opportunistic species (Waskowska, 2011). The short-term unpredictable and rapid changes associated with ashfalls can wholly change the environment and do not allow foraminiferal communities to adapt to the modified conditions (Waskowska, 2011). The sea floor experiences catastrophic conditions with low oxygen levels and food availability (Waskowska, 2011). Volcanism can also promote the growth of phytoplankton blooms, creating toxic conditions for planktic foraminifera (Frogner *et al.,* 2001; Keller and Pardo, 2004a,b; Duggen *et al.,* 2007; Tantawy *et al.,* 2009; Waskowska, 2011; Achterberg *et al.,* 2013). Ash particles deposited in the surface waters of the seaway release macronutrients and "bioactive" trace metals that can then become available to primary producers (Frogner *et al.,* 2001;

Duggen *et al.,* 2007; Achterberg *et al.,* 2013). The iron released from these particles can rapidly fertilize large areas (Frogner *et al.,* 2001; Duggen *et al.,* 2007; Achterberg *et al.,* 2013) and promote a rapid growth of algal blooms. These large blooms increase the turbidity of the water column and can cause eutrophication (Keller and Pardo, 2004a,b; Waskowska, 2011). Only after the organic matter in the water column is reduced can the foraminifera begin recovering (Keller and Pardo, 2004a,b; Waskowska, 2011). A study on the effect of ash falls on benthic foraminiferal communities noted that within and after each ash fall there was a decrease in benthic foraminiferal abundance and taxonomic diversity in conjunction with a high proportion of opportunistic species, as well as smaller tests and some that were abnormally developed (Waskowska, 2011). Similar changes in assemblage have also been noted for planktic foraminifers after volcanic events (Keller 2003, 2008).

In the shallow restricted setting of the eastern margin of the Canadian WIS, diversity was already low and biotic stress was high. In these conditions, the abundant ash falls resulted in extreme levels of biotic stress resulting in a strong foraminiferal response where only the most resistant opportunistic species continued to thrive while the less resistant foraminiferal species were reduced in abundance and in taxonomic diversity. Both sites contain abundant evidence of the increased volcanism of the Cenomanian-Turonian interval in the form of bentonites and bentonite swarms. The foraminiferal response to these short-lived events is dramatic. In BR3, the abundance of *H. globulosa* almost always increases above ashfalls beds, as does the abundance of dwarfed specimen (Fig. 20), most of which are *H. globulosa.* This trend is also seen in BDC: the proportion

of *H. globulosa* is higher within and above intervals containing multiple bentonite layers (Fig. 22).

At BDC, the foraminiferal assemblage at the top of the Carlile Formation is made up of 100% *Heterohelix globulosa.* This interval indicates a catastrophic event that caused the death of all but the most resistant species, *H. globulosa*. It is likely the response to the extremely high biotic stress resulting from the frequent ash falls here seen as a group of closely spaced bentonite layers in the middle of the Second White Specks Formation followed by more dispersed individual bentonites. These abundant ashfalls may have caused severe eutrophication of the surface waters. Due to excess productivity from the addition of nutrients from the volcanic ash, depletion of oxygen in bottom waters and the expansion of the oxygen minimum zone into surface waters takes place (Leckie *et al.,* 2002). Recurrent ash falls throughout the Cenomanian – Turonian interval each had a lasting effect on the foraminiferal assemblage and each ash fall, or series of ash falls (swarm), can be considered a catastrophic event (Waskowska, 2011).

6. CONCLUSION

The Cenomanian – Turonian interval was a particularly dynamic and enigmatic time during the Cretaceous Period. Two localities along the eastern margin of the Cretaceous WIS of Canada were investigated: an outcrop situated on the Bainbridge River (BR3) in eastern most central Sakatchewan, representing a proximal setting of the eastern margin, as well as a reference core (Bredenbury core - BDC: 11-36-22-1W2) situated in south east Saskatchewan, representing a more distal setting. Comparisons of these strata and their foraminiferal assemblages revealed a high-stress environment regularly disturbed by

catastrophic environmental changes. This portion of the WIS was warm and shallow with a flat gradient, causing the area to be susceptible to sea-level change.

The two studied localities represent high stress environments. However, because of its position in shallower waters, nearest to the edge of the seaway, BR3 displays a higher level of biotic stress. Several events and their foraminiferal responses were noted in each section and general trends were identified in order to recognize periods of "catastrophic environmental change".

1) The proportion of large foraminiferal species *W. aprica* in the assemblages is severely reduced during times of interpreted heightened biotic stress, matched by an increase in the proportion of *H. globulosa*. These intervals are often associated with low overall diversities and small test sizes.

2) The proportion of resistant opportunistic species *H. globulosa* increases within and above bentonite layers and bentonite swarms, while the abundance of spiral foraminifera is reduced. Bentonite swarms have a more severe and lasting effect on the diversity of the assemblages and can be considered catastrophic for the planktic foraminiferal assemblage

3) Decreases in diversity are matched by an increase in the number of dwarfed foraminiferal tests, indicating severe biotic stress. This was evident during the initial phase of planktic occurrence, before the short-term disappearance of planktics from the section, as well as (to a lesser degree) during/after ashfalls.

4) The drop in sea-level recorded by the bioclastic accumulation in the more proximal Favel Formation at BR3 was associated with a complete, short term loss of all

foraminifera from this section, and can be correlated to a period of extremely low diversity and abundance in the more distal section, BDC. This lowering of sea-level brought inhospitable environmental changes for the foraminiferal assemblage in both localities.

CHAPTER 4 – SUMMARY

Strata deposited near the eastern margin of the Canadian Cretaceous WIS document dynamic paleoenvironmental changes within a shallow part of the epicontinental sea. The Cenomanian-Turonian interval records a particularly enigmatic time characterized by extreme global warmth; rapidly fluctuating sea-level; significant changes in water chemistry including periods of anoxic bottom water conditions (sometimes expanding into the photic zone) and OAEs; increased volcanism, leading to frequent ashfalls; the impact of two bolides near or within the seaway (Deep Bay and Steen River Craters); in addition to other episodic events such as storms and possibly tsunami.

Vertebrate bioclast-rich accumulations found on the eastern margin of the seaway document changes in sea-level, transport energy, and sedimentation rate. They are influenced by a combination of background and episodic processes that result in their unique sedimentary and taphonomic characteristics. In the shallow setting of the eastern WIS with its very low angle (1°) gradient, slight sea-level fluctutations are a major control for the concentration of elements found within these accumulations and episodic events strongly influence the taphonomic character of each deposit. Their narrow timeframe of deposition allows these accumulations to be used to identify relative sea level fluctuations and the frequency of episodic events within the Cenomanian-Turonian.

The Late Cenomanian to Early Turonian foraminiferal assemblage is composed almost entirely of planktic foraminifera; the absence of benthic species indicating the pervasive dysoxic/anoxic bottom water conditions documented for this region and time slice. The low diversity planktic assemblage that is present in the Manitoba Escarpment and in

eastern Saskatchewan show high levels of biotic stress, increasing towards the paleoshoreline. Ecosystems were regularly disturbed by catastrophic environmental change including ashfalls, periods of anoxia reaching into the photic zone, and sea-level fluctuations.A better understanding of the foraminiferal response to changes in this warmer Earth and its drivers may provide insight into how modern environmental changes could affect biotic assemblages in the world's oceans and will aid in future predictions.

REFERENCES

Achterberg, E. P., Moore, C. M., Henson, S. A., Steigenberger, S., Stohl, A., Eckhardt, S., & Ryan-Keogh, T. J. 2013. Natural iron fertilization by the Eyjafjallajökull volcanic eruption. *Geophysical Research Letters,* **40(5):** 921-926.

Arthur, M. A., Dean, W. E., & Schlanger, S. O. 1985. Variations in the global carbon cycle during the Cretaceous related to climate, volcanism, and changes in atmospheric CO2. *Geophysical Monograph Series,* **32:** 504-529.

Bagshaw, R. L. 1977. Foraminiferal abundance related to bentonitic ash beds in the Tununk Member of the Mancos Shale (Cretaceous) in Southeastern Utah. M.Sc. Thesis. Brigham Young University, USA.

Bamburak, J. D. & Nicolas, M. P. B. 2009. Revisions to the Cretaceous stratigraphic nomenclature of southwest Manitoba. *Manitoba Geological Survey, Report on activities,* **19:** 183-192.

Barker, I. R., Moser, D. E., Kamo, S. L., & Plint, A. G. 2011. High-precision U–Pb zircon ID–TIMS dating of two regionally extensive bentonites: Cenomanian Stage, Western Canada Foreland Basin. *Canadian Journal of Earth Sciences,* **48(2):** 543-556.

Bhattacharya, J. P., & MacEachern, J. A. 2009. Hyperpycnal rivers and prodeltaic shelves in the Cretaceous seaway of North America. *Journal of Sedimentary Research*, **79(4):** 184-209.

Bice, K. L., Birgel, D., Meyers, P. A., Dahl, K. A., Hinrichs, K. U., & Norris, R. D. 2006. A multiple proxy and model study of Cretaceous upper ocean temperatures and atmospheric CO2 concentrations. *Paleoceanography,* **21(2):** 1-17.

Bloch, J., Schröder-Adams, C., Leckie, D. A., McIntyre, D. J., Craig, J., & Staniland, M. 1993. Revised stratigraphy of the lower Colorado Group (Albian–Turonian), western Canada. *Canadian Bulletin of Petroleum Geology*, **41:** 325–348.

Bloch, J., Schröder-Adams, C., Leckie, D. A., Craig, J., & McIntyre, D. J. 1999. Sedimentology, micropaleontology, geochemistry, and hydrocarbon potential of shale from the Cretaceous Lower Colorado Group in Western Canada. *Geological Survey of Canada Bulletin,* **531,** 185p.

Bondevik, S., Svendsen, J. I., Mangerud, J. 1997. Tsunami sedimentary facies deposited by the Storegga tsunami in shallow marine basins and coastal lakes, western Norway. *Sedimentology,* **44:** 1115-1131.

BouDagher-Fadel, M. K., Banner, F. T., & Whittaker, J. E. 1997. The Early evolutionary history of planktonic foraminifera. Chapman and Hall, New York. 269p.

Brett, C. E. 1995. Sequence stratigraphy, biostratigraphy, and taphonomy in shallow marine environments: *Palaios*, **10:** 597-616.

Brett, C. E., Kirchner, B. T., Tsujita, C. J., and Dattilo, B. F. 2008. Depositional dynamics recorded in mixed siliciclastic-carbonate marine successions: insights from the Upper Ordovician Kope Formation of Ohio and Kentucky, U.S.A. In: Pratt, B. R. and Holmden, C. (Eds.); Dynamics of Epeiric Seas. *Geological Association of Canada Special paper* **48**: 73-102.

Budd, D. A. 2002. The relative roles of compaction and early cementation in the destruction of permeability in carbonate grainstones; a case study from the Paleogene of west-central Florida, U.S.A. *Journal of Sedimentary Research,* **72(1):** 116-128.

Cadrin, A. A. J, Kyser, T. K. Caldwell, W. G. E, & Longstaffe, F. J. 1995. Isotopic and chemical compositions of bentonites as paleoenvironmental indicators of the Cretaceous Western Interior Seaway. *Palaeogeography, Palaeoclimatology, Palaeoecology,* **119:** 301-320.

Caldwell, W. G. E. 1975. The Cretaceous system in the Western Interior of North America. *Geological Association of Canada, Special Paper,* **13:** 666p.

Caldwell, W. G. E., North, B. R., Stelck, C. R., & Wall, J. H. 1978. A foraminiferal zonal scheme for the Cretaceous System in the Interior Plains of Canada. In: Stelck, C. R. & Chatterton , B. D. E. (Eds.); Canadian Biostratigraphy. *Geological Association of Canada Special Paper,* **18:** 495-575.

Canfield, D. E., & Raiswell, R. 1991. Pyrite formation and fossil preservation. In: Allison, P. A. & Briggs, D. E. (Eds.); Taphonomy: Releasing the data locked in the fossil record: 337-387.

Carsey, D. O. 1926. Foraminifera of the Cretaceous of Central Texas. *Texas University Bulletin,* **2612:** 56p.

Catuneanu, O., Sweet, A. R., & Miall, A. D. 1999. Concept and styles of reciprocal stratigraphies: Western Canada foreland system. *Terra Nova-Oxford*, **11(1):** 1-8.

Christopher, J., Yurkowski, M., Nicolas, M., & Bamburak, J. 2006a. The Cenomanian-Santonian Colorado formations of eastern southern Saskatchewan and southwestern Manitoba. In: Saskatchewan and Northern Plains Oil & Gas Symposium: 299-318.

Christopher, J., Yurkowski, M., Nicolas, M., & Bamburak, J. 2006b. The Upper Cretaceous (Turonian-Santonian) Carlile Formation of eastern southern Saskatchewan, and the correlative Morden and Boyne Members of southwestern Manitoba. In: Summary of Investigations. *Saskatchewan Geological Survey,* **1:** 16p.

Cobban, W. A., & Scott, G. R. 1972. Stratigraphy and ammonite fauna of the Graneros Shale and Greenhorn Limestone near Pueblo, Colorado: U.S. *Geological Survey Professional Paper,* **645:** 108p.

Coccioni, R., & Luciani, V. 2004. Planktonic foraminifera and environmental changes across the Bonarelli Event (OAE2, latest Cenomanian) in its type area: a high resolution

study from the Tethyan reference Bottaccione section (Gubbio, central Italy). *Journal of Foraminiferal Research,* **34:** 109-129.

Coccioni, R., & Luciani, V. 2005. Planktonic foraminifers across the Bonarelli Event (OAE2, latest Cenomanian): the Italian record. *Palaeogeography, Palaeoclimatology, Palaeoecology,* **224:** 167-185.

Coccioni, R., Luciani, V., & Marsili, A. 2006. Cretaceous oceanic anoxic events and radially elongated chambered planktonic foraminifera: Paleoecological and paleoceanographic implications. *Palaeogeography, Palaeoclimatology, Palaeoecology,* **235(1):** 66-92.

Collom, C. J. 2000. High-resolution stratigraphy, regional correlation, and report of molluscan faunas: Colorado group (Cenomanian to Coniacian interval, Late Cretaceous), east-central Saskatchewan. *Summary of Investigations,* **1**: 82-97.

Croizé, D. 2010. Mechanical and chemical compaction of carbonates - An experimental study. Dissertation for the degree of Philosophiae Doctor (Ph.D.) Faculty of Mathematics and Natural Sciences, Department of Geosciences, University of Oslo, Norway.

Cumbaa, S. L. & Tokaryk, T. T. 1999. Recent discoveries of Cretaceous marine vertebrates on the eastern margins of the Western Interior Seaway. *Saskatchewan Geological Survey Summary of Investigations,* **1:** 57-63.

Cumbaa, S. L., Schröder-Adams, C., Day, R. G., & Phillips, A. J. 2006. Cenomanian bonebed faunas from the northeastern margin, Western Interior Seaway, Canada.: 139-155. In: Lucas, S. G., & Sullivan, R. M. (Eds.); Late Cretaceous Vertebrates from the Western Interior. *New Mexico Museum of Natural History & Science Bulletin ,* **35:** 139-155.

Cumbaa, S. L., Shimada, K., & Cook, T. D. 2010. Mid-Cenomanian vertebrate faunas of the Western Interior Seaway of North America and their evolutionary, paleobiogeographical, and paleoecological implications. *Palaeogeography, Palaeoclimatology, Palaeoecology,* **295:** 199-214.

Cumbaa, S.L., Underwood, C.J., Schröder-Adams, C.J. 2013. Paleoenvironments and paleoecology of the vertebrate fauna from a Late Cretaceous marine bonebed, Canada. In: Arratia, G., Schultze, H.-P., & Wilson, M. V. H. (Eds.); Mesozoic fishes 5 - Global diversity and evolution: 509-524.

Dawson, A. G. & Stewart, I. 2007. Tsunami deposits in the geological record. *Sedimentary Geol*ogy, **200**: 166-183.

Dean, W. E. & Arthur, M. A. 1998. Cretaceous Western Interior Seaway drilling project: an overview. In: Dean, W. E. & Arthur, M. A. (Eds.); Stratigraphy and paleoenvironments of the Cretaceous Western Interior Seaway, U.S.A. *SEPM Concepts in Sedimentology and Paleontology*, **6:** 1-10.

Duggen, S., Croot, P., Schacht, U., & Hoffmann, L. 2007. Subduction zone volcanic ash can fertilize the surface ocean and stimulate phytoplankton growth: Evidence from biogeochemical experiments and satellite data. *Geophysical Research Letters*, **34(1):** 1-5.

Dypvik, H. & Jansa, L. F. 2003. Sedimentary signatures and processes during marine bolide impacts: a review. *Sedimentary Geology,* **161:** 309-337.

Earth Impact Database. Deep Bay. Online source: <http://www.passc.net/EarthImpact Database/deepbay.html >. Site developed and maintained by the Planetary and Space Science Centre University of New Brunswick Fredericton, New Brunswick, Canada.

Ehrenberg, C. G. 1840. Uber die Bildung der Kreidelfelsen und des Kreidelmergels durch unsichtbare Organismen. *K. Akad. Wiss. Berlin, Physik. Abh.* **(1838):** 59-147.

Eicher, D. L. and Diner, R. 1985. Foraninifera as indicators of water mass in the Cretaceous Greenhorn Sea, Western Interior. In: Pratt, L. M., Kauffman, E. G., and Zelt, F. B. (Eds.); Fine-grained deposits and biofacies of the Cretaceous Western Interior Seaway: Evidence of cyclic sedimentary processes. *SEPM Field Trip Guidebook*, **4:** 60-71.

Eicher, D. L., & Worstell, P. 1970. Cenomanian and Turonian foraminifera from the great plains, United States. *Micropaleontology,* **16(3):** 269-324.

Erbacher, J., Huber, B. T., Norris, R. D., & Markey, M. 2001. Increased thermohaline stratification as a possible cause for an ocean anoxic event in the Cretaceous period. *Nature,* **409(6818):** 325-327.

Espitalié, J., Laporte, J. L., Madec, M., Marquis, F., Leplat, P., Paulet, J., & Boutefeu, A. 1977. Méthode rapide de caractérisation des roches mètres, de leur potentiel pétrolier et de leur degré d'évolution. *Oil & Gas Science and Technology*, **32(1):** 23-42.

Fanti, F. 2009. Bentonite chemical features as a proxy of Late Cretaceous provenance changes: a case study from the Western Interior Basin of Canada. *Sedimentary Geology,* **217:** 112-127.

Fisher, C. G., Hay, W. W., and Eicher, D. L. 1994. Oceanic front in the Greenhorn Sea (late middle through late Cenomanian).*Paleoceanography,* **9(6):** 879-892.

Forster, A., Schouten, S., Moriya, K., Wilson, P. A., & Sinninghe Damsté, J. S. 2007. Tropical warming and intermittent cooling during the Cenomanian/Turonian oceanic anoxic event 2: Sea surface temperature records from the equatorial Atlantic. *Paleoceanography,* **22(1):** 1-14.

Friedrich, O. 2009. Benthic foraminifera and their role to decipher palaeoenvironment during mid-Cretaceous Oceanic Anoxic Events: the “anoxic benthic foraminifera” paradox. *Revue de Micropaléontologie,* **53:** 175–192.

Friedrich, O., Norris, R. D., Erbacher, J. 2012. Evolution of middle to Late Cretaceous oceans: A 55 my record of Earth's temperature and carbon cycle. *Geology,* **40(2):** 107-110.

Frogner, P., Gíslason, S. R., & Óskarsson, N. 2001. Fertilizing potential of volcanic ash in ocean surface water. *Geology,* **29(6):** 487-490.

Fujiwara, O., Kamataki, T. 2007. Identification of tsunami deposits considering the tsunami waveform: An example of subaqueous tsunami deposits in Holocene shallow bay on southern Boso Peninsula, central Japan. *Sedimentary Geology*, **200:** 295-313.

Fürsich, F. T., & Aberhan, M. 1990. Significance of time-averaging for paleocommunity analysis. *Lethaia* **23:** 143-152.

Gale, A. S., Voigt, S., Sageman, B. B., & Kennedy, W. J. 2008. Eustatic sea-level record for the Cenomanian (Late Cretaceous) extension to the Western Interior Basin, USA. *Geology,* **36(11):** 859-862.

Gardner, M. H. 1995. Tectonic and eustatic controls on the stratal architecture of mid-Cretaceous stratigraphic sequences, central western interior foreland basin of North America. In: Stratigraphic Evolution of Foreland Basins. *SEPM Special Publication,* **52:** 243-279.

Glancy, T. J., Jr., Arthur, M. A., Barron, E. J., and Kauffman, E. G. 1993. A paleoclimate model for the North American Cretaceous (Cenomanian-Turonian) epicontinental sea. In: Caldwell, W. G. E. and Kauffman, E. G. (Eds.); Evolution of the Western Interior Basin. *Geological Association of Canada, Special Paper,* **39:** 219-242.

Grieve, R. A. F. 1998. Extraterrestrial impacts on Earth: the evidence and the consequences. *London Geological Society Special Publications,* **140:** 105-131.

Grieve, R. A. F. 2006. Impact structures in Canada. Geological Association of Canada c/o Department of Earth Sciences Memorial University of Newfoundland, St. John's , Newfoundland & Labrador, Canada.

Guobiao, L. 2012. Foraminifera: environmental co-evolution during Cretaceous Oceanic Anoxic Event 2 in Gambia of southern Tibet, China. *Disaster Advances,* **5(4):** 383-390.

Hart, M. B., & Ball, K. C. 1986. Late Cretaceous anoxic events, sea-level changes and the evolution of the planktonic foraminifera. *London Geological Society Special Publications,* **21(1):** 67-78.

Hart, B. S., & Plint, A. G. 1993. Tectonic influence on deposition and erosion in a ramp setting: upper cretaceous cardium formation, Alberta foreland basin. *AAPG Bulletin,* **77(12):** 2092-2107.

Hasegawa, H., Tada, R., Jiang, X., Suganuma, Y., Imsamut, S., Charusiri, P., Ichnnorov, N., & Khand, K. 2012. Drastic shrinking of the Hadley circulation during the mid-Cretaceous Supergreenhouse. *Climatic Past*, **8:** 1323–1337.

Hattin, D. E. 1962. Stratigraphy of the Carlile Shale (Upper Cretaceous) in Kansas. *University of Kansas Bulletin*, **156:** 155p.

Hattin, D. E. 1964. Cyclic sedimentation in the Colorado Group of west-central Kansas. In: Symposium on Cyclic Sedimentation. *Kansas Geological Survey Bulletin,* **169:** 205-217.

Hattin, D. E. 1975. Stratigraphy and depositional environment of the Greenhorn Limestone (Upper Cretaceous) of Kansas. *Bulletin of the Kansas Geological Survey,* **209**: 128p.

Hattin, D. E. 1986. Carbonate substrates of the Late Cretaceous Sea, central Great Plains and southern Rocky Mountains: *Palaios* **1:** 347-367.

Hattin, D. E. 1996. Fossilized regurgitate from the Smoky Hill Member of the Niobrara Chalk (Upper Cretaceous) of Kansa, USA. *Cretaceous Research,* **17:** 443-450.

Hay, W. W., Eicher, D. L., and Diner, R. 1993. Physical oceanography and water masses in the Cretaceous Western Interior Seaway. In: Caldwell, W. G. E. and Kauffman, E. G. (Eds.); Evolution of the Western Interior Basin. *Geological Association of Canada, Special Paper,* **39:** 297-318.

Hay, W. W. 1996. Tectonics and climate. *Geologische Rundschau*, **85(3):** 409-437.

Hay, W. W. 2008. Evolving ideas about the Cretaceous climate and ocean circulation. *Cretaceous Research*, **29(5):** 725-753.

Hay, W. W., & Floegel, S. 2012. New thoughts about the Cretaceous climate and oceans. *Earth Science Reviews,* **115:** 262-272.

Huber, B. T. 1998. Tropical paradise at the Cretaceous poles. *Science*, **282(5397):** 2199-2200.

Huber, B. T., Leckie, R. M., Norris, R. D., Bralower, T. J., & CoBabe, E. 1999. Foraminiferal assemblage and stable isotopic change across the Cenomanian-Turonian boundary in the subtropical North Atlantic. *Journal of Foraminiferal Research*, **29(4):** 392-417.

Huber, B. T., Norris, R. D., & MacLeod, K. G. 2002. Deep-sea paleotemperature record of extreme warmth during the Cretaceous. *Geology,* **30(2):** 123-126.

Huber, B. T., and Leckie, R. A. 2011. Planktic foraminiferal species turnover across deep-sea Aptian-Albian boundary sections. *Journal of Foraminiferal Research,* **41(1):** 53-95.

Jansa, L. F. 1993. Cometary impacts into ocean : their recognition and the threshold constraint for biological extinctions. *Palaeogeography, Palaeoclimatology, Palaeoecology,* **104:** 271-286.

Jarvis, I., Carson, G. A., Cooper, M. K. E., Hart, M. B., Leary, P. N., Tocher, B. A., & Rosenfeld, A. 1988. Microfossil assemblages and the Cenomanian-Turonian (Late Cretaceous) oceanic anoxic event. *Cretaceous Research,* **9(1):** 3-103.

Jenkyns, H. C. 1980. Cretaceous anoxic events: from continents to oceans. *Journal of the Geological Society,* **137(2):** 171-188.

Jenkyns, H. C. 2010. Geochemistry of oceanic anoxic events. *Geochemistry, Geophysics, Geosystems*, **11(3). doi:** 10.1029/2009GC002788.

Jones, C. E., & Jenkyns, H. C. 2001. Seawater strontium isotopes, oceanic anoxic events, and seafloor hydrothermal activity in the Jurassic and Cretaceous. *American Journal of Science*, **301(2):** 112-149.

Junium, C. K., & Arthur, M. A. 2007. Nitrogen cycling during the Cretaceous, Cenomanian-Turonian oceanic anoxic event II. *Geochemistry, Geophysics, Geosystems*, **8(3):** 1-18.

Kauffman, E. G. 1977a. Upper Cretaceous cyclothems, biotas, and environments, Rock Canyon anticline, Pueblo, Colorado. *Mountain Geologist* **14(3,4):** 129-152.

Kauffman, E. G. 1977b. Geological and biological overview: Western Interior Cretaceous Basin. In: Kauffman, E. G. (Ed.); Cretaceous Facies, Faunas, and Paleoenvironments across the Western Interior Basin. Field Guide: North American Paleontological Convention II. *Mountain Geologist* **14(3,4):** 75-99.

Kauffman, E. G. 1984. Paleobiogeographic and evolutionary response dynamic in the Cretaceous Western Interior Seaway of North America. *Geological Association of Canada Special Paper,* **27:** 273-306.

Kauffman, E. G. 1990. Giant fossil inoceramid bivalve pearls. In: Boucot, A. J. (Ed.); Paleobiologic evidence for rates of behavioral evolution and co-evolution: 66-68.

Kauffman, E. G. & Caldwell, W. G. E. 1993. The Western Interior Basin in space and time. In: Caldwell, W. G. E. & Kauffman, E. G. (Eds.); Evolution of the Western Interior Basin. *Geological Association of Canada Special Paper,* **39:** 1-30.

Kauffman, E. G., Harries, P. J., Meyer, C., Villamil, T., Arango, C., & Jaecks, G. 2007. Paleoecology of giant inoceramidae (*Platyceramus*) on a Santonian (Cretaceous) seafloor in Colorado. *Journal of Paleontology,* **81:** 64-81.

Keller, G. 2003. Biotic effects of impacts and volcanism. *Earth and Planetary Science Letters,* **215:** 249-264.

Keller, G. 2008. Cretaceous climate, volcanism, impacts, and biotic effects. *Cretaceous Research,* **29:** 754-771.

Keller, G. & Abramovich, S. 2009. Lilliput effect in late Maastrichtian planktic foraminifera: Response to environmental stress. *Palaeogeography, Palaeoclimatology, Palaeoecology,* **284:** 47-62.

Keller, G., Han, Q., Adatte, T., & Burns, S. J. 2001. Palaeoenvironment of the Cenomanian–Turonian transition at Eastbourne, England. *Cretaceous Research*, **22(4):** 391-422.

Keller, G. & Pardo, A. 2004a. Disaster opportunists Guembelitrinidae: index for environmental catastrophes. *Marine Micropaleontology,* **53:** 83-116.

Keller, G. & Pardo, A. 2004b. Age and paleoenvironment of the Cenomanian–Turonian global stratotype section and point at Pueblo, Colorado. *Marine Micropaleontology*, **51(1):** 95-128.

Kidwell, S. M. 1986. Models for fossil concentrations: paleobiologic implications. *Paleobiology,* **12(1)**: 6-24.

Kidwell, S. M., Fürsich, F. T., & Aigner, T. 1986. Conceptual framework for the analysis and classification of fossil concentrations. *Palaios*, **1:** 228-238.

Kidwell, S. M. 1991. Condensed deposits in siliciclastic sequences: expected and observed features. In: Einsele, G., Ricken, W., & Seilacher, A. (Eds.); Cycles and Events in Stratigraphy: 682-695.

Kidwell, S. M. & Holland, S. M. 1991. Field description of coarse bioclastic fabrics. *Palaios,* **6:** 426-434.

Kump, L. R. and Slingerland, R. L. 1999. Circulation and stratification of the early Turonian Western Interior Seaway: Sensitivity to a variety of forcings. In: Barrera, E. and Johnson, C. C. (Eds.); Evolution of the Cretaceous Ocean-climate System. *Geological Society of America, Special Paper,* **332:** 181-190.

Kuroda, J., Ogawa, N. O., Tanimizu, M., Coffin, M. F., Tokuyama, H., Kitazato, H., & Ohkouchi, N. 2007. Contemporaneous massive subaerial volcanism and late cretaceous Oceanic Anoxic Event 2. *Earth and Planetary Science Letters,* **256(1):** 211-223.

Langenhorst, F. & Deutsch, A. 2012. Shock Metamorphism of Minerals. *Elements,* **8:** 31-36.

Langford, F. F. 1973. Geology of the Wapawekka area, Saskatchewan. *Saskatchewan Department of Mineral Resources, Report***, 147:** 36 p.

Laurin, J. & Sageman, B. B. 2007. Cenomanian–Turonian coastal record in SW Utah, USA: Orbital-scale transgressive–regressive events during Oceanic Anoxic Event II. *Journal of Sedimentary Research*, **77(9):** 731-756.

Leckie, R. M. 1987. Paleoecology of mid-Cretaceous planktonic foraminifera: a comparison of open ocean and epicontinental sea assemblages. *Micropaleontology*, **33(2):** 164-176.

Leckie, D. A., & Smith, D. G. 1992. Regional setting, evolution, and depositional cycles of the Western Canada Foreland Basin. *American Association of Petroleum Geologists, Memoir,* **55:** 9-46.

Leckie, D. A., Kjarsgaard, B. A., Block, J., McIntyrel, D., McNeil, D., Stasiuk, L., & Heaman, L. 1997. Emplacement and reworking of Cretaceous, diamond-bearing, crater facies kimberlite of central Saskatchewan, Canada. *Geological Society of America Bulletin,* **109(8):** 1000-1020.

Leckie, R. M. 1985. Foraminifera of the Cenomanian-Turonian boundary interval, Greenhorn Formation, Rock Canyon Anticline, Pueblo, Colorado. In: Pratt, L. M., Kauffman, E. G., and Zelt, F. B. (Eds.); Fine-grained deposits and biofacies of the Cretaceous Western Interior Seaway: Evidence of cyclic sedimentary processes. *SEPM Field Trip Guidebook* **4:** 139-149.

Leckie, R. M., Yuretich, R. F., West, O. L. O., Finkelstein, D., & Schmidt, M. 1998. Paleoceannography of the southwestern Western Interior Sea during the time of the Cenomanian-Turonian boundary (Late Cretaceous). *SEPM Concepts in Sedimentology and Paleontology,* **6:** 101-126.

Leckie, R. M., Bralower, T. J., & Cashman, R. 2002. Oceanic anoxic events and plankton evolution: Biotic response to tectonic forcing during the mid-Cretaceous. *Paleoceanography,* **17(3):** 13-1.

Loeblich, A. R. and Tappan, H. 1961. Cretaceous planktonic foraminifera: Part I – Cenomanian. *Micropaleontology,* **7(3):** 257-304.

Loeblich, A. R. and Tappan, H. 1964. Sarcodina, chiefly "thecamoebans" and foraminifera. In: Moore, R. C. (Ed.); Treatise on invertebrate paleontology, Part C, Protista 2. Geological Society of America and University of Kansas Press: 900p.

MacLeod, K. G., & Hoppe, K. A. 1992. Evidence that inoceramid bivalves were benthic and harbored chemosynthetic symbionts. *Geology*, **20:** 117-120.

MacLeod, K. G., & Orr, W. N. 1993. The taphonomy of Maastrichtian inoceramids in the Basque region of France and Spain and the pattern of their decline and disappearance. *Paleobiology,* **19(2):** 235-250.

Macleod, N., Ortiz, N., Fefferman, N., Clyde, W., Schulter, C., & Maclean, J. 2000. Phenotypic response of foraminifera to episodes of global environmental change. In: Culver, S. J. & Rawso P. F. (Eds.); Biotic response to global change: 51-78.

Marshak, S. 2012. Earth: portrait of a planet. 4th Edition. W.W. Norton & Company, Canada.

Meyers, W. J. 1980. Compaction in Mississippian skeletal limestones, southwestern New Mexico. *Journal of Sedimentary Petrology,* **50(2):** 457-474.

McNeil, D. H., & Caldwell, W. G. E. 1981. Cretaceous rocks and their foraminifera in the Manitoba Escarpmen*., Geological Association of Canada Special Paper,* **21:** 439p.

Mitchell, A. J., Allison, P. A., Piggott, M. D., Gorman, G. J., Pain, C. C., & Hampson, G. J. 2010. Numerical modelling of tsunami propagation with implications for sedimentation in ancient epicontinental seas: The Lower Jurassic Laurasian Seaway. *Sedimentary Geology,* **228:** 81-97.

Montenaro Gallitelli, E. 1958. Schackoina from the Upper Cretaceous of the northern Apennines Italy. *Micropaleontology,* **1(2):** 200-220.

Morrow, A. L. 1934. Foraminifera and ostracoda from the Upper Cretaceous of Kansas. *Journal of Paleontology,* **8(2):** 186-205.

Mort, H. P., Adatte, T., Föllmi, K. B., Keller, G., Steinmann, P., Matera, V., & Stüben, D. 2007. Phosphorus and the roles of productivity and nutrient recycling during oceanic anoxic event 2. *Geology,* **35(6):** 483-486.

Morton, R. A., Gelfenbaum, G., & Jaffe, B. E. 2007a. Physical criteria for distinguishing sandy tsunami and storm deposits using modern examples. *Sedimentary Geology,* **200**: 184-207.

Morton, R. A., Gelfenbaum, G., Jaffe, B. E., & Gibbons, H. 2007b. Distinguishing tsunami from storm deposits in the geologic record. *Sound Waves*: 2-3.

Munro, L. E. 2000. $^{18}O/^{16}O$ isotopes as temperature indicators in Late Cretaceous fossil shark and bony fish teeth. Bachelor of ScienceThesis, Department of Environmental Sciences, Carleton University, Ottawa, Ontario, Canada.

Nauss, A. W. 1947. Cretaceous microfossils of the Vermilion area, Alberta. *Journal of Paleontology,* **21(4):** 329-343.

Nichols, G. 2009. Sedimentology and stratigraphy. John Wiley & Sons. 419p.

Nicolas, M. P. B. 2009. Williston Basin Project (Targeted Geoscience Initiative II): summary report on Mesozoic stratigraphy, mapping and hydrocarbon assessment, southwestern Manitoba; Manitoba Science, Technology, Energy and Mines. *Manitoba Geological Survey Geoscientific Paper,* **1:** 19p.

Nicholls, E. L. & Russell, A. P. 1990. Paleobiogeography of the Cretaceous Western Interior Seaway of North America; the vertebrate evidence. *Palaeogeography, Palaeoclimatology, Palaeoecology,* **79:** 149-169.

Nielsen. K. S., Schröder-Adams, C. J., & Leckie, D. A. 2003. A new stratigraphic framework for the Upper Colorado Group (Cretaceous) in southern Alberta and southwestern Saskatchewan, Canada. *Bulletin of Canadian Petroleum Geology,* **51(3):** 304-346.

Norris, R. D., Bice, K. L., Magno, E. A., & Wilson, P. A. 2002. Jiggling the tropical thermostat in the Cretaceous hothouse. *Geology,* **30:** 299-302.

Ohkouchi, N., Kashiyama, Y., Kuroda, J., Ogawa, N. O., & Kitazato, H. 2006. The importance of diazotrophic cyanobacteria as primary producers during Cretaceous Oceanic Anoxic Event 2. *Biogeosciences,* **3(4):** 467-478.

Ormo, J. and Lindstrom, M. 2000. When a cosmic impact strikes the sea bed. *Geology Magazine,* **137:** 67-80.

Peryt, D. 2004. Benthic foraminiferal response to the Cenomanian-Turonian and Cretaceous-Paleogene boundary events. *Przeglad Geologiczny,* **52:** 827-832.

Petrizzo, M. R., & Huber, B. T. 2006. Biostratigraphy and taxonomy of late Albian planktonic foraminifera from ODP Leg 171B (western North Atlantic Ocean). *Journal of Foraminiferal Research,* **36(2):** 166-190.

Phillips, A. 2008. A late Cretaceous (Cenomanian) marine vertebrate-rich bioclastic horizon from the northeastern margin of the Western Interior Seaway, Canada. Master's Thesis, Department of Earth Sciences, Carleton University, Ottawa-Carleton Geoscience Centre, Ottawa, Ontario, Canada.

Pirrie, D., & Marshall, J. D. 1990. Diagenesis of Inoceramus and Late Cretaceous paleoenvironmental geochemistry: a case study form James Ross Island, Antarctica. *Palaios,* **5(4):** 336-345.

Plint, A. G., Hart, B. S., & Donaldson, W. S. 1993. Lithospheric flexure as a control on stratal geometry and facies distribution in Upper Cretaceous rocks of the Alberta foreland basin. *Basin Research,* **5(2):** 69-77.

Plint, A. G., & Kreitner, M. A. 2007. Extensive thin sequences spanning Cretaceous foredeep suggest high-frequency eustatic control: Late Cenomanian, Western Canada foreland basin. *Geology,* **35(8):** 735-738.

Plint, A. G. 2009. High-frequency relative sea level oscillations in Upper Cretaceous shelf clastics of the Alberta foreland basin: possible evidence for a glacio-eustatic control. In: Sedimentation, Tectonics and Eustasy. *Special Publication of the International Association of Sedimentol*ogy, **12:** 409-428.

Poulsen, C. J., Barron, E. J., Arthur, M. A., & Peterson, W. H. 2001. Response of the Mid-Cretaceous global oceanic circulation to tectonic and CO2 forcings. *Paleoceanography,* **16(6):** 576-592.

Price, G. D., Sellwood, B. W., & Valdes, P. J. 1995. Sedimentological evaluation of general circulation model simulations for the "greenhouse" Earth: Cretaceous and Jurassic case studies. *Sedimentary Geology,* **100:** 159-180.

Price, R. A. 1994. Cordilleran tectonics and the evolution of the Western Interior Sedimentary Basin. In: Geological Atlas of the Western Interior Sedimentary Basin: 13-24.

Reeburgh, W. S. 1983. Rates of biochemical processes in anoxic sediments. *Annual Review of Earth and Planetary Sciences,* **11:** 269-298.

Reimold, W. U. & Jourdan, F. 2012. Impact! - Bolides, Craters, and Catastrophes. *Elements,* **8:** 19-24.

Reolid, M., Sebane, A., Rodríguez-Tovar, F. J., & Marok, A. 2012. Foraminiferal morphogroups as a tool to approach the Toarcian Anoxic Event in the Western Saharan Atlas (Algeria). *Palaeogeography Palaeoclimatology Palaeoecology* **323-325:** 87-99.

Russell, D. A. 1993. Vertebrates in the Western Interior Sea. In: Caldwell, W. G. E. & Kauffman, E. G. (Eds.); Evolution of the Western Interior Basis. *Geological Association of Canada Special Paper,* **39:** 665-680.

Sageman, B. B. 1989. The benthic boundary biofacies model: Hartland Shale Member, Greenhorn Formation (Cenomanian), Western Interior, North America. *Palaeogeography, Palaeoclimatology, Palaeoecology,* **74:** 87-110.

Sageman, B. B. 1996. Lowstand tempestites: depositional model for Cretaceous skeletal limestones, Western Interior, U.S. *Geology,* **24:** 888-892.

Sageman, B. B., & Bina, K. R., 1997, Diversity and species abundance patterns in Late Cenomanian black shale biofacies, Western Interior, U.S. *Palaios,* **12:** 449-466.

Schlanger, S. O., & Jenkyns, H. C. 1976. Cretaceous oceanic anoxic events: causes and consequences. *Geologie en mijnbouw*, **55(3-4):** 179-184.

Schröder-Adams, C. J., Leckie, D. A. Bloch, J., Craig, J., McIntyre, D. J., & Adams, P. J. 1996. Paleoenvironmental changes in the Cretaceous (Albian to Turonian) Colorado Group of Western Canada: Microfossil, sedimentological and geochemical evidence. *Cretaceous Research,* **17:** 311-365.

Schröder-Adams, C. J., Cumbaa, S. L., Bloch, J., Leckie, D. A., Craig, J., El-Dein, S. A. S., Simons, D.-J. H. A. E., & Kenig, F. 2001. Late Cretaceous (Cenomanian to Campanian) paleoenvironmental history of the Eastern Canadian margin of the Western Interior Seaway: bonebeds and anoxic events. *Palaeogeography, Palaeoclimatology, Palaeoecology,* **170:** 261-289.

Schröder-Adams, C. J., Herrle, J. O., & Tu, Q. 2012. Albian to Santonian carbon isotope excursions and faunal extinctions in the Canadian Western Interior Sea: Recognition of eustatic sea-level controls on a forebulge setting. *Sedimentary Geology*, **281:** 50-58.

Schröder-Adams, C. J. 2014. The Cretaceous Polar and Western Interior seas: paleoenvironmental history and paleoceanographic linkages. *Sedimentary Geology*, **301:** 26-40.

Scott, D. B., Medioli, F. S., & Schafer, C. T. 2001. Monitoring in coastal environments using foraminifera and thecamoebian indicators. Cambridge University Press, Cambridge, United Kingdoms.

Shimada, K., Schumacher, B. A., Parkin, J. A., & Palermo, J. M. 2006. Fossil marine vertebrates from the lowermost Greenhorn Limestone (Upper Cretaceous: middle Cenomanian) in southeastern Colorado. *Journal of Paleontology,* **80(63):** 1-45.

Singh, C.1983. Cenomanian microfloras of the Peace River area, northwestern Alberta. *Alberta Research Council, Bulletin,* **44:** 322p.

Simons, D. J. H., & Kenig, F. 2001. Molecular fossil constraints on the water column structure of the Cenomanian–Turonian Western Interior Seaway, USA. *Palaeogeography, Palaeoclimatology, Palaeoecology,* **169(1):** 129-152.

Simonson, B. M. & Glass, B.P. 2004. Spherule layers – records of ancient impacts. *Annual Review Earth and Planetary Science,* **32:** 329-361.

Slingerland, R., Kump, L. R., Arthur, M. A., Fawcett, P. J., Sageman, B. B., and Barron, E. J. 1996. Estuarine circulation in the Turonian Western Interior Seaway of North America. *Geological Society of America Bulletin,* **108(8):** 941-952.

Snow, L. J., & Duncan, R. A. 2001. Hydrothermal links between ocean plateau formation and global anoxia. *AGU Fall Meeting Abstracts,* **1:** 437.

Snow, L. J., Duncan, R. A., & Bralower, T. J. 2005. Trace element abundances in the Rock Canyon Anticline, Pueblo, Colorado, marine sedimentary section and their relationship to Caribbean plateau construction and oxygen anoxic event 2. *Paleoceanography*, **20(3):** 1-14.

Speyer, S. E. & Brett, C. E. 1991. Taphofacies controls: background and episodic processes in fossil assemblage preservation. In : Allison, P. A. and Briggs, D. E. G. (Eds); Taphonomy: releasing the data locked in the fossil record: 500-545.

Stewart, C., Jonhson, D. M., Leonard, G. G., Horwell, C. J., Thordarson, T., & Cronin, S. J. 2006. Contamination of water supplies by volcanic ashfall: a literature review and simple impact modeling. *Journal of Volcanology and Geothermal Research,* **158:** 296-306.

Stoffler, D. & Langenhorst, F. 1994. Shock metamorphism of quartz in nature and experiment: I. Basic observation and theory. *Meteoritics,* **29:** 155-181.

Tantawy, A. A. A., Keller, G., & Pardo, A. 2009. Late Maastrichtian volcanism in the Indian Ocean: Effect on calcareous nannofossils and planktic foraminifera. *Palaeogeography, Palaeoclimatology, Palaeoecology,* **284:** 63-87.

Tappan, H. 1940. Foraminifera from the Grayson Formation of northern Texas. *Journal of Paleontology,* **14:** 93-126.

Tappan, H. 1943. Foraminifera from the Duck Creek formation of Oklahoma and Texas. *Journal of Paleontology,* 476-517.

Tappan, H. 1962. Foraminifera of the Artic slope of Alaska; Part 3-Cretaceous foraminifera. *U.S. Geological Survey, Professional Paper,* **236-C:** 91-209.

Tarduno, J. A., Brinkman, D. B., Renne, P. R., Cottrell, R. D., Scher, H., & Castillo, P. 1998. Evidence for extreme climatic warmth from Late Cretaceous Arctic vertebrates. *Science*, **282(5397):** 2241-2243.

Then, D. R. & Dougherty, B. J. 1983. A new procedure for extracting foraminifera from indurated organic shale. In: Current Research, Part B. *Geological Survey of Canada Paper,* **83-1B:** 413-414.

Tokaryk, T. T., Cumbaa, S. L., & Storer, J. E. 1997. Early Late Cretaceous birds from Saskatchewan, Canada: the oldest diverse avifauna known from North America. *Journal of Vertebrate Paleontology,* **17:** 172-176.

Trueman, C. N. & Martill, D. M. 2002. The long term preservation of bone: the role of bioerosion. *Archaeometry,* **44:** 371-382.

Trueman, C. N., Benton, M. J., & Palmer, M. R. 2003. Geochemical taphonomy of shallow marine vertebrate assemblages. *Palaeogeography, Palaeoclimatology, Palaeoecology,* **197**: 151-169.

Tsandev, I., & Slomp, C. P. 2009. Modeling phosphorus cycling and carbon burial during Cretaceous Oceanic Anoxic Events. *Earth and Planetary Science Letters,* **286(1):** 71-79.

Turgeon, S. C., & Creaser, R. A. 2008. Cretaceous oceanic anoxic event 2 triggered by a massive magmatic episode. *Nature,* **454(7202):** 323-326.

Twitchett, R. J. 2006. The palaeoclimatology, palaeoecology and palaeoenvironmental analysis of mass extinction events. *Palaeogeography, Palaeoclimatology, Palaeoecology*, **232(2):** 190-213.

Twitchett, R. J. 2007. The Lilliput effect in the aftermath of the end-Permian extinction event. *Palaeogeography, Palaeoclimatology, Palaeoecology*, **252(1):** 132-144.

Tyagi, A., Plint, A. G., & McNeil, D. H. 2007. Correlation of physical surfaces, bentonites, and biozones in the Cretaceous Colorado Group from the Alberta Foothills to

southwest Saskatchewan, and a revision of the Belle Fourche-Second White Specks formational boundary. *Canadian Journal of Earth Sciences*, **44(7):** 871-888.

Underwood, C. J., & Cumbaa, S. L., 2010, Chondrichthyans from a Cenomanian (Late Cretaceous) bonebed, Saskatchewan, Canada. *Palaeontology,* **53:** 903-944.

Urbanek, A. 1993. Biotic crises in the history of Upper Silurian graptoloids: a palaeobiological model. *Historical Biology*, **7(1):** 29-50.

Wade, B. S., & Olsson, R. K. 2009. Investigation of pre-extinction dwarfing in Cenozoic planktonic foraminifera. *Palaeogeography, Palaeoclimatology, Palaeoecology*, **284(1):** 39-46.

Walker, K. R., and Bambach, R. K. 1971. The significance of fossil assemblages from fine-grained sediments: time-averaged communities. *Geological Society of America Abstracts with Programs,* **3**: 783-784.

Waśkowska, A. 2011. Response of Early Eocene deep-water benthic foraminifera to volcanic ash falls in the Polish Outer Carpathians: Palaeoecological implications. *Palaeogeography, Palaeoclimatology, Palaeoecology,* **305:** 50-64.

Williams, J. W. 1995. Factors controlling the formation of fossiliferous beds in the Devonian Columbus limestone at Marblehead Quarry, Marblehead, Ohio. *Ohio Journal of Science,* **95(5):** 325-330.

Williams-Mitchell, E. 1948. The zonal value of foraminifera in the chalk of England. *Proceedings of the Geological Association*, **59:** 91-112.

Wilson, P. A., & Norris, R. D. 2001. Warm tropical ocean surface and global anoxia during the mid-Cretaceous period. *Nature,* **412(6845):** 425-429.

Zielinski, G. A. 2000. Use of paleo-records in determining variability within the volcanism–climate system. *Quaternary Science Reviews,,***19(1):** 417-438.

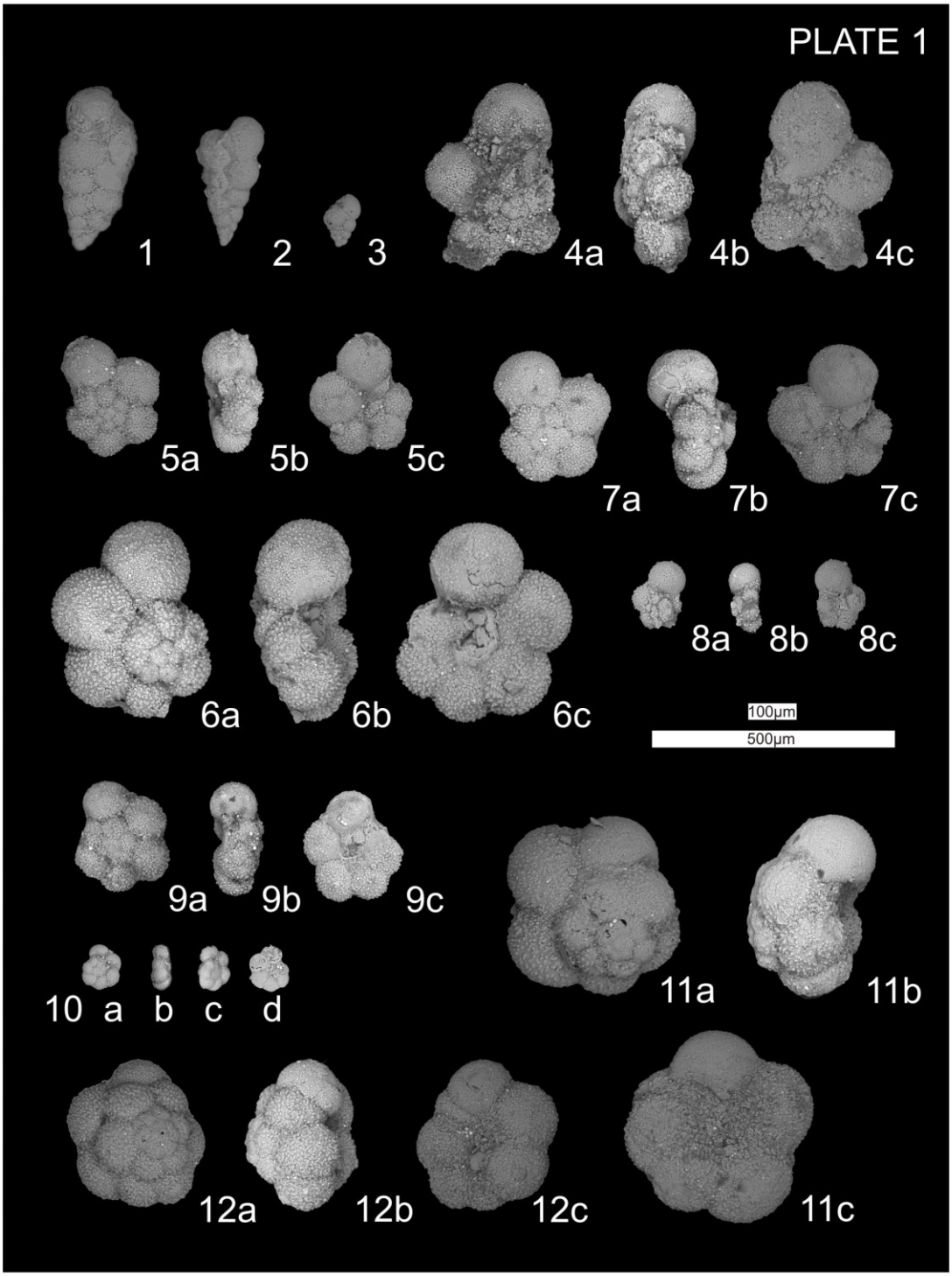
PLATE 1
1
2
3
4a
4b
4c
5a
5b
5c
7a
7b
7c
8a
8b
8c
6a
6b
6c
100µm
500µm
9a
9b
9c
10 a b c d
11a
11b
12a
12b
12c
11c

Explanation of plate 1

Figures 1, 2, 3. *Heterohelix globulosa* (Ehrenberg) – Sample localities 1:BR3-20, 2:BR3-32, 3:BR3-30.

Figures 4 a-c, 5 a-c. *Clavihedbergella amabilis* (Loeblich and Tappan) – spiral views; 4a, 5a, edge view; 4b, 5b, umbilical view; 4c, 5c. Sample localities 4:BDC-32, 5:BDC-33.

Figures 6 a-c, 7 a-c, 8 a-c. *Muricohedbergella delrioensis* (Carsey) – spiral views; 6a, 7a, 8a, edge view; 6b, 7b, 8b, umbilical view; 6c, 7c, 8c. Sample localities 6:BDC-28, 7:BDC-33, 8:BR3-17.

Figures 9 a-c, 10 a-d. *Muricohedbergella planispira* (Tappan) – spiral views; 9a, 10a, edge view; 9b, 10b-c, umbilical view; 9c, 10d. Sample localities 9:BDC-33, 10:BR3-20.

Figures 11 a-c, 12 a-c. *Muricohedbergella portsdownensis* (Williams-Mitchell) – spiral views; 11a, 12a, edge view; 11b, 12b, umbilical view; 11c, 12c. Sample localities 11:BDC-28, 12:BDC-27.

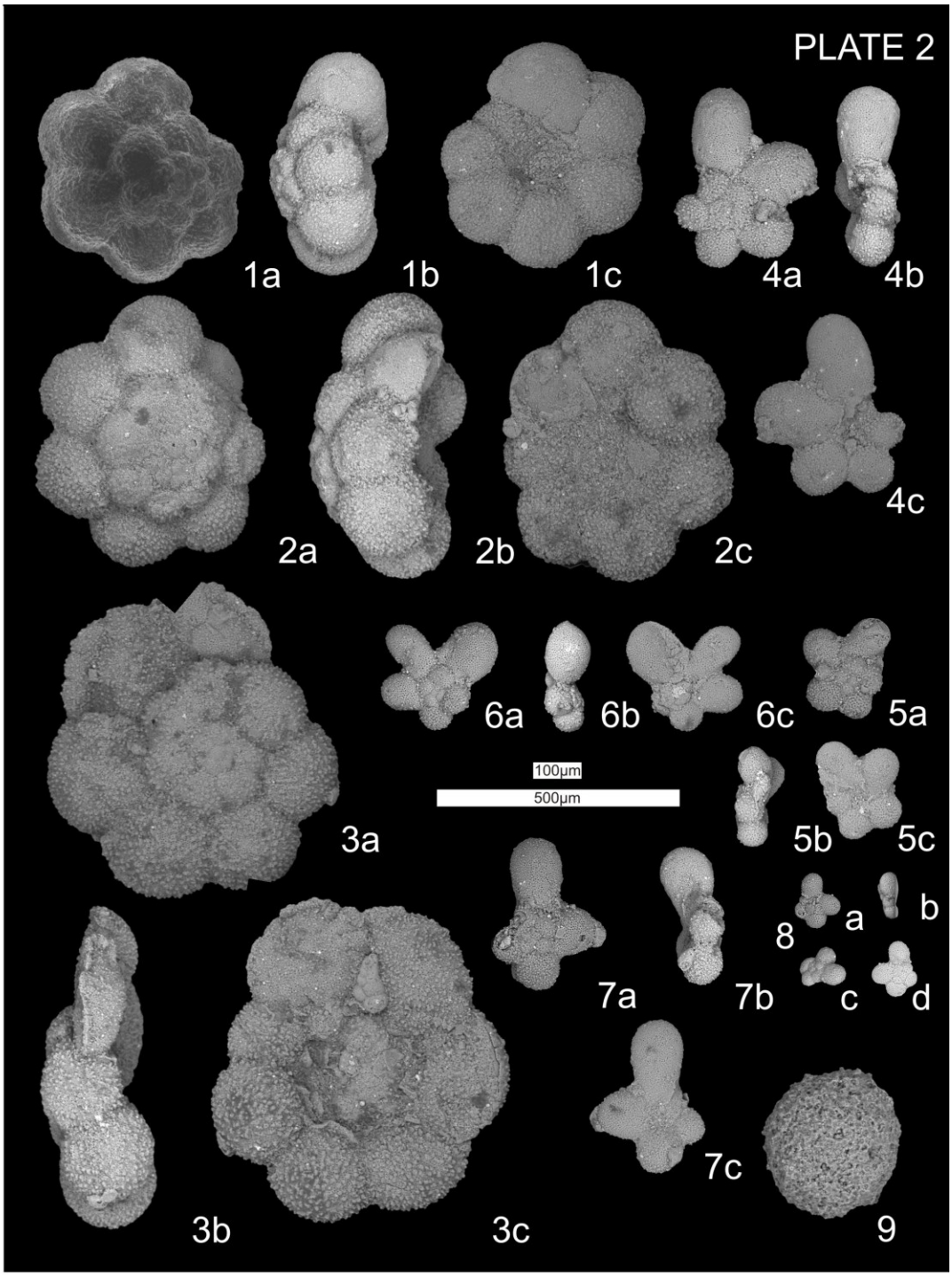
PLATE 2
1a
1b
1c
4a
4b
2a
2b
2c
4c
6a
6b
6c
5a
100µm
500µm
3a
5b
5c
8
a
b
c
d
7a
7b
7c
3b
3c
9

Explanation of plate 2

Figures 1 a-c. *Muricohedbergella loetterlei* (Nauss) – spiral views; 1a, edge view; 1b, umbilical view; 1c. Sample locality 1:BDC-27.

Figures 2 a-c, 3 a-c. *Whiteinella aprica* (Loeblich and Tappan) – spiral views; 2a, 3a, edge view; 2b, 3b, umbilical view; 2c, 3c. Sample localities 2:BDC-28, 3:BDC-28.

Figures 4 a-c, 5 a-c, 6 a-c. *Clavihedbergella subcretacea* (Tappan) – spiral views; 4a, 5a, 6a, edge view; 4b, 5b, 6b, umbilical view; 4c, 5c, 6c. Sample localities 4:BR3-17, 5:BR3-17, 6:BR3-30.

Figures 7 a-c, 8 a-d. *Clavihedbergella simplex* (Morrow) – spiral views; 7a, 8a, edge view; 7b, 8b-c, umbilical view; 7c, 8d. Sample localities 7:BR3-17, 8:BR3-30.

Figure 9. *Siliceous radiolarian test* (sp.?) – Sample locality 9:BR3-23.

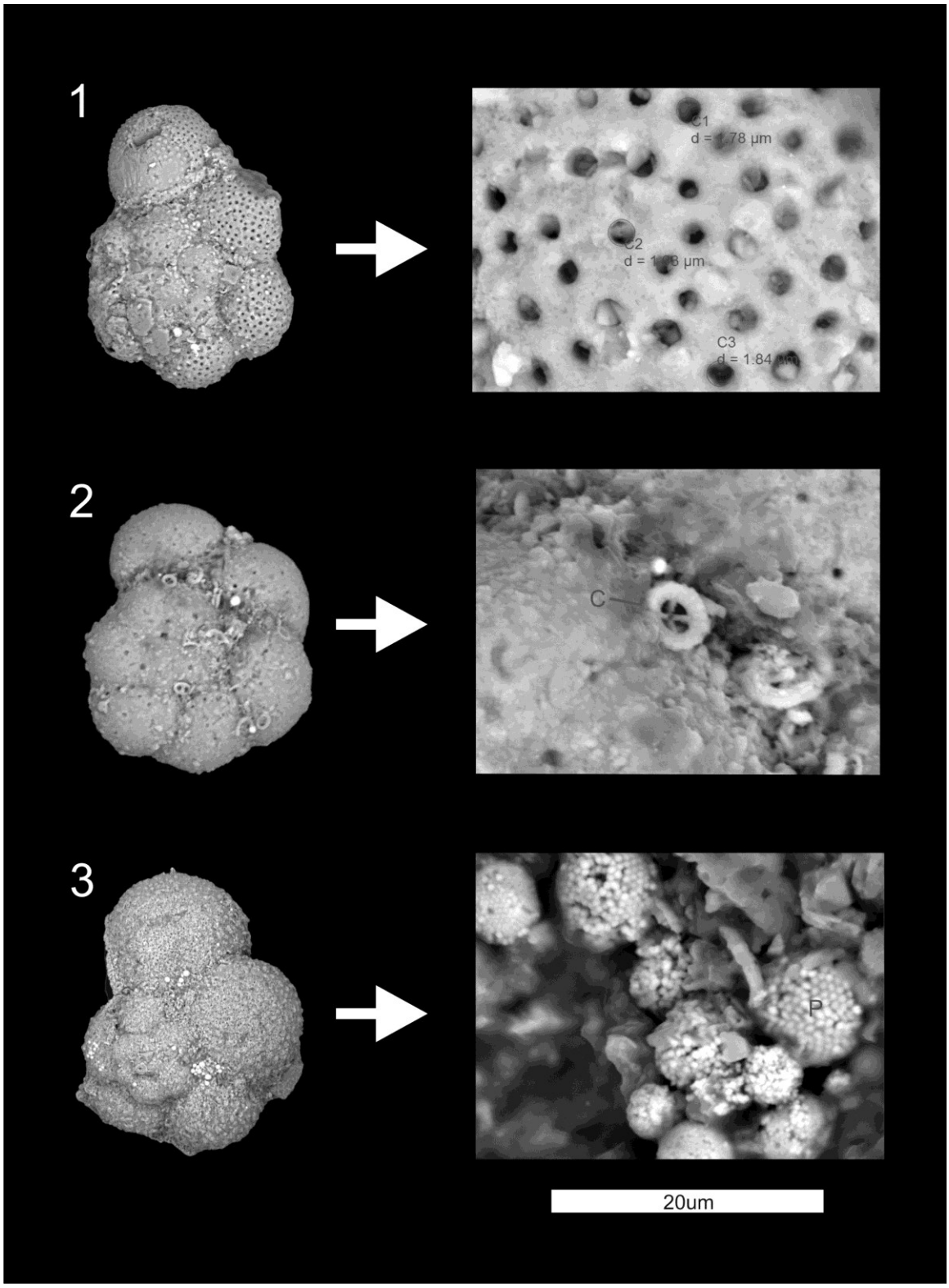
1
C1
d = 1.78 µm
C2
C3
2
C
3
P
20um

Explanation of plate 3

Figures 1. *Clavihedbergella amabilis* – Chamber walls are finely perforate with the wall pores (C1, C2, C3) measuring 1-2.5µm in diameter on adult chambers and variably spaced. Sample locality 1: BDC-33.

Figures 2. *Muricohedbergella planispira.* – Foraminiferal test covered by smaller coccolithophore (C) fragments. Sample locality 2:BR3-20.

Figures 3. *Muricohedbergella delrioensis* – Foraminiferal test showing growth of pyrite framboids (P). Sample locality 3: BDC-28.

APPENDIX 1: Planktic foraminiferal listings for Bainbridge River outcrop. For the listing of agglutinated species, readers are refered to Schröder-Adams *et al.* (2001).

Formation	Sample #	*H. globulosa*	*W. aprica*	*M. loetterlei*	*M. ports-downensis*	*M. delrio-ensis*	*M. planispira*	*C. amabilis*	*C. simplex*	*C. sub-cretacea*	*M. sp?*	planktic fragments
Ashville Fm. Belle Fourche Member	1	x	x	x	x	x	x	x	x	x	x	x
	2	x	x	x	x	x	x	x	x	x	x	x
	3	x	x	x	x	x	x	x	x	x	x	x
	4	x	x	x	x	x	x	x	x	x	x	x
	5	x	x	x	x	x	x	x	x	x	x	x
	6	x	x	x	x	x	x	x	x	x	x	x
	7	x	x	x	x	x	x	x	x	x	x	x
	8	x	x	x	x	x	x	x	x	x	x	x
	9	x	x	x	x	x	x	x	x	x	x	x
	10	x	x	x	x	x	x	x	x	x	x	x
	11	x	x	x	x	x	x	x	x	x	x	x
Favel Fm. Keld Member	12	x	x	x	x	x	x	x	x	x	x	x
	N28	**6**	x	**6**	x	**27**	**18**	**6**	x	x	x	**10**
	13	x	x	x	x	x	x	x	x	x	x	x
	14	**159**	x	x	x	**3**	**4**	x	x	x	x	**1**
	15*	**133**	x	**57**	**4**	**103**	**18**	**1**	x	x	**3**	**12**
	16	**222**	x	**31**	**15**	**57**	**17**	**3**	**6**	x	**55**	x
	17	**154**	x	**10**	**13**	**58**	**5**	**19**	**35**	**3**	**12**	**0**
Favel Fm. Assiniboine Member	18	**238**	**24**	**32**	**18**	**116**	**22**	**61**	x	x	**15**	**11**
	19	**278**	x	x	x	**8**	x	**1**	x	x	**1**	**3**
	20	**251**	**2**	x	x	**51**	**149**	x	x	x	**6**	**64**
	21	**500**	x	**20**	x	**15**	**55**	x	x	x	**32**	**65**
	22	**304**	**81**	**102**	**15**	**51**	**24**	**4**	x	x	**30**	**45**
	23	**65**	**6**	**24**	**5**	**38**	**6**	x	x	x	**96**	x
	24	**517**	**23**	**21**	**11**	**117**	**143**	x	x	x	**39**	**31**
	25	**17**	**107**	**108**	**45**	**78**	**3**	**5**	x	x	**48**	**73**
Carlile Fm. Morden Member	26	x	x	x	x	x	x	x	x	x	x	x
	27	x	x	x	x	x	x	x	x	x	x	x
	28	x	x	x	x	x	x	x	x	x	x	x
	29	x	x	x	x	x	x	x	x	x	x	x
Favel Fm. Keld Member	30	**247**	**18**	**12**	**4**	**83**	**1**	**12**	**51**	**9**	**2**	x
	31	**330**	**18**	**16**	**7**	**23**	**10**	**2**	x	**1**	**1**	**6**
	32	**347**	**157**	**131**	**30**	**106**	**62**	**13**	x	x	**26**	**4**
	33	**439**	**87**	**61**	**10**	**171**	**26**	**37**	x	x	**16**	**38**
Favel Fm. Assiniboine Member	34	**366**	**57**	**88**	**25**	**122**	**36**	**6**	x	x	**26**	**21**
	35	**19**	x	x	x	**8**	**2**	x	x	x	x	**35**
	36	**99**	x	x	**2**	**2**	**1**	**1**	**1**	x	**1**	**9**
	37	x	x	x	x	x	x	x	x	x	x	x
	38	**160**	x	**3**	x	**24**	**9**	**2**	**1**	x	**13**	**2**
	39	**129**	x	**2**	x	**102**	**256**	x	**1**	x	**18**	**3**

*one specimen of *Neobulimina albertensis.*

APPENDIX 2: Planktic foraminiferal listings for Bredenbury reference core. For agglutinated species, readers are refered to Bloch *et al.* (1999).

Formation	Sample #	*H. globulosa*	*W. aprica*	*M. loetterlei*	*M. ports-downensis*	*M. delrio-ensis*	*M. planispira*	*C. amabilis*	*C. simplex*	*C. sub-cretacea*	*M. sp?*	planktic fragments
Carlile Fm.	18	x	x	x	x	x	x	x	x	x	x	x
	19	x	x	x	x	x	x	x	x	x	x	x
	20*	x	x	x	x	x	x	x	x	x	x	x
Second White Specks Fm.	21	x	x	x	x	x	x	x	x	x	**1**	x
	22	**32**	x	x	x	x	x	x	x	x	x	x
	23	**3**	x	x	x	x	x	x	x	x	x	x
	24	**59**	x	x	x	x	x	x	x	x	x	x
	25	**57**	x	x	x	x	x	x	x	x	x	x
	26	**40**	**169**	**300**	**24**	**401**	**263**	**12**	x	x	x	x
	27	**131**	**388**	**1026**	**210**	**764**	**2073**	**39**	**1**	x	**49**	**35**
	28	**233**	x	**28**	**19**	**458**	**1220**	**225**	x	x	**41**	**25**
	29	x	x	x	x	x	x	x	x	x	**38**	x
	30**	**445**	**159**	**1005**	**987**	**525**	**1152**	**293**	**2**	**10**	**114**	**1**
	31	**384**	**744**	**1255**	**183**	**492**	**380**	**115**	x	x	**271**	**33**
	32	**25**	**337**	**650**	**199**	**1022**	**794**	**596**	**27**	**5**	**42**	**2**
	33	x	**4**	**219**	**228**	**776**	**1868**	**551**	**5**	**1**	**37**	**3**
Belle Fourche Fm.	34*	x	x	x	x	x	**2**	x	x	x	x	x
	35*	**2**	x	x	x	x	x	x	x	x	x	x
	36	x	x	x	x	x	x	x	x	x	x	x
Fish Scales Fm.	37	x	x	x	x	x	x	x	x	x	x	x
	38	x	x	x	x	x	x	x	x	x	x	x
Westgate Fm.	39*	x	x	x	x	x	x	x	x	x	x	x

*agglutinated foraminifera are present.
*very abundant, fine fraction 10% picked.

APPENDIX 3: Rock-Eval pyrolysis data for Bainbridge River outcrop.

Formation	Sample #	Height	TOC	HI
Ashville Fm. Belle Fourche Member	1	0.40	6.30	226.0
	2	0.51	1.73	85.0
	3	0.56	6.74	201.0
	4	0.85	6.12	174.5
	5	1.00	6.62	188.5
	6	2.00	4.34	294.5
	7	3.45	6.31	295.5
	8	3.60	1.54	227.5
	9	3.80	5.86	139.0
	10	4.80	5.69	444.5
	11	5.00	0.03	37.5
Favel Fm. Keld Member	12	5.21	11.63	498.0
	13	6.21	---	---
	14	7.15	10.55	464.0
	15	8.11	9.02	468.5
	16	9.25	9.15	488.0
	17	9.41	5.70	433.5
Favel Fm. Assiniboine Member	18	10.31	6.61	441.5
	19	11.31	9.52	476.5
	20	12.31	12.38	469.0
	21	13.31	11.93	392.0
	22	14.41	11.78	466.0
	23	15.31	2.65	377.5
	24	16.31	8.23	363.0
	25	17.31	0.20	112.5
Carlile Fm. Morden Member	26	17.80	15.27	573.0
	27	18.80	14.82	551.0
	28	19.80	12.83	562.5
	29	20.80	11.22	393.5
Favel Fm. Keld Member	30	2.50	8.28	408.0
	31	2.53	11.47	396.0
	32	2.91	8.24	453.5
	33	2.93	1.93	309.5
Favel Fm. Assiniboine Member	34	3.13	4.21	375.5
	35	4.08	2.58	313.0
	36	4.15	9.03	428.0
	37	4.35	3.43	269.0
	38	4.48	7.81	420.5
	39	4.98	13.71	499.0

APPENDIX 4: Rock-Eval pyrolysis for Bredenbury reference core.

Formation	Sample #	Depth	TOC	HI
Carlile Fm.	18	255.4	7.91	134
	19	256.3	6.91	120
	20	258.3	6.46	274
Second White Specks Fm.	21	260.3	9.14	177
	22	262.3	7.23	447
	23	264.9	4.65	374
	24	266.9	10.26	423
	25	268.9	11.95	434
	26	270.9	12.62	429
	27	272.7	10.20	455
	28	273.7	0.82	255
	29	275.6	1.40	346
	30	277.5	8.14	446
	31	279.4	8.17	373
	32	281.3	4.88	415
	33	283.2	7.87	375
Belle Fourche Fm.	34	285.1	8.99	419
	35	287.0	7.22	421
	36	288.9	5.51	401
Fish Scales Fm.	37	290.8	4.95	181
	38	291.7	4.20	191
Westgate Fm.	39	296.7	3.91	147

APPENDIX 5: Reference list of planktic foraminiferal species.

***Heterohelix globulosa* (Ehrenberg), 1840**

Textularia globulosa: Ehrenberg, C. G. 1840. Uber die Bildung der Kreidelfelsen und des Kreidelmergels durch unsichtbare Organismen. *K. Akad. Wiss. Berlin, Physik. Abh.* **(1838):** 59-147.

Montenaro Gallitelli, E. 1958. *Schackoina* from the Upper Cretaceous of the northern Apennines Italy. *Micropaleontology,* **1(2):** 200-220.

***Whitinella aprica* (Loeblich and Tappan), 1961**

Ticinella aprica: Loeblich, A. R. and Tappan, H. 1961. Cretaceous planktonic foraminifera: Part I – Cenomanian. *Micropaleontology,* **7(3):** 257-304.

Eicher, D. L., & Worstell, P. 1970. Cenomanian and Turonian foraminifera from the great plains, United States. *Micropaleontology,* **16(3):** 269-324.

***Muricohedbergella loetterlei* (Nauss), 1947**

Globigerina loetterlei: Nauss, A. W. 1947. Cretaceous microfossils of the Vermilion area, Alberta. *Journal of Paleontology,* **21(4):** 329-343.

Huber, B. T., and Leckie, R. A. 2011. Planktic foraminiferal species turnover across deep-sea Aptian-Albian boundary sections. *Journal of Foraminiferal Research*, **41(1):** 53-95.

***Muricohedbergella portsdownensis* (Williams-Mitchell), 1948**

Hedbergella portsdownensis: Williams-Mitchell, E. 1948. The zonal value of foraminifera in the chalk of England. *Proceedings of the Geological Association,* **59:** 91-112.

Huber, B. T., and Leckie, R. A. 2011. Planktic foraminiferal species turnover across deep-sea Aptian-Albian boundary sections. *Journal of Foraminiferal Research,* **41(1):** 53-95.

***Muricohedbergella delrioensis* (Carsey), 1926**

Hedbergella delrioensis: Carsey, D. O. 1926. Foraminifera of the Cretaceous of central Texas. *University of Texas Bulletin,* **2612:** 56p.

Huber, B. T., and Leckie, R. A. 2011. Planktic foraminiferal species turnover across deep-sea Aptian-Albian boundary sections. *Journal of Foraminiferal Research,* **41(1):** 53-95.

***Muricohedbergella planispira* (Tappan), 1940**

Hedbergella planispira: Tappan, H. 1940. Foraminifera from the Grayson Formation of northern Texas. *Journal of Paleontology,* **14:** 93-126.

Huber, B. T., and Leckie, R. A. 2011. Planktic foraminiferal species turnover across deep-sea Aptian-Albian boundary sections. *Journal of Foraminiferal Research,* **41(1):** 53-95.

***Clavihedbergella* amabilis* (Loeblich and Tappan), 1961**

Hedbergella amabilis: Loeblich, A. R. and Tappan, H. 1961. Cretaceous planktonic foraminifera: Part I – Cenomanian. *Micropaleontology,* **7(3):** 257-304.

***remark:** This species has been assigned to the genus *Clavihedbergella* due to its radially elongated chambers, a feature that excludes it from the genus *Muricohedbergella*.

***Clavihedbergella simplex* (Morrow), 1934**

Hastigerinella simplex: Morrow, A. L. 1934. Foraminifera and Ostracoda from the Upper Cretaceous of Kansas. *Journal of Paleontology,* **8(2):** 186-205.

Loeblich, A. R. and Tappan, H. 1961. Cretaceous planktonic foraminifera: Part I – Cenomanian. *Micropaleontology,* **7(3):** 257-304.

***Clavihedbergella subcretacea* (Tappan), 1943**

Hastigerinella subcretacea: Tappan, H. 1943. Foraminifera from the Duck Creek Formation of Oklahoma and Texas. *Journal of Paleontology,* **7:** 476-517.

Loeblich, A. R. and Tappan, H. 1964. Sarcodina, chiefly "thecamoebans" and foraminifera. In: Moore, R. C. (Ed.); Treatise on invertebrate paleontology, Part C, Protista 2. Geological Society of America and University of Kansas Press: 900p.